Western &Graduate&PostdoctoralStudies

Electronic Thesis and Dissertation Repository

8-14-2019 9:30 AM

A role for Shh and Bmp4 in regulating the dorsal-ventral patterning of the developing pharyngeal region

Alex Szpak, *The University of Western Ontario*

Supervisor: Drysdale, Thomas A., *The University of Western Ontario*
A thesis submitted in partial fulfillment of the requirements for the Master of Science degree in Biology

Follow this and additional works at: https://ir.lib.uwo.ca/etd

Part of the Developmental Biology Commons

Abstract

  The pharynx is crucial to the survival of all vertebrates since it facilitates respiration by connecting the nasal and oral cavity to the larynx and digestion by connecting the oral cavity to the esophagus. The developing pharyngeal region displays dorsoventral patterning, and currently there is little information identifying the underlying mechanisms that regulate this patterning. This is in part due to the complexity of the developing pharyngeal region that requires contributions from all three germ layers along with neural crest cells. The expression profiles of Sonic Hedgehog (Shh) and Bone Morphogenetic Protein 4 (Bmp4) adjacent to the developing pharyngeal region are reminiscent of their expression around the developing neural tube where they regulate dorsoventral patterning. By pharmacologically altering these signalling pathways I was able to support the hypothesis that the correct dorsoventral gene expression pattern observed in the developing pharyngeal region is regulated by opposing gradients of Shh and Bmp4.

Keywords: Sonic Hedgehog, Bone Morphogenetic Protein 4, *hand1*, pharyngeal region, *Xenopus laevis*

Summary for Lay Audience

The pharynx is the part of the throat that connects the mouth and nasal cavity to the larynx and esophagus. The purpose of the pharynx is to facilitate respiration by connecting the mouth and nasal cavity to the larynx and allow digestion by connecting the mouth to the esophagus. The developing pharyngeal region can be observed on the lateral side of vertebrate embryos just below the developing head and can be identified by a series of tissue outgrowths called pharyngeal arches. During early development, the pharyngeal region displays patterning of genes along the anteroposterior axis (front to back) and dorsoventral axis (top to bottom). The signaling molecule retinoic acid regulates the patterning of genes along the anteroposterior axis, however, the signaling molecules that regulate the gene pattern along the dorsoventral axis remains unknown. The main aim of this thesis is to uncover those signaling molecules that regulate the dorsoventral patterning of the developing pharyngeal region. The signaling molecules Sonic Hedgehog (Shh) and Bone Morphogenetic Protein 4 (Bmp4) have been shown to regulate the dorsoventral patterning of the neural tube and are expressed later in development on the dorsal and ventral sides of the developing pharyngeal region, respectively. Therefore, I hypothesized that Shh and Bmp4 work in opposing gradients to pattern genes along the dorsoventral axis of the developing pharyngeal region. The hypothesis was tested by chemically inhibiting or activating Shh and Bmp4 signaling, staining the mRNA of genes located within the developing pharyngeal region and assessing the localization of the genes' expression domains along the dorsoventral axis following treatment of the *Xenopus laevis* embryos. The results were able to support the hypothesis that the correct gene expression along the dorsoventral axis of the developing pharyngeal region is regulated by opposing gradients of Shh and Bmp4.

Co-authorship

The initial observations that Shh signalling was regulating the dorsoventral patterning of the developing pharyngeal region in *X. laevis* was investigated by Kevin Fan and Dr. Thomas A. Drysdale. I have personally performed all of the writing and experiments defined within this thesis. Dr. Drysdale is attributed with co-authorship of this thesis due to his supervision, assistance in designing experiments, examining data, and editing the thesis.

Acknowledgements

Table of Contents

List of Tables

List of Figures

List of Abbreviations

μg – Micrograms

μL – Microlitres

μM – Micromolar

bHLH – basic helix-loop-helix

Bmp4 – Bone morphogenetic factor 4

cDNA – complementary deoxyribonucleic acid

CRISPR/Cas9 – clustered regularly interspaced short palindromic repeats/ caspase 9

CY – cyclopamine

$_dH_2O$ – distilled water

DIG – digoxigenin

DMH1 – dorsomorphin homolog 1

DMSO – dimethyl sulfide

DNA - deoxyribonucleic acid
RNA - ribonucleic acid

EtOH – ethanol

g - grams

gcm2 – Glial Cells Missing Homolog 2

h - hour

hand1 – Heart and Neural Crest Derivatives Expressed 1

hoxa3 – Homeobox A3

L - litres

M – molar

mg - milligram

mL - millilitre

mM – millimolar

mn - minute

mRNA – messenger ribonucleic acid

ºC – Degrees Celsius

pax1 – Paired Box 1

PCR – polymerase chain reaction

PMA – purmorphamine

prrx2 – Paired Related Homeobox 2

RA – retinoic acid

rpm – revolutions per minute

sgDNA – single guide deoxyribonucleic acid

Shh – Sonic Hedgehog

T7E1 – T7 endonuclease 1

TGF-β - Transforming growth factor beta 1

UV – ultraviolet

Wnt - Wingless-related integration site

X. laevis – Xenopus laevis

Chapter 1: Introduction

Craniofacial morphogenesis is a complex developmental process that requires the precise orchestration of many molecular and morphogenetic events (Ataliotis et al., 2005; Ferguson and Graham, 2004; Graham and Smith, 2001; Ho et al., 1994; Noden and Trainor, 2005; Rinon et al., 2007). Structures such as the muscles of mastication, nerves needed for facial expression and the thyroid and parathyroid glands are a few of the important adult structures of the head and neck region that require proper early embryonic development of the pharyngeal region (Frisdal and Trainor, 2014). Since many adult structures and features of the head and neck region originate from the developing pharyngeal region, this area has been the focus of many studies to understand how patterning occurs and potential developmental origins of disorders and diseases (Escriva et al., 2002; Jones and Trainor, 2004; Scambler, 2000; Stewart et al., 2013). The purpose of this thesis is to advance the knowledge of how the pharyngeal region develops and to determine the factors that are regulating the dorsoventral patterning of the developing pharyngeal complex.

1.1 *Xenopus laevis* as a model for development

The South African clawed frog, *Xenopus laevis*, is a well-characterized model of development that has been used extensively over the past century to investigate many aspects of early embryogenesis. Some of the numerous advantages it has for studying early development include that many early developmental signalling pathways, morphological processes, and genes are all conserved between *X. laevis* and mammalian development. These conserved characteristics make *Xenopus* an appropriate model of development when investigating developmental events and diseases that occur in humans (Dickinson, 2016; Haremaki et al., 2015; Nie and Bronner, 2015).

One of the significant advantages of using *X. laevis* as a model of development is the ability of the embryos to tolerate extensive manipulation. Embryos can be exposed to reagents, have essential tissue extirpated, or DNA, mRNA or proteins can be injected to test specific hypotheses about the roles of signalling pathways or specific genes during early embryonic development (Blum and Ott, 2018; Tandon et al., 2017; Wheeler and Brändli, 2009). Exposure to reagents is easily performed because embryonic development

occurs externally in very simple culture conditions. *Xenopus* embryos can be treated directly by adding the reagents to the media in which the embryos are developing. (Gordon et al., 2010; Tabler et al., 2014).

Pertinent to this thesis is that the conserved biological characteristics of *Xenopus* also enables the use of CRISPR/Cas9 genome editing technology. The ability to rapidly inject large numbers of embryos with CRISPR/Cas9 reagents allows one to generate large numbers of embryos with mutations in specific genes that are required in conserved developmental events (Bhattacharya et al., 2015; Tandon et al., 2017).

X. laevis also has a well-documented fate map of the early blastomeres allowing for physical or chemical manipulation of specific embryonic regions (Dale and Slack, 1987). The ease of manipulation coupled with the well-defined fate map allows for the investigation into the exact developmental stages when specific tissues or signalling pathways are required. *Xenopus* embryos all develop at the same rate that is strictly dependent on temperature and this allows one to manipulate the rate of development by simply changing temperature. Lastly, perhaps the most beneficial property of *Xenopus* as a model of development is that the females can produce hundreds of eggs which synchronously develop once fertilized. This is advantageous to studies comparing experimental and control embryos, often using whole-mount *in situ* hybridization to study the localization of RNA, because large cohorts of embryos can be easily obtained. This allows for hundreds of observations and hence a large N-value when statistically analyzing those images.

One of the few complexities of using *X. laevis* as a model system is that these frogs are tetraploid. Specifically, *X. laevis* is an allelotetraploid species because it is a result of a hybridization event between two parental species. Two diploid progenitors, one closely related to *Xenopus tropicalis* and another ancient diploid *Xenopus* are the sources of the two diploid sets of chromosomes. Those two progenitor species had 20 chromosomes and the reason that *X. laevis* has 38, rather than 40 chromosomes, is that chromosome 9 and 10 have fused (Matsuda et al., 2015; Session et al., 2016). The two sets of chromosomes are referred to as the long chromosome and the short chromosome and individual genes have "l" or "s" behind their name if both sets of genes are still present: (for example *hand1l* and

hand1s) (Session et al., 2016). Therefore, genetic studies, specifically ones dealing with mutating genes, can be more complex. For example, *X. laevis* has four potential targets in the one cell embryo for a particular gene product if using CRISPR/Cas9 gene editing. In order to circumvent this complexity, multiple guide RNAs for CRISPR/Cas9 studies may be required to target both the long and short chromosome version of a particular gene in order to ensure that all gene copies are mutated (Tandon et al., 2017).

As mentioned earlier the vast majority of cellular pathways and developmental events are conserved between *X. laevis* and their mammalian counterparts. Two of the signalling pathways that are conserved are the Sonic hedgehog (Shh) and Bone morphogenetic protein (Bmp) signalling pathways which regulate morphological and patterning events throughout *X. laevis* development (Briscoe et al., 1999; Liem et al., 2000; Liem Jr. et al., 1997; Timmer et al., 2002). Not only are signalling pathways conserved but embryonic structures are conserved as well. One such structure is the developing pharyngeal region. In fact, segmentation and the creation of slits in the developing pharyngeal region is a defining characteristic of all chordates. The pharyngeal region and its patterning are the focus of this thesis.

1.2 Early embryonic development of the pharynx

The fully developed pharynx is located in the neck region and is situated between the oral and nasal cavity and the esophagus and larynx. The pharynx is crucial to the survival of all vertebrates given that the pharynx facilitates respiration by connecting the nasal and oral cavity to the larynx, while, also connecting the oral cavity to the esophagus allowing for digestive functions. One of the key reasons why the developing pharyngeal region is the focus of many developmental studies is that this area later gives rise to bones, cartilages, tissues, arteries, veins, and nerves of the head and neck region (Frisdal and Trainor, 2014). Pharyngeal endoderm also gives rise to the thymus, parathyroid, thyroid, and ultimobranchial bodies and disruptions in patterning can give rise to defects in these organs (Graham and Smith, 2001). Developmental studies of the pharyngeal region are also important because one in three congenital disorders affects the head and neck region and those defects may have developmental origins starting in the pharyngeal region including

Pierre Robin sequence and DiGeorge syndrome (Jones and Trainor, 2004; Scambler, 2000; Stewart et al., 2013).

As mentioned earlier, the basic pharyngeal region structure is conserved across all vertebrates (Square et al., 2015). This allows one to study the development of the pharynx and facial malformations associated with human disorders in model organisms that can be easily manipulated, either pharmacologically or genetically, including mice, zebrafish, and *X. laevis* (Ataliotis et al., 2005; Stewart et al., 2013).

During early embryonic development, the developing pharyngeal region can be identified as the reiterated series of outgrowths called pharyngeal arches on the lateral side of the embryo towards the ventral side of the developing head (**Fig. 1A**). The number of pharyngeal arches is species-dependent and can range from four to nine. *X. laevis* possesses seven pharyngeal arches which develop in sequential order. The first pharyngeal arch first develops at stage 23 and by stage 35 (**Appendix**) the first five pharyngeal arches can be identified on the lateral sides of the embryo (**Fig. 1A**). The development of the pharyngeal region is complex since it requires interaction between all three germ layers (endoderm, mesoderm and ectoderm) along with migrating neural crest cells (Ataliotis et al., 2005; Ferguson and Graham, 2004; Graham and Smith, 2001; Ho et al., 1994; Noden and Trainor, 2005; Rinon et al., 2007). The ectoderm surrounds the exterior of the pharyngeal arches which is defined as the pharyngeal cleft and groove. The interior portion of the pharyngeal arches, which is referred to as the pharyngeal pouch, is laminated with the endoderm (**Fig. 1B**). The ectoderm and endoderm come in close proximity with one another in the pharyngeal clefts, therefore, it is suspected that this close interaction between the two layers may be required for the complete perforation and opening of the pharyngeal gill slits in *X. laevis* embryos. This hypothesis is based on previous research showing that proximity of ectoderm and endoderm control the opening of the mouth in *X. laevis* embryos (Dickinson and Sive, 2006; Tabler et al., 2014). In the arch region between the clefts where the ectoderm and endoderm are adjacent, the space found between the ectoderm and endoderm is made up of mesoderm and neural crest cells that have delaminated from the mid- and hindbrain border (Frisdal and Trainor, 2014; Graham and Smith, 2001). Later in

the development of the pharyngeal region, each of the pharyngeal arches will give rise to specific skeletal, vascular, and muscle derivatives (Frisdal and Trainor, 2014).

In frogs the first pharyngeal arch will give rise to structures including but not limited to gill primordium, maxilla, and mandible, while the second pharyngeal arch later develops into the second aortic arch, upper part of the hyoid bone and stapes (Frisdal and Trainor, 2014). In the later stages of development the lower hyoid bone and common carotid artery originate from the third pharyngeal arch, whereas the thyroid and thymus derive from the fourth pharyngeal arch (Frisdal and Trainor, 2014). The fifth pharyngeal arches later gives rise to laryngeal cartilage and muscle (Frisdal and Trainor, 2014).
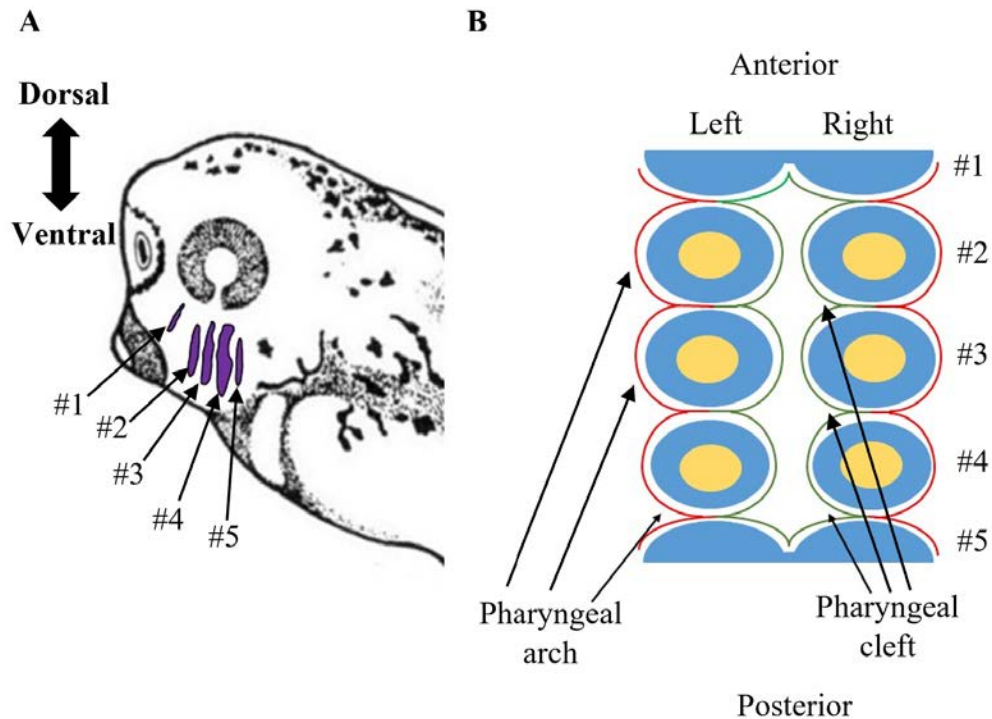
Figure 1. Diagrams displaying where the pharyngeal arches are located in a stage 35 *X. laevis* embryos and the organization of the germ layers and neural crest cells within the pharyngeal region. (**A**) The pharyngeal arches (purple) of a stage 35 *X. laevis* embryos can be identified by the reiterated series of outgrowths on lateral side of the head region of the embryo. (**B**) A schematic through the transverse section of the pharyngeal region of *X. laevis*. The exterior of the pharyngeal arches is covered by ectoderm (red), while, the interior of the pharyngeal arches is covered by a layer of endodermal cells (green). Within the pharyngeal arches the ectoderm and endoderm cover a layer of neural crests cells (blue) and at the centre of the group of neural crest cells is a mesodermal core (yellow).

During development of the arches, there is a clear anteroposterior pattern to the developing arches as evident by the different tissues formed from pharyngeal arches (Escriva et al., 2002; Frisdal and Trainor, 2014). This anteroposterior pattern is in part, regulated by retinoic acid (RA) signalling (Escriva et al., 2002). In *Amphioxus*, addition of exogenous RA results in an anterior shift in the expression of *AmphiTR2/4* which is found within the second pharyngeal arch while blocking RA signalling by exposing *Amphioxus* to BMS009, an RA inhibitor, was able to shift the expression of *AmphiTR2/4* to the posterior region of the developing pharyngeal region (Escriva et al., 2002). Furthermore, it has been established that the *Hox* genes are key elements of the anteroposterior pattern in the developing pharyngeal region (Hunt et al., 1991; Maconochie et al., 1999). More specifically, different *Hox* genes are expressed in different neural crest cell subpopulations and the presence or absence of certain *Hox* genes will give neural crest cells positional identity. The identity of neural crest cells found in specific pouches along the anteroposterior axis of the developing pharyngeal region are co-linear with the *Hox* gene numbers in the region of the neural tube where the neural crest cells are derived (Hunt et al., 1991a, 1991b; Maconochie et al., 1999; Trainor and Krumlauf, 2000; Tümpel et al., 2002, 2008). If the *Hox* genes are misregulated, such as by silencing *Hoxa3*, skeletal elements, normally found in the first pharyngeal arch, shift into the second pharyngeal arch and structures such as Meckel's cartilage, incus, and malleus which are normally found in the second pharyngeal arch are shifted into the first pharyngeal arch region (Gendron-Maguire et al., 1993; Kontges and Lumsden, 1996; Rijli et al., 1993). This anteroposterior patterning has been extensively studied due to the role of individual arches in forming specific structures such as a the thyroid, thymus and bones of the face (Frisdal and Trainor, 2014; Minoux and Rijli, 2010).

Not only does the developing pharyngeal region display anteroposterior patterning but it also displays patterning along the dorsoventral axis (Square et al., 2015). In order to understand the evolution of skeletal components derived from the arches during development, Square et al. (2015) demonstrated that several specific genes are differentially expressed along the dorsoventral axis of the developing pharyngeal region in *Xenopus* embryos (Square et al., 2015). This dorsoventral pattern within the pharyngeal region has also been observed in zebrafish and mice (Jeong et al., 2008; Talbot et al., 2010).

In both studies, expression of genes such as *hand2, dlx2/4* and *pou3f3* were restricted to the ventral, intermediate or dorsal regions of the developing pharyngeal region (Jeong et al., 2008; Talbot et al., 2010). Also *dlx* genes were demonstrated to play important roles in patterning the developing pharyngeal region and in regulating proper formation of skeletal structures arising from this area (Jeong et al., 2008; Talbot et al., 2010). Although these studies have shown that the developing pharyngeal region displays dorsoventral patterning, to my knowledge the signalling molecules that are responsible for establishing that pattern remain unknown (Jeong et al., 2008; Square et al., 2015; Talbot et al., 2010).

Perhaps the best understood example of dorsoventral patterning of a structure in the early embryo is in the neural tube where opposing gradients of Shh and Bmp4 signalling are necessary to establish a pattern of neuronal identities along that axis (Briscoe et al., 1999; Liem et al., 2000; Liem Jr. et al., 1997; Timmer et al., 2002). Expression profiles of Shh and Bmp4 around the pharyngeal region suggest that they may be available to help generate the dorsoventral pattern in the developing pharyngeal region (**Fig. 2**). If so, it should be noted that the gradients would be inverted as compared to the neural tube (**Fig. 3**) with Shh found on the dorsal side and Bmp4 found on the ventral side of the developing pharyngeal region (Barnett et al., 2012; Rankin et al., 2012).
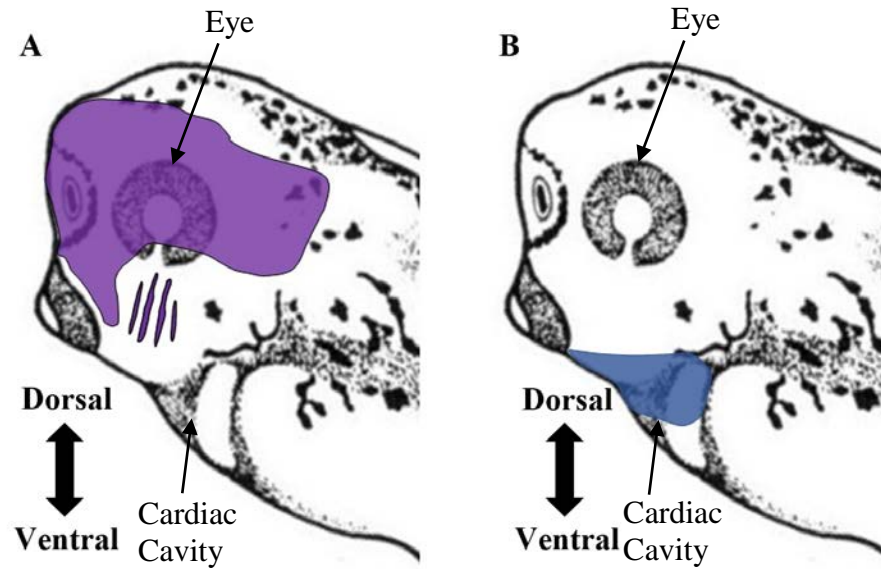
Figure 2. Diagrams depicting the localization of *Shh* and *Bmp4* mRNA in the head and neck region of stage 35 *X. laevis* embryos. (**A**) *Shh* expression (purple) is observed anterior to the pharyngeal region including and up to the first pharyngeal arch, and dorsal to the five pharyngeal arches. (**B**) *Bmp4* expression (blue) is observed ventral to the pharyngeal region. Data is based on previous expression studies (Koide et al., 2006; Rankin et al., 2012).

1.3 Axial Patterning in the Embryo

The anteroposterior, dorsoventral, and left-right axes are three axes along which an embryo develops. *X. laevis* has been extensively used to study how these three axes are generated and the possible consequences of their malformation due to aberrant molecular signalling or incorrect cellular divisions (Altaba and Melton, 1989; Campione et al., 1999; Suzuki et al., 1994). In particular, the molecular mechanisms that establish the dorsoventral axis of the embryo is particularly well understood in *Xenopus*. A microtubule-based mechanism initiated by entry of the sperm centriole drives beta-catenin to the dorsal side of the just fertilized embryo causing a canonical wingless (wnt) signal that defines that side of the embryo as being dorsal (Weaver and Kimelman, 2004). Later in the developing *Xenopus* embryo the neural plate forms from ectoderm on the dorsal side of the embryo. That plate then rolls to form the neural tube and the subsequent tube then establishes its own dorsoventral pattern (Christen and Slack, 1997; McMahon et al., 1998; Yost, 1990).

A neural tube is found in all vertebrate embryos and is the precursor to the brain and spinal cord, thereby making correct patterning of the neural tube crucial to the embryo's survival. One characteristic of dorsoventral patterning in the neural tube is that specific subtypes of neurons differentiate according to their position in the dorsoventral axis and this is crucial for proper motor, sensory and interneuron neuron development (Barth et al., 1999; Basler et al., 1993; Ericson et al., 1996; McMahon et al., 1998; Nguyen et al., 2000; Sander et al., 2000; Vallstedt et al., 2001; Yamada et al., 1993).

A key element in establishing the dorsoventral axis in the neural tube is secretion of the Shh ligand (Ericson et al., 1996; Roelink et al., 1995). The secretion of the Shh ligand from the notochord initiates the secretion of Shh in the floor plate. The further from this ventral source of the ligand within the neural tube, the lower the concentration of the Shh ligand resulting in the formation of a Shh gradient (Ericson et al., 1996; Roelink et al., 1995). Concurrently, Bmp4 is secreted from the epidermis dorsal to the neural tube, prompting the cells found in the roof plate of the neural tube to also secrete Bmp4 (Liem Jr. et al., 1995, 1997). The Bmp4 concentration is high at the dorsal pole of the neural tube with levels of Bmp4 decreasing ventrally along the dorsoventral axis (Liem Jr. et al., 1995, 1997). Thus, Shh and Bmp4 form opposing gradients along the dorsoventral axis (**Fig. 3**)

(Briscoe et al., 1999; Liem et al., 2000; Liem Jr. et al., 1997; Timmer et al., 2002). The levels of signalling ligand that the cells in the neural tube receive provides cells with positional information along the dorsoventral axis so that they can express and/or repress specific transcription factors (Nguyen et al., 2000; Sander et al., 2000). A combinatorial code based on the expression of these transcription factors specifies the different subtypes of neurons according to their position along the dorsoventral axis. For example, sensory neurons differentiate near the dorsal side of the neural tube and motor neurons are clustered near the ventral pole of the neural tube (Briscoe et al., 1999; Ericson et al., 1995; Liem et al., 2000; Liem Jr. et al., 1995, 1997; Roelink et al., 1995; Timmer et al., 2002).

The dorsoventral patterning of the neural tube is just one case of many processes where proper expression of Shh and Bmp4 are required for correct embryonic development. Another such developmental event that requires these signalling pathways is during the development of the kidneys (Nishinakamura and Sakaguchi, 2014; Yu et al., 2002). More specifically Shh signalling is required to promote mesenchymal cell proliferation, and regulates the time point at which differentiation of smooth muscle progenitor cells occurs in the ureteral mesenchyme (Yu et al., 2002). Mice in which Shh was mutated displayed phenotypes of renal hypoplasia, hydronephrosis and hydroureter demonstrating the necessity of expressing Shh at the correct time points and locations during the development of the kidney (Yu et al., 2002). Whereas Bmp4 is required to prevent ureteric bud attraction and combined with the Bmp antagonist, Gremlin, are required to initiate ureteric budding (Nishinakamura and Sakaguchi, 2014). Mice in which Bmp4 is mutated exhibit characteristics similar to human congenital anomalies of the kidney and the urinary tract including hypoplastic kidneys and hydroureter (Nishinakamura and Sakaguchi, 2014). A third region of the developing embryo where these signalling ligands displayed a similar expression profiles to the neural tube is around the developing pharyngeal region (**Fig. 2**) (Barnett et al., 2012; Rankin et al., 2012). The location of Shh and Bmp4 expression within the developing pharyngeal region is the inverse of their positioning within the neural tube with respect to the dorsoventral axis. Shh is expressed dorsal to the developing pharyngeal region and Bmp4 is expressed ventral to the developing pharyngeal region (**Fig. 2**) (Barnett et al., 2012; Rankin et al., 2012).
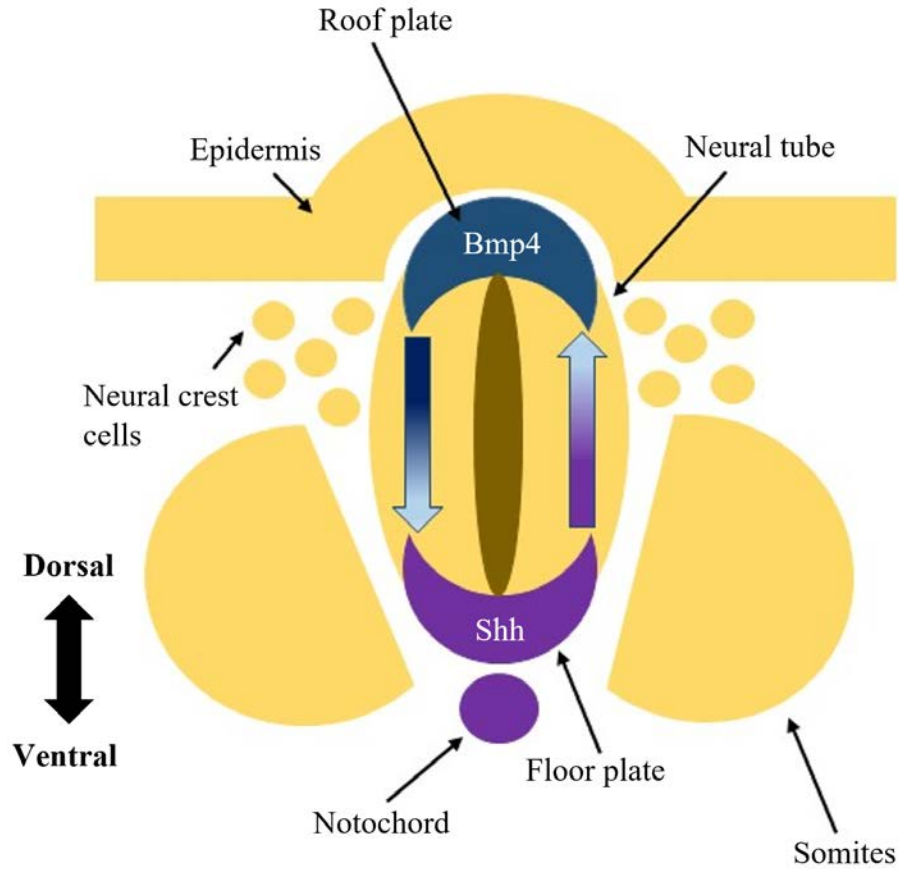
Figure 3. Diagram demonstrating the expression localization of Shh and Bmp4 in the neural tube. In the neural tube, the initial secretion of the Shh ligand (purple) originates from the notochord at the ventral side of the neural tube and causes cells located in the floor plate to also secrete the Shh ligand. Along the dorsoventral axis, there is a gradient of Shh protein from a high concentration found around the ventral pole and decreasing levels moving towards the dorsal side of the neural tube. A similar pattern is observed with the Bmp4 (blue) protein levels along the dorsoventral axis. A higher concentration of Bmp4 ligand is observed at the dorsal pole and decreases moving towards the ventral pole. Together these signalling molecules create opposing gradients which pattern the neural tube along the dorsoventral axis.

1.4 Sonic hedgehog (Shh) signalling

Sonic hedgehog (Shh) is one of the three Hedgehog signalling proteins (the other two are Indian and Desert hedgehog) and has been implicated in many biological processes throughout an organism's lifespan including events in early development, tissue regeneration, stem cell renewal and cancer (Bailey et al., 2008; Ericson et al., 1995; Machold et al., 2003). In addition to its role in patterning the neural tube, Shh is required for many critical patterning events in invertebrates and vertebrates (Ericson et al., 1995; Laufer et al., 1994; Rankin et al., 2016). One such place that Shh plays a critical role is during the development of the limb (Laufer et al., 1994; Tickle and Towers, 2017). Here Shh not only provides positional information for cells along the anteroposterior axis (thumb to little finger) but also stimulates mesenchymal cell proliferation to control the width of the limb and regulates the anteroposterior length of the apical ectodermal ridge which is important for developing the correct structures along the proximo-distal axis of the developing limb (Laufer et al., 1994; Tickle and Towers, 2017). With respect to *Xenopus,* Shh is expressed in defined locations during specific stages of development such as ventral to the neural tube, in the floor plate, in the limb bud, and dorsal to the pharyngeal region (Ericson et al., 1995; Koide et al., 2006; Laufer et al., 1994).

The Shh ligand is a protein that requires multiple modifications for the ligand to become a functional signalling protein. The Shh protein precursor is initially proteolytically cleaved into an amino terminus (Shh-N) and a carboxy terminus (Shh-C) peptides (Choudhry et al., 2014). Shh-N has been demonstrated to be the peptide which is crucial for Shh signalling (Choudhry et al., 2014). Following cleavage, auto-proteolysis occurs which then allows for a cholesterol moiety to be added to the C-terminus of Shh-N peptide (Choudhry et al., 2014). Next, Skinny hedgehog acyltransferase attaches a palmitoyl group on the N-terminal of Shh which is vital for regulating the secretion of Shh and the ability for Shh to signal at longer-ranges (Chamoun et al., 2001; Lewis et al., 2001; Liu et al., 2016; Zeng et al., 2001). Once it has undergone these post-translational modifications it can be used in intercellular signalling.

When there is an absence of the fully post-translationally modified Shh ligand, the co-receptor, Smoothened, which is located at the cell surface of the target cell, is kept in an

inactive form by the transmembrane receptor protein, Patched, and regulating the activity of the downstream transcription factors Gli1, Gli2, and Gli3. With no ligand present, Gli1 will be phosphorylated, targeting it for degradation, and Gli2 and Gli3 will be proteolyzed to produce their repressor forms by the glycogen synthase kinase (GSK3), tyrosine-protein kinase (CSK) and protein kinase A (PKA) complex preventing upregulation of Shh target genes.

However, when the fully post-translationally modified Shh ligand is present and bound to Patched, Smoothened is no longer negatively regulated by Patched. This allows Smoothened to locate to the cilium thereby allowing Gli1 and Gli2 to be processed into their activator conformations. Therefore, the Gli1 and Gli2, in their transcriptional activator forms, are then able to translocate to the nucleus where they up regulate Gli-responsive target genes by outcompeting the Gli3 repressor (**Fig. 4**).

Two of the most effective small molecular reagents that are used to either pharmacologically activate or inhibit the Shh signalling pathway are purmorphamine and cyclopamine, respectively (Chen et al., 2002; Sinha and Chen, 2006). Purmorphamine, the Shh signalling activator, has been shown to activate Shh signalling by directly targeting the heptahelical bundle of Smoothened causing a conformational change that results in Smoothened remaining in its active form even in the absence of the Shh ligand (Sinha and Chen, 2006). Consequently, Smoothened retains its active conformation and Gli3 repressor is marked for degradation while, Gli1 and Gli2 are no longer marked for degradation allowing them to translocate to the nucleus where they upregulate Shh target genes leading to the pathway being constitutively active.

Cyclopamine is a well-established Shh signalling inhibitor (Chen et al., 2002). Cyclopamine inhibits the Shh signalling pathway by directly binding to the heptahelical bundle of the co-receptor, Smoothened, consequentially causing a conformational change of Smoothened (Chen et al., 2002). This conformational change results in Smoothened remaining in its inactive form even when the Shh ligand is bound to Patched (Chen et al., 2002). Since Smoothened is restricted to its inactive conformation, the Gli1 activators are phosphorylated, priming them for degradation, while, Gli2 and Gli3 transcription factors are modified to become repressors. As repressors, Gli2 and Gli3 translocate to the nucleus

where the transcription factors repress Shh target genes leading to the inhibition of the Shh signalling pathway.
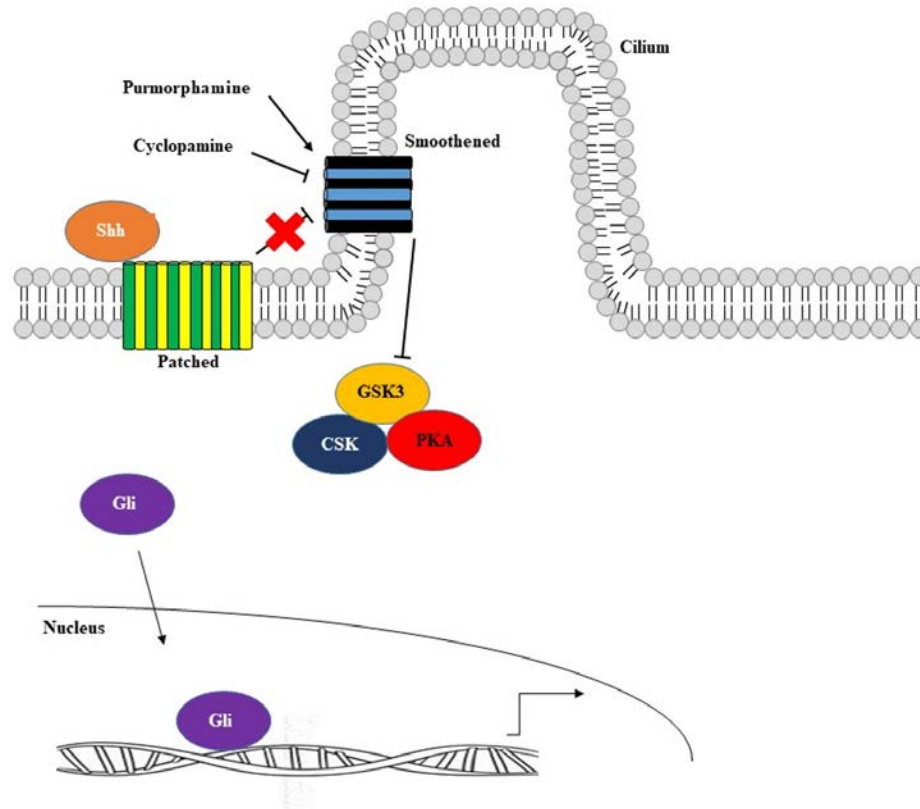
Figure 4. The Shh signalling pathway. The Shh signalling pathway is initiated when the Shh ligand binds to the transmembrane receptor, Patched. As a result of this interaction, Patched which is localized near the base of the cilium exits and Smoothened now migrates into the cilium. Since Smoothened is now present in the cilium, Smoothened's activity is no longer inhibited and it can now prevent the Gli proteins from being degraded or converted into repressors by the GSK3, CSK and PKA complex. Therefore, the Gli proteins can act as activators and then translocate to the nucleus where they upregulate Gli-responsive target genes. Purmorphamine is a small molecule activator of the Shh signalling pathway which results in the constrictive upregulation of Shh target genes. Conversely, cyclopamine is used as a small molecule inhibitor of the Shh signalling pathway and when administered it causes inhibition of the Shh signalling pathway even in the presence of the Shh ligand.

1.5 Bmp4 signalling

Bone morphogenetic proteins (Bmps) are a group of signalling molecules that are a part of the Transforming Growth Factor-β (TGF- β) superfamily of secreted proteins. Bone morphogenetic protein 4 (Bmp4) is highly conserved among vertebrates and plays crucial roles in embryogenesis and maintenance of adult tissue homeostasis (Bei and Maas, 1998; Qian et al., 2013; Timmer et al., 2002). Bmp4 is particularly well known for its role as the dorsal signal during the dorsoventral patterning of the neural tube in vertebrates (Timmer et al., 2002). Bmp4 also regulates dorsoventral patterning of somite derivatives and anteroposterior patterning of the limbs (Beck et al., 2001; Drossopoulou et al., 2000; Schmidt et al., 1995).

Bmp4 signalling is first initiated when the Bmp4 ligand binds to the Bmp type I receptors ALK2, ALK3, and ALK6 and type II serine/threonine kinase heterodimeric receptors causing the type II receptor to transphosphorylate the type I receptor. This in turn leads to the phosphorylation of the receptor-regulated Smad 1/5/8 intracellular proteins which then form a complex with Smad 4 protein, a common-mediator. The Smad 1/5/8 – Smad 4 complex then translocates to the nucleus where the complex upregulates Bmp4 target genes (**Fig. 5**).

Several small molecular reagents have been identified that can broadly and selectively inhibit the Bmp pathways. One common broad inhibitor of the Bmp pathways is dorsomorphin although it is also known to inhibit 5' AMP-activated protein kinase signalling (Gao et al., 2008; Yu et al., 2008). A more commonly used specific inhibitor of the Bmp4 pathway is Dorsomorphin Homolog 1 (DMH1) (Hao et al., 2010, 2014). Dorsomorphin blocks the Bmp signalling pathway by preventing phosphorylation of the BMP type I receptors by the Bmp type II receptor while DHM1 inhibits the Bmp4 signalling pathway by binding to the intracellular kinase domain of the Bmp type I receptor (Hao et al., 2010, 2014; Yu et al., 2008). Therefore, following treatment with Dorsomorphin or DMH1, Smad 1/5/8 proteins are no longer able to be phosphorylated and thus cannot form a complex with Smad 4 protein in order to translocate to the nucleus to upregulate Bmp target genes.
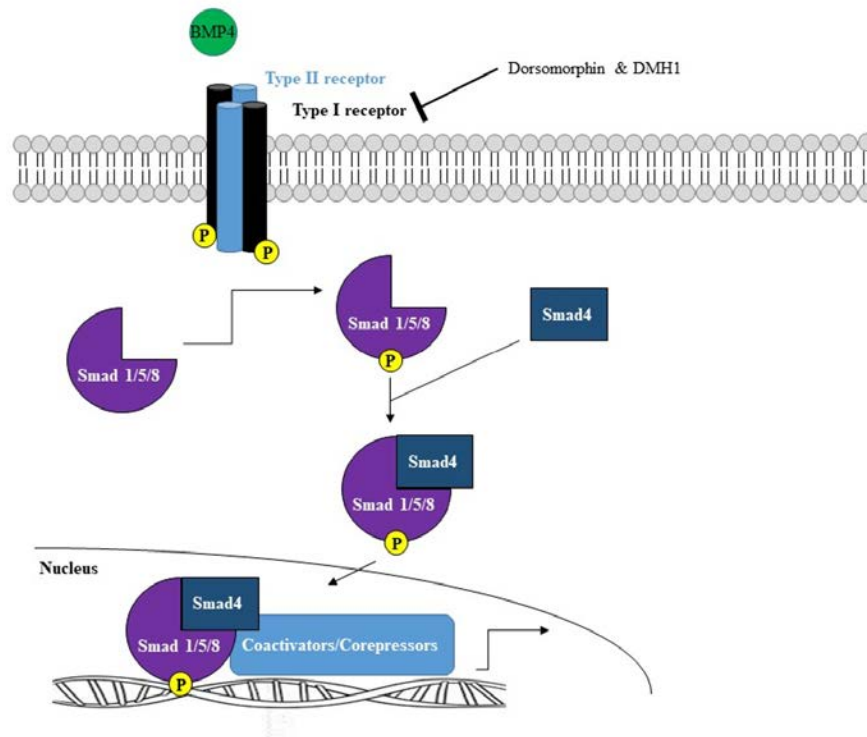
Figure 5. Bmp4 signalling pathway. The Bmp4 signalling pathway is initiated when a Bmp4 ligand binds to the Bmp type I and II heterodimeric receptors resulting in the phosphorylation of the Bmp type I receptor. This phosphorylation event leads to the phosphorylation of Smad 1/5/8 which then is able to form a complex with a Smad 4 protein. This Smad complex then translocates to the nucleus where it upregulates Bmp4 target genes. Two small molecular reagents that are used to inhibit the Bmp signalling pathway are dorsomorphin and DMH1.

1.6 Regional dorsoventral pattern within the developing pharyngeal complex

In order to understand dorsoventral patterning, I have examined the expression of genes that have regional expression within the developing pharyngeal complex. I have roughly divided the expression domains into three regions based on their expression along the dorsoventral axis: ventral, intermediate and dorsal expression domains. The expression domains are visualized using whole-mount *in situ* hybridization. All of the genes used as regional markers encode transcription factors that are critical in the development of structures originating from the pharyngeal region such as the thyroid, bones of the ear, and cartilage of the head and pharynx (Berge et al., 1998; Firulli et al., 2014; Günther et al., 2000; Jeong et al., 2008; Liu et al., 2007; Manley and Capecchi, 1998; Su et al., 2001).

1.6.1 Ventral pharyngeal region marker

The transcription factor whose expression profile was chosen as the ventral developing pharyngeal marker was *hand1*. Expression of *hand1* is initiated following gastrulation at the end of stage 12 (Session et al., 2016). Following stage 12, *hand1* is expressed in the cardiac progenitor cells, lateral plate mesoderm, and the developing pharyngeal region (Angelo et al., 2000; Deimling and Drysdale, 2009, 2011). Specifically, with respect to the pharyngeal region at stage 35, *hand1* is expressed in the ventral region of the developing pharyngeal complex between the posterior of the cement gland and the posterior of the developing pharyngeal complex (**Fig. 6F**). Along the dorsoventral axis *hand1* expression begins at the most ventral edge of the developing pharyngeal complex and extends roughly 1.4 µm ventrally. The expression profile of *hand1* has also been used to investigate whether retinoic acid (RA) signalling regulates the anteroposterior patterning of the lateral plate mesoderm (Deimling and Drysdale, 2009). More specifically, *hand1* expression was used as a marker of the anterior-middle domain of the lateral plate mesoderm (Collop et al., 2006; Deimling and Drysdale, 2009).

Hand1 is not only important as a marker of the developing ventral pharyngeal region but also could be a possible downstream regulator of the dorsoventral patterning of the developing pharyngeal region. *Hand1* is a basic helix-loop-helix transcription factor, and its expression was first characterized in *X. laevis* as a regulator of cardiovascular development (Sparrow et al., 1998). *Hand1*-null mouse embryos present with defects in

placentation and the linear heart tube fails to loop in the correct direction resulting in either a linear heart tube at the midline or slight looping to the right then left (Riley et al., 1998). If the placentation defects are rescued, the embryos still die from cardiovascular defects (Riley et al., 1998). Not only is *hand1* a vital transcription factor in the initial morphogenesis of the heart, but it also plays an essential role in ventricular myocyte differentiation and expression of a subset of cardiac genes (Smart et al., 2002).

Hand1 also plays a role in the development of other lineages including the lung and trachea along the anteroposterior axis of the developing embryo (Fernandez-Teran et al., 2003; Hoyos et al., 2016; Rankin et al., 2016). Here *hand1* expression is restricted to the heart, pharyngeal mesenchyme, and the posterior lateral plate mesoderm, but lacking expression in the foregut lateral plate mesoderm region (Rankin et al., 2016). This *hand1* expression which outlines the presumptive lung field is crucial for later development of the lung demonstrating one of many key roles the *hand1* transcription factor plays during embryonic development (Rankin et al., 2016).

The *hand1* gene is of particular interest to this study because *hand1* is expressed in the developing ventral pharyngeal region and has been demonstrated to be necessary for proper morphogenesis (Firulli et al., 2014). I found that not only is *hand1* expression regulated by Shh and Bmp4 signalling during the dorsoventral patterning of the developing pharyngeal region, but I hypothesize that *hand1* is itself is a regulator of the pattern.

1.6.2 Intermediate pharyngeal region markers

The expression domain of the transcription factors g*cm2* and *pax1* were chosen as markers of the intermediate developing pharyngeal region. This is the region where the gill slits will eventually open to the pharyngeal cavity. *Gcm2* is a master regulator of the parathyroid which is derived from endoderm of the pharyngeal region (Correa et al., 2002; Kebebew et al., 2004). *Gcm2* has been demonstrated to be necessary for proper parathyroid gland development, expression of the parathyroid hormone, and proper expression prevents conditions like hyperparathyroidism (Correa et al., 2002; Günther et al., 2000; Liu et al., 2007). Detection of *gcm2* mRNA begins in the oocyte and is observed until stage 12 at which point the expression becomes barely detectable until stages 29-30 when its expression returns. The expression of *gcm2* is solely restricted to the intermediate region

of the second, third, and fourth pharyngeal arches of the developing pharyngeal region at stage 35 (Lee et al., 2013) (**Fig. 6D**).

The second RNA chosen as a marker for the intermediate region of the developing pharyngeal complex was *pax1*. The *pax1* gene encodes a transcription factor that plays important roles during embryonic development. With respect to the developing pharyngeal complex, it is crucial for the proper development of the parathyroid glands and for complete separation of the pharyngeal pouch (Su et al., 2001). During *X. laevis* development *pax1* is expressed between stages 22 and 38 where it is constrained to the pharyngeal and the perinotochordal regions of the embryo (Gray et al., 2009; Sánchez and Sánchez, 2013, 2015). Within the developing pharyngeal region at stage 35, *pax1* expression is restricted to the first five pharyngeal arches (**Fig. 6E**).

1.6.3 Dorsal pharyngeal region markers

The expression domains that were used to mark the developing dorsal pharyngeal region were those of *hoxa3*, and *prrx2*, and *pou3f3*. The *hoxa3* gene encodes a transcription factor and is part of the A cluster of homeobox genes on chromosome 7 which are known to be regulators of patterning during embryonic development (Chojnowski et al., 2016; Manley and Capecchi, 1998). Proper expression of *hoxa3* is crucial for many craniofacial derivatives of the developing pharyngeal region such as cranial nerves, throat cartilage, thyroid and the parathyroid glands (Chojnowski et al., 2016; Manley and Capecchi, 1998). The expression of *hoxa3* is detectable from the end of gastrulation at stage 12 and continues beyond stage 40 (Session et al., 2016). Expression of *hoxa3* is observed in several regions including the hindbrain, spinal cord, and developing pharyngeal region (McNulty et al., 2005; Square et al., 2015). At stage 35 when the developing pharyngeal region can be observed on either side of the head region of the embryo, the *hoxa3* expression is restricted to the pharyngeal tissue which surrounds the third and fourth pharyngeal arches (**Fig. 6A**).

The transcription factor, *prrx2*, is crucial for proper development of select facial bones and if misexpressed, can lead to severe craniofacial malformations (Berge et al., 1998). Within the developing pharyngeal region its expression is necessary for the proper development of the mandibular processes, dentaries and the nasal cavity (Balic et al., 2009; Berge et al., 1998). There is maternal mRNA for *prrx2* in the oocyte, however, expression

is low and *prrx2* expression does not become prominent until stage 20 and declines to low levels again by stage 40 (Session et al., 2016). Throughout, these developmental stages *prrx2* expression can be detected in the head region, mouth primordium and the developing pharyngeal region (Square et al., 2015). With respect to the developing pharyngeal region and this study at stage 35, *prrx2* expression is found just posterior to the cement gland extending to the posterior of the developing pharyngeal region. Though the *prrx2* expression can be observed in the ventral and dorsal regions of the developing pharyngeal complex, no expression is present in the intermediate region (**Fig. 6B**). The dorsal expression domain of *prrx2* is the focus of this thesis when comparing the expression domain between control embryosand embryos in which signaling was altered or *hand1* expression knocked-down.

The last gene whose expression is used in this thesis as a marker for the dorsal region of the developing pharyngeal complex was *pou3f3*. The transcription factor, *pou3f3*, is a member of the POU domain family of genes which have been implicated in many development processes, however, *pou3f3* expression has been specifically demonstrated to be crucial for proper development of pharyngeal derivatives such as squamosal bone, jugal bone, and if it is lost, there is failure of the stapes to detach from the styloid process (Cosse-Etchepare et al., 2018; Jeong et al., 2008; Ryan and Rosenfeld, 1997). In *Xenopus,* its mRNA is first detected at stage 8. After stage 12, *pou3f3* is once again expressed until stage 40 where the expression returns to levels similar to those at stage 8 (Session et al., 2016). Throughout stages 12 to 40 *pou3f3* expression is mainly localized to the anterior region of the embryo including the anterior neural fold, fore- and hindbrain, and the developing pharyngeal region (Cosse-Etchepare et al., 2018; Square et al., 2015). Expression of *pou3f3* in that area of the developing embryo is localized to the dorsal region of the first, and second pharyngeal arches at stage 35 (**Fig. 6C**) (Square et al., 2015).
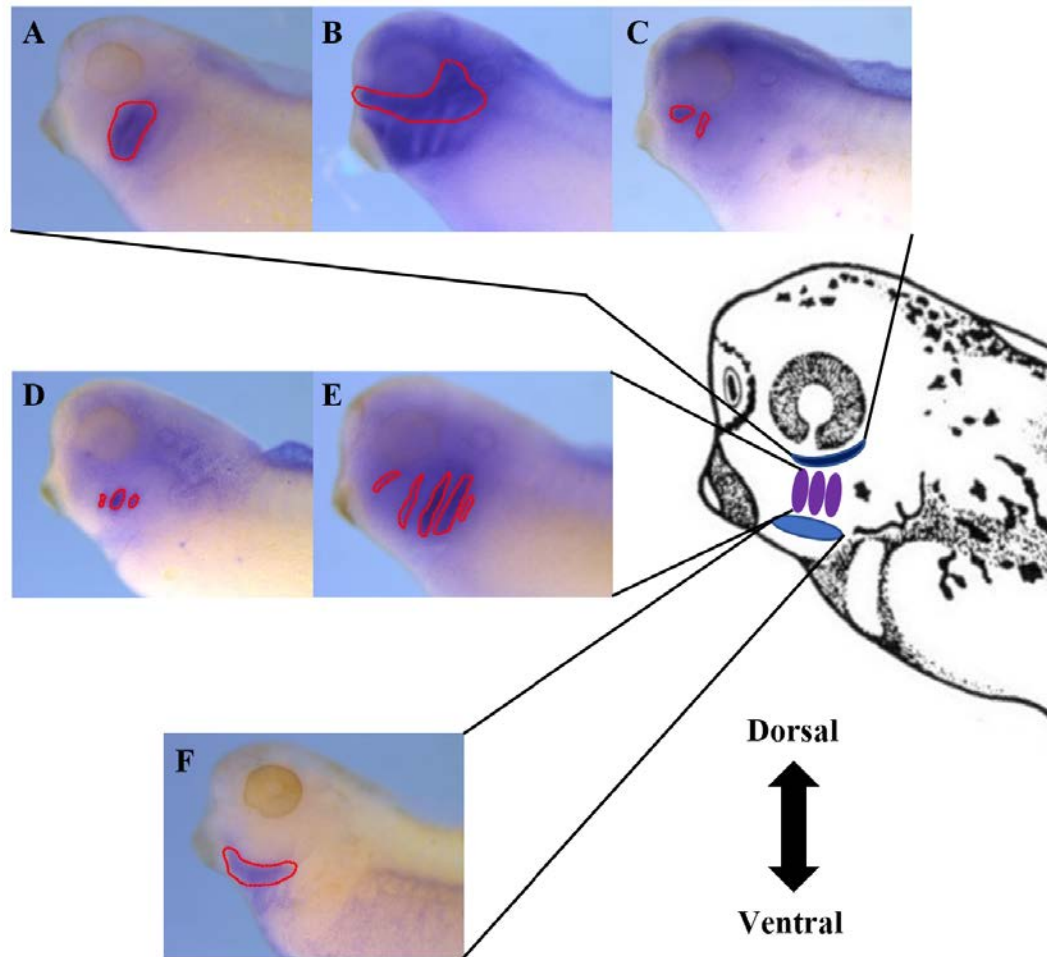
Figure 6. Diagram displaying the expression domains of the markers of ventral, intermediate and dorsal regions of the developing pharyngeal complex. The mRNA expression profiles used as markers for the dorsal region of the developing pharyngeal complex were *hoxa3* (**A**), *prrx2* (**B**), and *pou3f3* (**C**). The mRNA expression profiles used as markers for the intermediate region were *gcm2* (**D**), and *pax1* (**E**). The mRNA expression profile used as a marker for the ventral region was *hand1* (**F**).

1.7   CRISPR/Cas9 Genome Editing

Over the past ten years one approach to modifying the genome that has gained tremendous popularity is CRISPR/Cas9 genome editing technology. Instead of using morpholinos to knock-down gene expression, many laboratories are now using CRISPR/Cas9 to cause mutations in genes which in turn result in the knocking-down of their expression (Tandon et al., 2017). The two key molecules that cause the mutations in the gene of interest are the Cas9 enzyme, and a portion of RNA called the guide RNA (gRNA). The enzyme and gRNA work together as a complex inside the cell's nucleus where the complex searches along the DNA for small sequences called protospacer adjacent motifs (PAM) sites (Pickar-Oliver and Gersbach, 2019). These PAM sites allow the Cas-9 enzyme to grip the DNA resulting in its destabilization leading to the unzipping of the double-stranded helix (Pickar-Oliver and Gersbach, 2019). Following, the opening of the DNA, the gRNA moves along the DNA searching for the complementary sequence (Pickar-Oliver and Gersbach, 2019). Once the complementary sequence is found the gRNA activates the Cas-9 enzyme which in turn cleaves the DNA into two separate pieces (Pickar-Oliver and Gersbach, 2019). The double-stranded break is repaired by non-homologous end-joining which is an error-prone repair mechanism that introduces insertions or deletions at the site of the break (Pickar-Oliver and Gersbach, 2019). One of the possible outcomes of the insertions or deletions is a frameshift mutation leading to a premature stop codon resulting in a non-functional gene (Pickar-Oliver and Gersbach, 2019).

Using CRISPR-Cas9 genome editing technology in the model system, *X. laevis* offers a few more challenges than to researchers working with other models of development such as mice or human cells. This is because *X. laevis* are tetraploid meaning that they carry two complete genomes. The two sets can be differentiated based on small differences in chromosome size and so one set has been designated long and the other short (Session et al., 2016). Although there has been some evolutionary loss of one copy of many genes, for the majority of the genes there are essentially four functional copies (Session et al., 2016). Therefore, when attempting to knock-down genes in *X. laevis* multiple gRNAs may have to be injected in order to target both the long and short genes

(Yang et al., 2013). Nevertheless, CRISPR/Cas9 technology is able to efficiently mutate both sets of genes without any clear toxic effects (Bhattacharya et al., 2015; Blitz et al., 2013; DeLay et al., 2018). CRISPR/Cas9 genome editing will be the method used to mutate *hand1* to test the hypothesis that the *hand1* gene regulates the dorsoventral pattern of the developing pharyngeal region downstream of Shh and Bmp4 signalling.
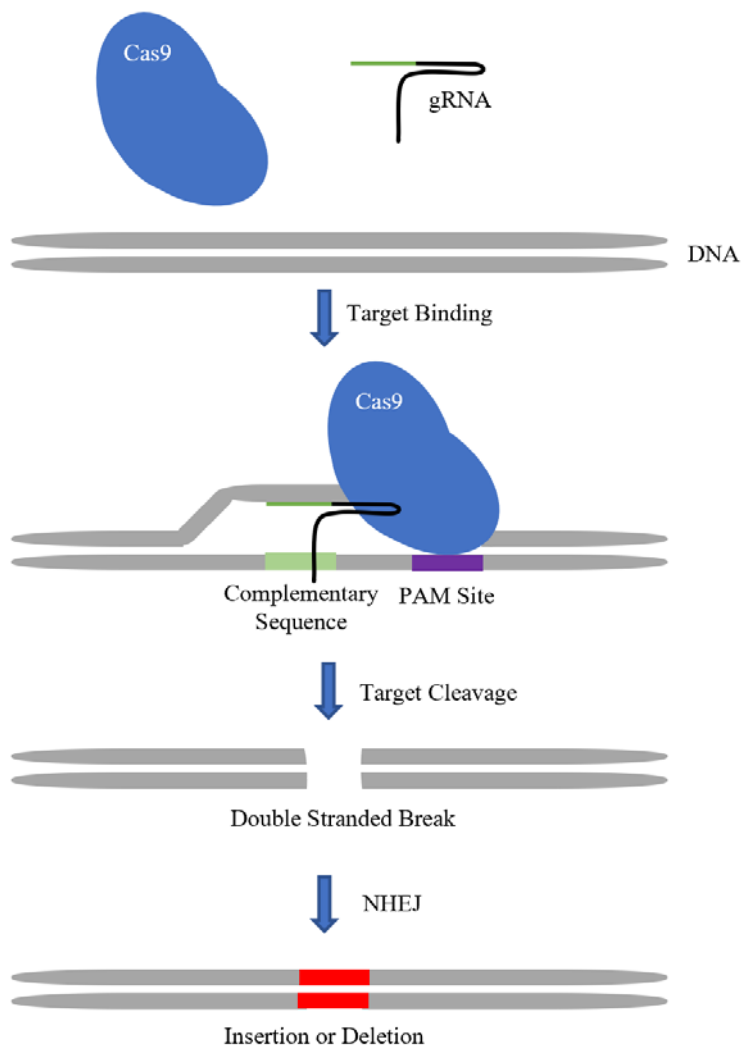
Figure 7. Diagram depicting how CRISPR/Cas9 genome editing technology introduces an insertion or deletion into the gene of interest. The enzyme and gRNA work together as a complex searching along the DNA for small sequences called protospacer adjacent motifs (PAM) sites. These PAM sites allow the Cas9 enzyme to grip the DNA resulting in its destabilization leading to the unzipping of the double-stranded helix. The gRNA then searches for the complementary sequence. Once the complementary sequence is found the gRNA activates the Cas9 enzyme which in turn creates a double stranded break. The break is repaired by non-homologous end-joining which is an error-prone repair mechanism that introduces an insertion or deletion at the site of the break. The insertion or deletions may cause a coding frameshift leading to the knock-down of the gene of interest.

1.8 Purpose of the research

The purpose of this study is to discover underlying signalling mechanisms that regulate the dorsoventral patterning of the developing pharyngeal region in *X. laevis*. I utilized information from previous studies that have demonstrated clear patterns of gene expression along the dorsoventral axis in the developing pharyngeal region. Based on the observation that Shh is located dorsal to the developing pharyngeal region, while Bmp4 is located ventral to the developing pharyngeal region, there is the potential for a counter gradient role for these molecules in the dorsoventral patterning of the pharyngeal complex, similar to the known patterning described for the neural tube (Barnett et al., 2012; Le Dréau and Martí, 2012; Rankin et al., 2012; Square et al., 2015). Therefore, *I hypothesize that the correct dorsoventral gene expression pattern observed in the developing pharynx is regulated by opposing gradients of Shh and Bmp4 signalling.* This thesis will investigate whether Shh and Bmp4 provide positional information to cells found along the dorsoventral axis so that the cells can activate and/or repress specific transcription factors known to be involved in craniofacial development. Small molecule reagents were used to alter the signalling pathways in embryos prior to the pharyngeal patterning. I predict that activating Shh signalling by exposing the embryos to purmorphamine will result in a ventral shift of the mRNA expression profiles (**Fig. 8**). In contrast, I predict that exposing embryos to cyclopamine, thereby inhibiting Shh signalling, will cause a dorsal shift in the mRNA expression domains in the three regions of the developing pharyngeal complex (**Fig. 9**). Similarly, in purmorphamine treated embryos, I predict a ventral shift of the mRNA expression domains in the three regions of the developing pharyngeal complex when exposed to the Bmp inhibitors dorsomorphin and DMH1 (**Fig. 10**). Finally, a second hypothesis is that *hand1 regulates the dorsoventral patterning of the developing pharyngeal region.* This is due to the ventrally restricted localization of *hand1* mRNA in the developing pharyngeal region and Shh signaling and the *hand* genes have been demonstrated to cooperatively regulate embryonic morphogenetic events (Firulli et al., 2017; Rankin et al., 2016; Riley et al., 1998). I predict that when the *hand1* gene is mutated, the mRNA expression profiles in the intermediate and dorsal regions will be shifted dorsally (**Fig. 11**). These findings will provide new information on how the developing

pharyngeal region is patterned and could be later used to predict the origin of defects in craniofacial development.
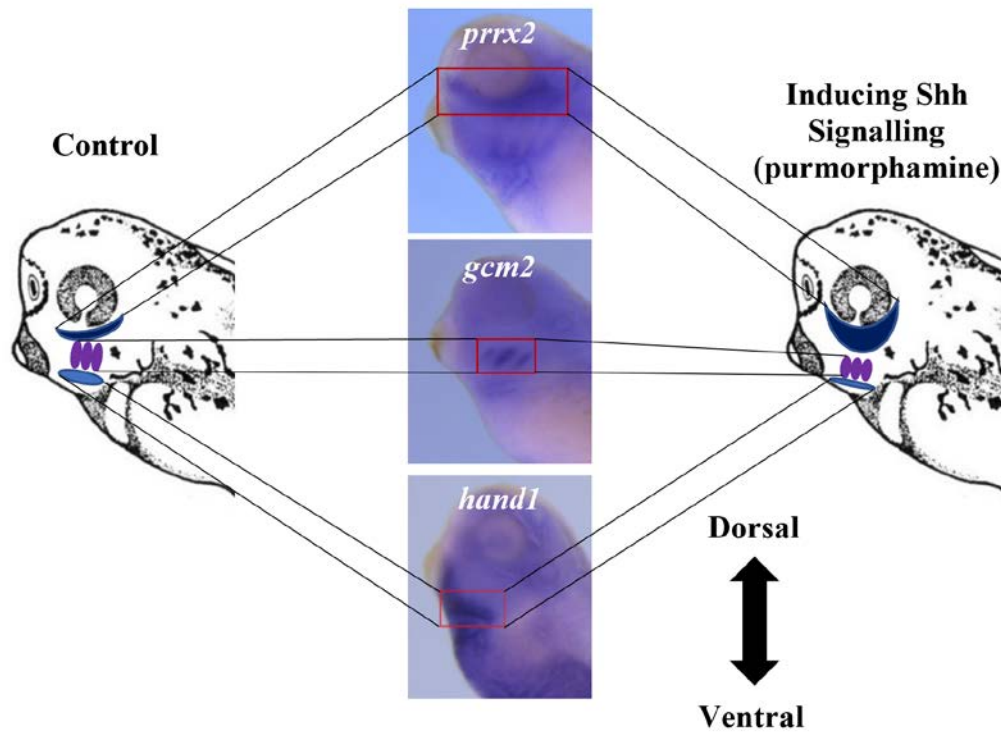
Figure 8. Diagram depicting the prediction of the change in the mRNA localization when inducing Shh signalling by exposing the *X. laevis* embryos to purmorphamine. On the left side of the diagram is a *X. laevis* head and neck region with the light blue, purple and dark blue coloured areas marking the ventral, intermediate and dorsal regions of the developing pharyngeal complex, respectively. The three centre images are *X. laevis* embryos stained for *hand1, gcm2*, and *prrx2* which are markers for the ventral, intermediate and dorsal regions, respectively. On the right side is a diagram predicting the ventral shift of the markers of the three regions when inducing Shh signalling through the exposure of the embryos to purmorphamine.
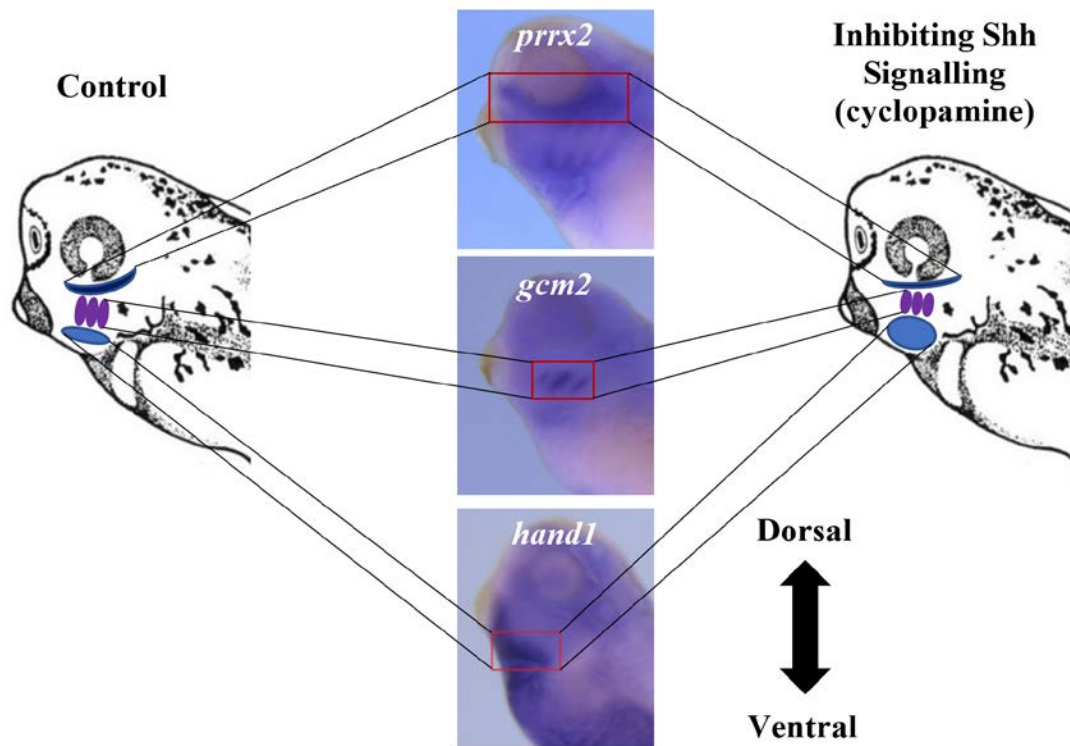
Figure 9. Diagram depicting the predictions of the change in the mRNA localization following cyclopamine inhibition of Shh. On the left side of the diagram is a *X. laevis* head and neck region with the light blue, purple and dark blue coloured areas marking the ventral, intermediate and dorsal regions of the developing pharyngeal complex, respectively. The three centre images are *X. laevis* embryos stained for *hand1, gcm2*, and *prrx2* which are markers for the ventral, intermediate and dorsal regions, respectively. On the right side is a diagram predicting the dorsal shift of the markers of the three regions when inhibiting Shh signalling through the exposure of the embryos to cyclopamine.
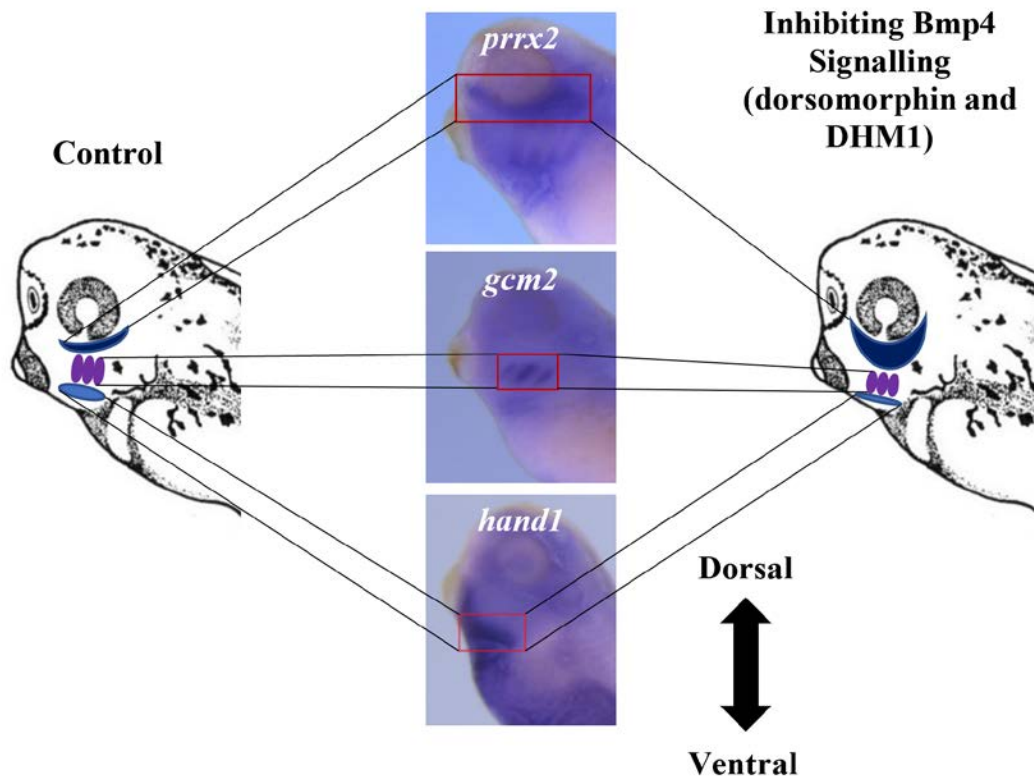
Figure 10. Diagram depicting the predictions of the change in the mRNA localization when inhibiting Bmp4 signalling by exposing the *X. laevis* embryos to dorsomorphin and DMH1. On the left side of the diagram is a *X. laevis* head and neck region with the light blue, purple and dark blue coloured areas marking the ventral, intermediate and dorsal regions of the developing pharyngeal complex, respectively. The three centre images are *X. laevis* embryos stained for *hand1, gcm2*, and *prrx2* which are markers for the ventral, intermediate and dorsal regions, respectively. On the right side is a diagram predicting the ventral shift of the markers of the three regions when inhibiting Bmp4 signalling through the exposure of the embryos to dorsomorphin and DMH1.
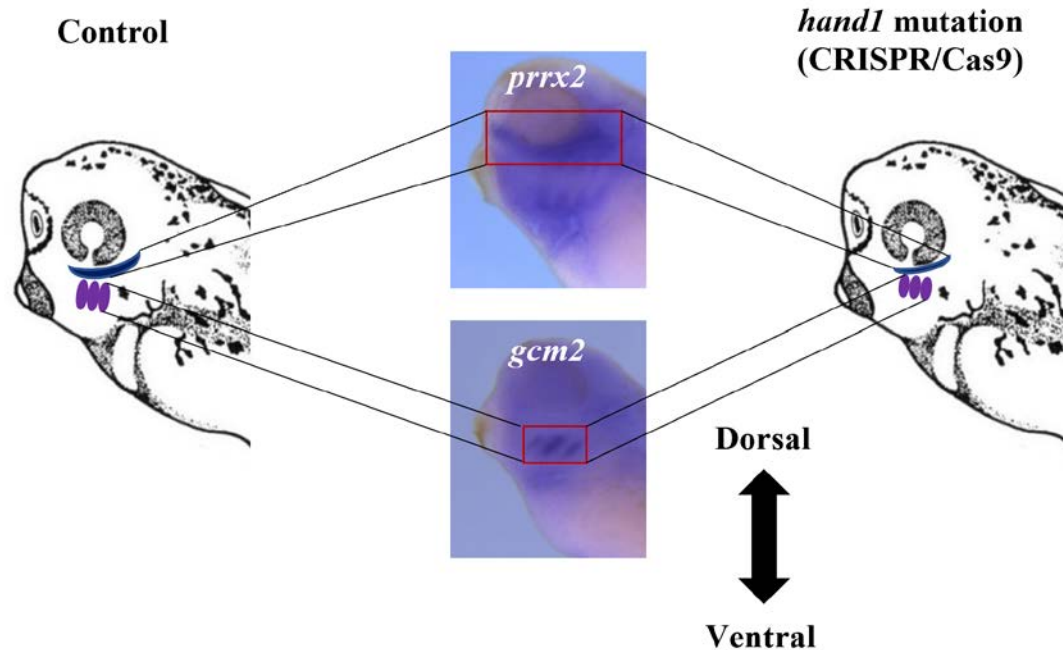
Figure 11. Diagram depicting the predictions of the change in the mRNA localization after *hand1* mutation by CRISPR/Cas9 technology. On the left side of the diagram is a *X. laevis* head and neck region with the purple, and dark blue coloured areas marking the intermediate, and dorsal regions of the developing pharyngeal complex, respectively. The two centre images are *X. laevis* embryos stained for *gcm2*, and *prrx2* which are markers for the intermediate, and dorsal regions, respectively. On the right side is a diagram predicting the dorsal shift of the markers of the intermediate and dorsal regions when mutating the *hand1* gene by use of CRISPR/Cas9 genome editing technology.

Chapter 2: Materials and Methods

2.1 Generation of *X. laevis* embryos

In order to induce ovulation, female *X. laevis* were injected with 800 IU of human chorionic gonadotrophin (Intravet) the night before eggs were to be fertilized. Male *X. laevis* were sacrificed, and testes were removed and stored in 200% Steinberg's solution. All Steinberg's solutions were prepared from Steinberg's stock solution A (68g NaCl, 1g KCl, 4.09g MgSO$_4$-7H$_2$O, 1.58g Ca(NO$_3$)$_2$-4H$_2$O) and Steinberg's stock solution B (11.2g Tris-HCl pH 7.4). Eggs were squeezed from the females into 80% Steinberg's solution and *in vitro* fertilization was accomplished using minced testes. Embryos were de-jellied at stage 4 with 2.5% cysteine (pH 8.0) and washed several times with 20% Steinberg's solution to remove excess 2.5% cysteine. Embryos were staged according to the Nieuwkoop and Faber staging (**Appendix**) (P.D. Nieuwkoop and J. Faber, 1994). All embryos were cultured in 3 mL of 20% Steinberg's solution at 18ºC.

2.2 Shh activator and inhibitor

Cyclopamine and purmorphamine (Toronto Research Chemicals) were prepared as 20 mM and 10 mM stock solutions in 95% ethanol and DMSO, respectively, and stored at -20ºC. Based on research by Lewis and Krieg (2014) that determined effective concentrations for *Xenopus* embryos, I treated stage 13 embryos with 100 μM cyclopamine or 20 μM purmorphamine. Control embryos were treated with either 15 μL of 95% ethanol or 3 μL of DMSO in 3 mL of 20% Steinberg's solution. Embryos were continuously exposed to cyclopamine or purmorphamine from stage 13 until stage 35 when they were fixed for whole-mount *in situ* hybridization. The embryos were treated starting at stage 13 (**Appendix**) to avoid interfering with gastrulation and were fixed at stage 35 (**Appendix**) since this is the optimal stage to view the developing pharyngeal region.

2.3 Bmp4 inhibitors

In order to inhibit Bmp signalling, embryos were treated with 40 μM DMH1 (Adooq Bioscience) (Rankin et al., 2015) or 10 μM dorsomorphin (Fisher Scientific) (Pieper et al., 2012; Yu et al., 2008). DMH1 and dorsomorphin were both prepared as 40 mM stock

solutions in DMSO and stored at 4ºC. The control treatments were 3 µL of DMSO in 3mL of 20% Steinberg's solution. DMH1 and dorsomorphin was added to the culture media containing the embryos at stage 13 and continued until stage 35 when the embryos were fixed for whole-mount *in situ* hybridization.

2.4 Embryo fixation

Embryos used for whole-mount *in situ* hybridization were fixed at stage 35 in MEMPFA (4% paraformaldehyde, 2 mM EGTA (ethylene glycol tetraacetic acid), 0.1 mM MOPS (3-(N-morpholino) propanesulfonic acid), 1mM $MgSO_4$, pH 8.0) and placed in a nutator (LabQuake) for two hours. After the MEMPFA fixation, embryos were transferred into 100% methanol at -20ºC until processing for *in situ* hybridization.

2.5 Plasmid transformations to prepare probes

DH5α *Escherichia coli* bacteria were used as competent cells in the plasmid transformations. For transformations, approximately 100 ng of plasmid DNA was added to 50 µL of competent cells, and the solution was then placed on ice for thirty minutes. The bacteria-DNA mixture was then placed on a 42ºC heating block for sixty seconds and then returned to ice for five minutes. Following the ice treatment, 1 mL of Luria's broth (LB) was added to the mixture and placed in the 37ºC shaking incubator for one hour. The whole LB and competent cell-plasmid solution were plated on LB plates (5 g bacto-tryptone, 2.5 g bacto-yeast extract, 5 g NaCl, 7.5 g bacto-agar for 500 mL) containing ampicillin (50 mg/mL) and incubated overnight at 37ºC. Colonies were then picked using a tungsten loop tool and suspended in 5 mL of LB and 100 mg/mL ampicillin in a culture tube. The mixture was then placed in the 37ºC incubator and shaken at 225 rpm overnight. Following the incubation, the plasmids were isolated and purified using the QIAprep® Spin Miniprep kit (QIAGEN) according to the manufacturer's instructions.

2.6 Restriction digest to prepare probes

The restriction digests were performed in a 1.5 ml Eppendorf tube using 10 µg of isolated and purified DNA, 1 µl of the appropriate restriction enzyme (**Table 1**), 5 µl of the appropriate buffer solution and brought to a total volume of 50 µl using dH_2O. The tubes were then placed in a 37ºC incubator for three hours. Following the incubation, 50 µl of

dH_2O was added to produce a total volume of 100 μl. A 1:1 volume of phenol/chloroform isopropanol was added and vortexed. The solution was then centrifuged at 14,000 rpm for three minutes. The aqueous layer was removed and placed in a fresh 1.5 ml Eppendorf tube and purified by adding 1/10th volume of ammonium acetate (3M) and 2:1 volumes of 100% ethanol. The tubes were placed in the -20ºC freezer for thirty minutes and then centrifuged at 14,000 rpm for fifteen minutes. Following the centrifugation, the supernatants were removed, and the DNA pellet was air dried, washed with 70% ethanol and then centrifuged again at 14,000 rpm for ten minutes. Following the centrifugation, the ethanol was removed, and the DNA was left to air dry. The pellet was then resuspended in 15 μl of dH_2O, and 1 μl was then run on a 1% gel and visualized under a UV transilluminator.

Table 1. List of the antisense RNA probes used for marking the ventral, intermediate and dorsal regions of the pharyngeal complex. Accompanying the names of the cDNA are the vector backbone inserted into, restriction enzymes used to digest the plasmid DNA, the RNA polymerase to synthesize the probe and from whom the cDNA was obtained from.

cDNA	Vector	Restriction Enzyme	RNA Polymerase	Source Reference
hand1	pBluescript SK +	BamHI	T7	(Sparrow et al., 1998)
gcm2	pBluescript SK +	NotI	T7	Unpublished (Kevin Fan and Taisaku Nogi)
pax1	pBluescript II SK(-)	NotI	T7	Dr. Ueno (Sánchez and Sánchez, 2013)
hoxa3	pSport6	SalI	T7	(Lee et al., 2013)
prrx2	pJet1.2	NotI	SP6	(Square et al., 2015)
pou3f3	pJet1.2	NotI	SP6	(Square et al., 2015)

2.7 Probe synthesis for *in situ* hybridization

Using the linearized DNA template, RNA was transcribed and labeled with Digoxygenin so that whole-mount *in situ* hybridizations could be performed to determine the localization of mRNA of interest. The antisense Digoxygenin-labeled probe synthesis was set up as follow: 1 – 2 μg of linearized template DNA, 4 μl of digoxygenin-labeled NTP mixture (2.5 mM CTP, 2.5 mM GTP, 2.5 mM ATP, 1.625 mM UTP and 0.875 mM Dig-11-UTP (Roche), 0.5 μl of RNase inhibitor (Invitrogen), 2 μl of transcription buffer (Invitrogen), 2 μl of appropriate RNA polymerase and brought to a total volume of 20 μl with dH_2O (see **Table 1 for PCR conditions**). The transcription reactions were incubated for two hours at 37°C followed by the addition of 1 μl of DNAse (Invitrogen) and incubated for another ten minutes at 37°C. After incubation 1 μl was removed to check on 1% agarose gels. To the remaining 19 μl, 80 μl of 1% SDS in TE buffer (10 mM Tris pH 8.0, 1 mL EDTA), 10 μl of ammonium acetate (5 M) and 220 μl of cold 100% ethanol were added. The mixture was then vortexed and set aside on ice until results of the RNA quality check were known. The remaining RNA probes that were set aside on ice were precipitated by centrifuging at 14,000 rpm for fifteen minutes and allowed to dry briefly. The RNA probes were then resuspended in 1 ml of RNA hybridization buffer and vortexed. The probes were then briefly heated to 37ºC and vortexed again. The probes were then transferred to a 15 ml polystyrene tube and brought to a total volume of 10 ml with RNA hybridization buffer.

2.8 Whole-mount *in situ* hybridization

Whole-mount *in situ* hybridization was performed as previously described by (Deimling et al., 2015). Embryos were contained in 3 ml glass vials (VWR) all steps were carried out on a nutator (LabQuake) and at room temperature unless noted. Embryos stored in 100% methanol were rehydrated in a series of methanol washes (75%, 50%, and 25%) and then washed with TTW buffer (Tris buffered saline: 50 mM Tris (pH 7.4), 200 mM NaCl, 0.1% Tween-20) three times for ten minutes each. Embryos were fixed in MEMPFA for 20 minutes and subsequently washed with TTW three times for five minutes each. Embryos were then washed with pre-warmed RNA hybridization buffer for ten minutes and once again at 65ºC for one hour. Probe, previously heated to 65ºC, was then added to the vials

and incubated at 65ºC overnight. The following day the probe(s) were removed and stored at -20ºC for further use and the embryos were incubated again at 65ºC for ten minutes in pre-warmed RNA hybridization buffer. The embryos were then subjected to two twenty-minute washes of 2 X SSC (from a 20 X SSC stock: 3 M NaCl, 0.3 M $Na_3C_6H_5O_7$, pH 7.0) at 37ºC followed by three one-hour washes of 0.2 X SSC at 65ºC. Embryos were then submerged in blocking solution (MAB (pH 7.5) (100 mM maleic acid, 150 mM NaCl), 2% blocking reagent (Roche) and 20% heat-treated sheep serum) and then in a blocking solution containing DIG-labelled antibodies (anti-Digoxygenin-AP, Fab Fragments; (Roche)) and incubated at 4ºC overnight. The next day the embryos were subjected to twelve thirty-minute washes of MAB. Embryos were stained by BM Purple (Roche, Indianapolis, IN) overnight. The following day the colourimetric reaction was fixed by dehydrating the embryos in a series of five methanol washes (25%, 50%, 75%, 100% and 100%) for five minutes each and then rehydrating the embryos in a series of methanol washes (75%, 50%, 25%) once again for five minutes each. Incubating the embryos in MEMPFA for thirty minutes further fixed the stain and was followed up by three five-minute washes of 25% methanol. The embryos were then bleached (5% formamide, 0.5 X SSC, 1% hydrogen peroxide) for four hours or until excess pigmentation was removed. After bleaching, embryos were then dehydrated in a series of five methanol washes (25%, 50%, 75%, 100%, and 100%) and stored at -20°C until images were ready to be taken.

2.9 Single guide RNA (sgRNA) of the *hand1* gene synthesis

The first step of synthesizing the *hand1* sgRNA was generation of template DNA through a PCR reaction, and the conditions are listed in **Table 2**. The sgRNA primer sequences used and the universal reverse primer sequence are listed in **Table 3**. The beginning of each sgRNA encodes a T7 promoter site followed by a specific target sequence followed by a universal reverse sequence. The universal reverse primer contained a universal reverse sequence and codes for the Cas9 association site. The *hand1l* and *hand1s* gene maps outlining the forward and reverse primer start sites, gRNA associated PAM sites and HLH domain are outlined in **Figure 12**. After completion of the PCR, the products were purified on a QIAGEN Quickspin PCR column according to

manufacturers' instructions. The quantity of the PCR product was calculated by Nanodrop, and the quality was checked on a 1% agarose gel containing EtBr.

   To generate the sgRNA for the *hand1* gene, an *in vitro* transcription was performed at 37ºC overnight using T7 RNA polymerase (Ambion Megascript Kit) in a total volume of 20 μl containing 300 ng of PCR product, 2 μl each of ATP, CTP, GTP and UTP, 2 μl 10 X reaction buffer and 2 μl T7 RNA polymerase. Following the incubation 1 μl of TurboDNase (Invitrogen) was added and incubated for another fifteen minutes. Next, the sgRNA was purified using GE Illustra Sephadex G-50 NICK columns. To prepare the columns for use, the columns were washed three times with 4 ml of TE Buffer (10 mM Tris (pH 8) 1 mM EDTA (pH 8)). Afterwards, 80 μl of TE Buffer was added to the sgRNA reaction and applied to the column. Once the column stopped dripping, the column was washed with 400 μl of TE buffer, and when the column stopped dripping again, the sgRNA was eluted by applying 400 μl of TE Buffer to the column. The sgRNA was collected in an Eppendorf tube containing 1 ml of 100% EtOH and 10 μl of NH_4 Acetate (Megascript Kit). The mixture was then inverted several times followed by an incubation at -20ºC for forty-five minutes and then at -80ºC for fifteen minutes. The tubes were then centrifuged in a microcentrifuge at 13,000 rpm for twenty minutes at 4ºC. The pellet was washed with 70% ethanol and air dried on the 55ºC heat block. The pellet was resuspended in 20 μl of dH_2O, followed by calculating the quantity using the spectrophotometer and the quality was checked by running on a 2% agarose and TAE gel containing EtBr. Once the quantity was known and quality was confirmed, the sgRNA was diluted to 1500 ng/μl and 10 μl aliquots were stored at -20ºC. Cas9 protein was received from PNA Bio Inc. (Thousand Oaks, CA) and resuspended in nuclease-free dH_2O and stored in aliquots at -20ºC.

Table 2. The sgRNA template synthesis PCR cycling conditions.

Temperature (°C)	Time (seconds)	Number of Cycles
98	30	1
98	10	
62	20	10
72	20	
98	10	
72	30	25
72	300	1
4	Hold	1

Table 3. Primer sequences for the synthesis of sgRNA. The beginning of each sgRNA matches to the T7 promoter site, the nucleotides underlined are the specific target sequences corresponding to a region of the *hand1* gene and the bolded nucleotides are universal primer sequences which anneal to both the target primers and the Cas9 association site located on the universal reverse primer. The remaining nucleotides (Bold) on the universal reverse primer are the Cas9 association site.

Primer Name	Sequence
sgT1	CAGCTAATACGACTCACTATA<u>GGAAGTAAGGTCTCTCCTGG</u>**GTTTTAGAGCTAGAAATAG**
sgT2	CAGCTAATACGACTCACTAT<u>AAGGGATCAGGCATCATGTCC</u>**GTTTTAGAGCTAGAAATAG**
sgT3	CAGCTAATACGACTCACTATA<u>AGGATGGGTGCTCAACCCTG</u>**GTTTTAGAGCTAGAAATAG**
Universal Reverse Primer	**CAAAATCTGATCTTTATC**GTTCAATTTTATTCCGATCAGGCAATAGTTGAACTTTTTCACCGTGGCTCAGCCACGAAAA
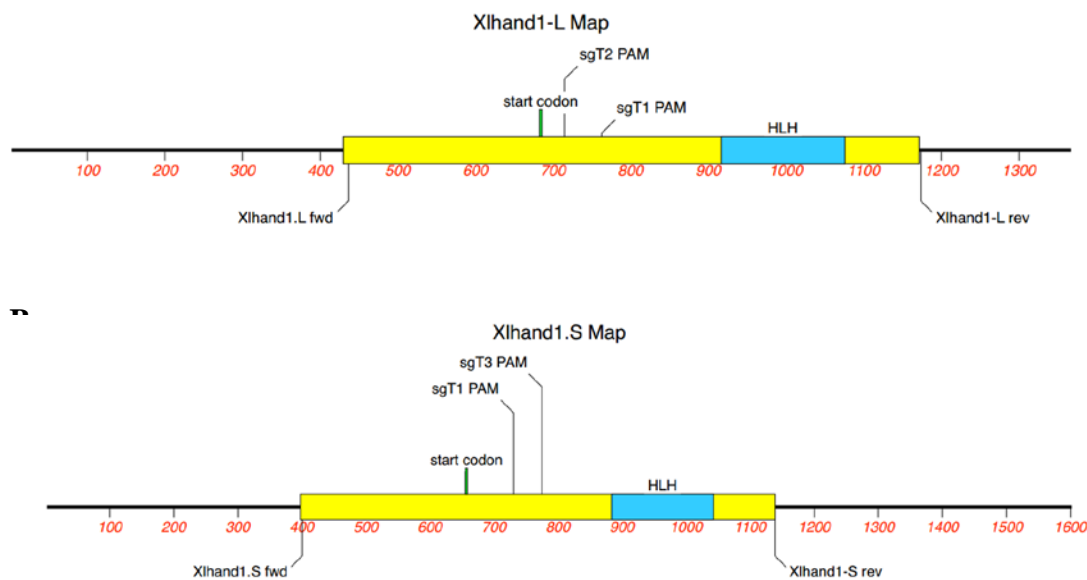
Figure 12. Diagram showing the location of the forward and reverse primers as well as the gRNA PAM sites. (**A**) Diagram of *hand1l* gene map demonstrating the locations of the forward and reverse primers, the start codon, the sgT1 PAM site and the sgT2 PAM site. (**B**) Diagram of *hand1s* gene map demonstrating the locations of the forward and reverse primers, the start codon, the sgT1 PAM site and the sgT3 PAM site. The maps were created by Victoria Deveau and permission was granted to use in this thesis. HLH – Helix-Loop-Helix.

2.10 Microinjection of the *hand1* guide RNA and Cas9 protein

Embryos for injection were de-jellied 20 minutes post-fertilization and transferred to Petri dishes containing 3% Ficoll (GE Life Sciences) in 1 X MMR solution (1 mM $MgSO_4$, 2 mM $CaCl_2$, 5 mM Hepes (pH 7.8), 0.1 mM NaCl, 0.1 mM EDTA (pH 8.0), 2 mM KCl). Following incubation at 14ºC for 15 minutes the embryos were microinjected at the one-cell stage using a Nanoject 3 Microinjector (Drummond Scientific Company; Broomall, PA). Each embryo was injected with 1.5 ng of Cas9 protein and 750 pg of each of the 3 sgRNA in a total volume of 7 nl. The sgRNA was heated to 70ºC for two minutes before being added to the injection stock solution. To control for microinjection of the *hand1* guide RNA and Cas9 protein embryos were injected with dH_2O. Un-injected embryos from the same batch were also allowed to develop until stage 35 so that whole-mount *in situ* hybridization could be performed to control for any abnormal effects caused by the injections process.

2.11 T7E1 assay to determine efficiency of CRISPR/Cas9

DNA was extracted from five non-injected embryos, five dH_2O-injected embryos and ten *hand1* injected embryos and were placed into individual 1.5 mL Eppendorf tubes. The embryos were then homogenized at 55ºC overnight in 0.5 mL of homogenization buffer (1% SDS, 10 mM EDTA, 20 mM Tris (pH 7.5) and 100 mM NaCl), and 2.5 μL of proteinase K (20mg/mL). The DNA was then extracted with 1 volume of aqueous phenol, followed by extracting with 1:1 mix of phenol:chloroform and once with chloroform. Following the extractions, the DNA was precipitated by adding 1/10 volume of 5 M ammonium acetate and 0.6 volumes of isopropanol. The solution was then placed on ice for thirty minutes. The precipitate was recovered by centrifuging at 12,000g for five minutes. The pellet was washed with 70% ethanol and resuspended in 100 μL of TE buffer and treated with 10 μg/mL of RNase A and incubated at room temperature for thirty minutes. The DNA was then precipitated by adding 1/10 volume of 5 M ammonium acetate and 0.6 volumes of isopropanol. The precipitate was then centrifuged at 12,000g for 5 minutes, and the pellet was resuspended in 20 μL of TE Buffer (10 mM Tris-HCl (pH 8), 1 mM EDTA).

PCR reactions were performed using the extracted DNA to amplify 750 bp of the *hand1* gene surrounding the sgRNA target sites. The first of the two sets of primers were used so that both *hand1l* and *hand1s* could be examined. Primers and the PCR conditions are listed in **Table 4** and **Table 5**, respectively. Following the PCR, 20 µl was run on a 1% agarose and TAE gel containing EtBr so that a single product was amplified. The remaining 20 µl of PCR product was denatured at 95°C for three minutes, and then the temperature was dropped 1°C every sixty seconds until 4°C was reached. Next 0.3 U of T7 endonuclease I (NEB) and NEB Buffer 2 was transferred to the remaining 20 µl of PCR product and incubated for one hour at 37ºC. Following the digest, 15 µl of the product was run on a 2% agarose gel containing EtBr and analyzed on the UV transilluminator. Three bands appear in a lane on the gel when a mismatch of DNA was present indicating that the Cas9 has altered the DNA at the predicted target site.

Table 4. T7 endonuclease assay primer sequences targeting the area around the *hand1* gene on the short and long chromosomes.

Primer Name		Sequence
hand1.S	Fwd	GCAGCACAGACTGAACCTGG
	Rvs	CCAATTTGAGCGATTTCTACTCAC
hand1.L	Fwd	TGCAGTGTAAGACTTTGCCTGGA
	Rvs	CCTATATTCATACAACCCTACTC

Table 5. PCR cycling conditions for amplifying the area of the *hand1* gene surrounding the sgRNA target sites.

Temperature (°C)	Time (seconds)	Number of Cycles
95	30	1
95	60	
55 (*hand1.S*) Or 59 (*hand1.L*)	30	40
72	30	
4	Hold	1

2.12 Imaging and statistical analysis

To prepare for imaging, embryos were first rehydrated in a series of methanol washes (75%, 50%, and 25%) and placed in 1 X PBS and imaged on a 1% agarose plate. Following rehydration, the embryos were imaged using the Leica M205 FA microscope and the accompanying program Leica Application Suite (version 4.4.0). Before placing markers on the morphological land marks and expression domain limits, the images were assigned random numbers. This was done so that I was unaware of the treatment administered to the embryos when assessing images in order to prevent observer bias.

In all of the images, lines that act as markers were placed along the embryo to perform quantitative analysis so that the change of RNA localization along the dorsoventral axis of the developing pharyngeal region could be assessed. One of those lines was placed at the bottom of the cardiac cavity to act as a reference point from which all distances were calculated (**Fig. 13**). This bottom reference line placed at the bottom of the cardiac cavity was orientated so that it was always parallel with the top and bottom of the staining limits. A third line was placed at the top of the head of each embryo from which the total distance of the head and neck region was calculated from the bottom reference line (**Fig. 13**). This total distance of the head and neck region was used to create ratios to normalize the head and neck regions between embryos (**Fig. 13**).

For the ventral developing pharyngeal region that expresses *hand1*, a line was also placed at the top of the staining region and the distance from the bottom reference line to the top of the staining was determined (**Fig. 13A**). A ratio was then created using this distance and the distance between the bottom reference line and the line at the top of the head. This represented the entire head and neck region and was used to compare between treatment groups to determine if RNA localization shifted along the dorsoventral axis of the developing pharyngeal region (**Fig. 13A**).

For the genes with expression profiles that are found within the intermediate pharyngeal region, the marker at the bottom of the cardiac cavity was used as a reference point. From which distances to the lower and upper limit of the staining were taken to calculate the distance from the bottom of the cardiac cavity to the centre of the staining (**Fig. 13B**). The distances from the bottom reference line to the middle of the staining was then converted

into a ratio of the entire head and neck region using the distance between the reference line and the line at the top of the head (**Fig. 13B**). This ratio was used to assess if the small molecular activator and inhibitors had an effect on the patterning of the genes within the developing pharyngeal region.

With respect to the dorsal region, a line was placed at the top of the staining limit of *hoxa3* and *pou3f3,* while, a line was placed at the bottom of the staining limit when examining the *prrx2* expression domains (**Fig. 13C & D**). Similar to the ventral, and intermediate regions, the distances to these lines were converted into a ratio of the entire head and neck region. This was accomplished by using the distance between the bottom reference line and the line at the top of the head to assess whether shifts of the expression domains had occurred when Shh and Bmp4 signalling was altered or following the mutation of the *hand1* gene (**Fig. 13C & D**).

Statistical analysis was performed using Microsoft Excel (2013) and IBM SPSS statistical analysis package (IBM SPSS Statistics 25 2017). Following the data collection, a two-sample t-test assuming equal variances was performed to compare control and treatment groups from which Shh signalling was altered. One-way ANOVA test compared the phenotypes between different treatment groups resulting from disrupted Bmp4 signalling and *hand1* gene mutations. This analysis was followed by a Tukey's test to determine the differences between the spatial area of staining patterns observed in the control and experimental treatment groups.

A ventral (*hand1*)

B intermediate (*gcm2*)

C dorsal (*prrx2*)

D dorsal (*pou3f3*)
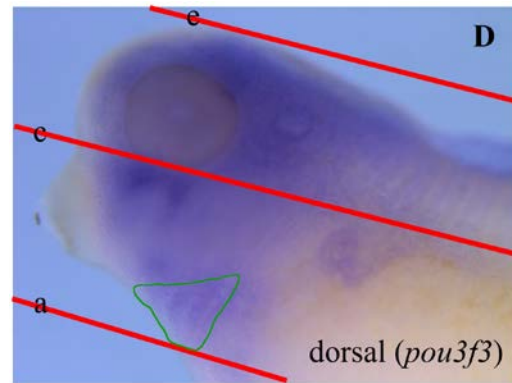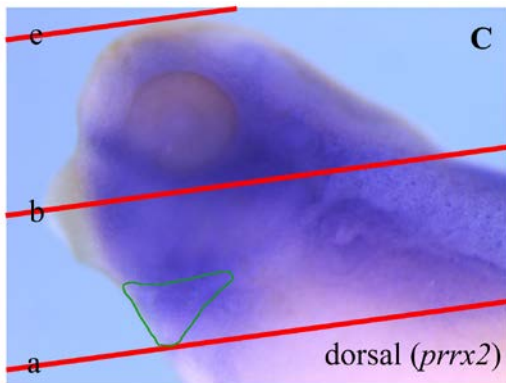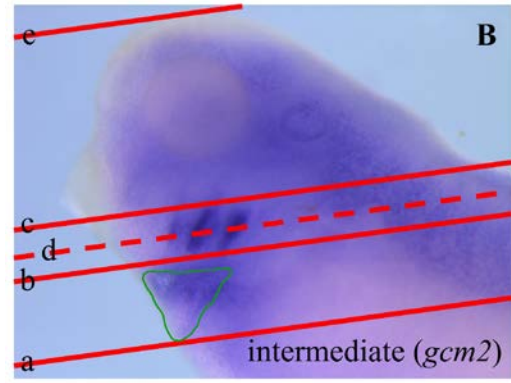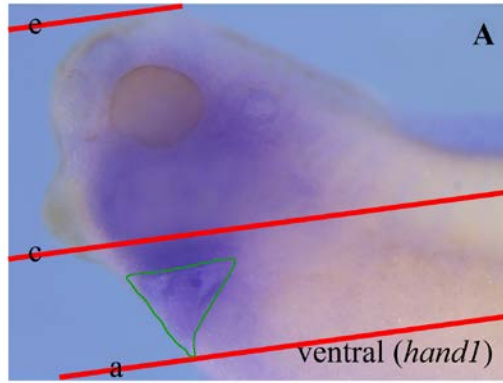
Figure 13. Images of *X. laevis* embryos displaying the markers to determine the effect of the reagents and mutation of the *hand1* gene. A lateral view of a *X. laevis* stage 35 embryo stained with *hand1* RNA probe (ventral marker) (**A**), *gcm2* RNA probe (intermediate marker) (**B**), *prrx2* RNA probe (dorsal marker) (**C**) and *pou3f3* RNA probe (dorsal marker) (**D**). For all RNA probes, a reference line was placed at the bottom of the developing cardiac cavity (green) (a), and the top of the head of the embryo (e) to normalize measurements across all embryos. A parallel line (b) was placed at the lower limit of the staining for the intermediate (**B**) and dorsal markers (**C**). An additional parallel line (d) was placed at the upper limit of the staining for the ventral (**A**), intermediate markers (**B**) and dorsal marker (**D**). For the intermediate markers (**B**) the distance between the lower (b) and the upper limit (c) of the staining were subtracted to calculate the distance from the bottom of the cardiac cavity (green) to the middle of the staining (d). For the ventral (**A**) and dorsal (**D**) markers the distance between the reference line and upper limit (c) of the staining was determined. For the dorsal (**C**) marker the distance between the reference line and the lower limit (b) of the staining was calculated. The distances were then converted into ratios of the developing pharyngeal region (a-e) which were then used to analyze the effects of the small molecular reagents and mutating the *hand1* gene on the dorsoventral patterning of the developing pharyngeal region.

Chapter 3: Results

3.1 Altering Shh signalling caused a disruption in the dorsoventral patterning of the developing pharyngeal region

To test whether Shh plays a role in patterning gene expression within the developing pharyngeal region, the pathway was manipulated in *X. laevis* embryos by pharmacologically activating or inhibiting Smoothened, a key transducer of Shh pathway. Following activation or inhibition of Shh signalling, genes that have expression localized to the three regions of the developing pharyngeal complex were used to assess whether a shift occurred in their pattern of expression along the dorsoventral axis (Jeong et al., 2008; Square et al., 2015; Talbot et al., 2010).

The ventral pharyngeal marker, *hand1,* expression can also be observed in the heart, and lateral plate mesoderm, but for this thesis its broad staining patterning across the ventral pharyngeal region was the focus (**Fig. 14A, B & D**) (Deimling and Drysdale, 2009; Rankin et al., 2012). Embryos were treated with either purmorphamine, a Shh activator, or cyclopamine, a Shh inhibitor, or treated with the vehicle controls (3µL of DMSO and 15µl of 95% ethanol, respectively) (**Fig. 14B-E**). All control embryos showed the expected expression pattern described in previous studies (**Fig. 14B & D**) (Deimling and Drysdale, 2009; Rankin et al., 2012). Embryos in which Shh signalling was activated showed no significant change in staining localization when compared to the control embryos (**Fig. 14D & E**). However, when Shh signalling was inhibited, the embryos displayed a significant dorsal shift in the *hand1* staining localization with respect to morphological landmarks when compared to the control embryos (t (127) = -2.64, p<0.05) (**Fig. 14B, C & F; Supplementary Figure 1**). Therefore, the distance between the bottom of the cardiac cavity and the top of the staining increased for embryos treated with cyclopamine. The dorsal shift of *hand1* expression when Shh signalling was inhibited supported the hypothesis that presence of Shh signalling results in restriction of the expression domain of *hand1* in the developing pharyngeal region.

A *hand1*

B EtOH

C 100 µM CY

D DMSO

E 20 µM PMA

F

The distance between the bottom of the cardiac cavity and upper staining limit as a ratio of the height of the head and neck region

N = 96 (EtOH)
N = 33 (CY)
N = 49 (DMSO)
N = 34 (PMA)

*

Treatments
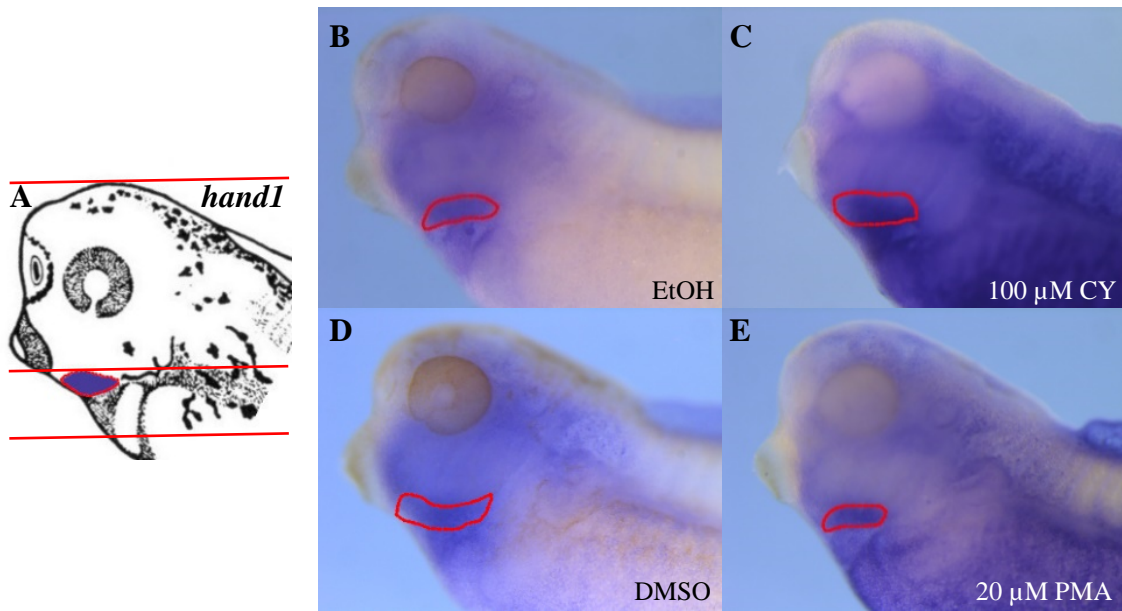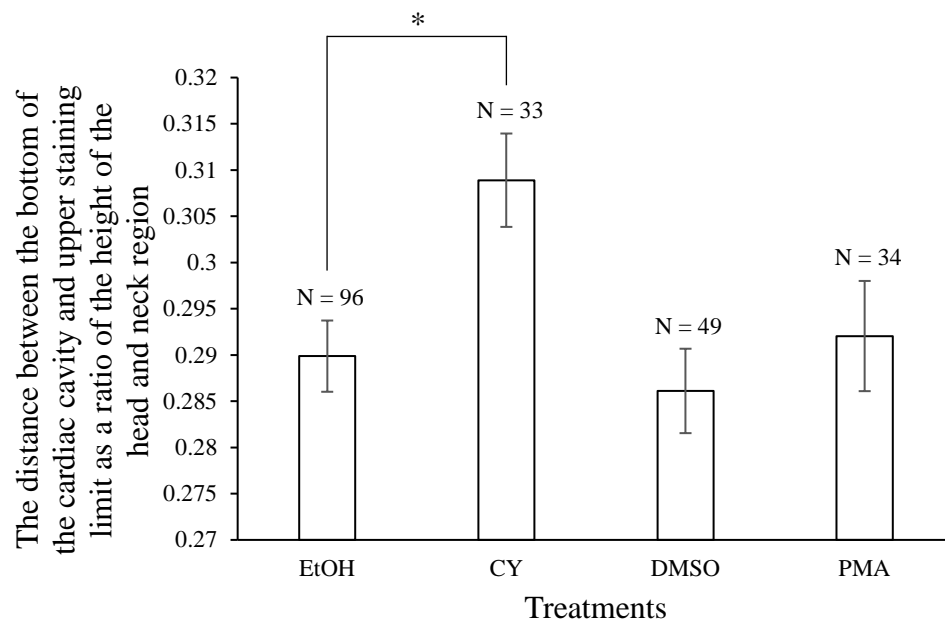
Figure 14.   Inhibiting Shh signalling resulted in a dorsal shift of *hand1* expression within the developing pharyngeal region.   **(A)** Schematic diagram depicting the localization of *hand1* expression in the developing pharyngeal region with lines demonstrating where markers were placed. *Hand1* is expressed in the broad ventral region of the developing pharyngeal region (**B & D**). Activating Shh signalling by exposing the embryos to purmorphamine resulted in no significant difference in localization of *hand1* expression **(E)** compared to the control embryos **(D)**. Inhibition of Shh signalling by exposing embryos to cyclopamine resulted in a significant dorsal shift of the *hand1* expression domain **(C)** when compared to control embryos **(B)** (t (127) = -2.64, p<0.05). Significant differences between the control and treated embryos are marked with an asterisk (P < 0.05) according to the two-sample t-test assuming equal variance (**F**). EtOH – ethanol, PMA – purmorphamine, and CY – cyclopamine.

To further test the hypothesis that Shh signalling regulates the dorsoventral patterning of the developing pharyngeal region, genes that are expressed in the intermediate section were examined under conditions of altered Shh signalling. The genes whose expression domains were examined were *gcm2*, and *pax1*. The expression of *gcm2* is solely restricted to the intermediate region of the 2nd, 3rd, and 4th pharyngeal arches during embryonic development (**Fig. 15A, B & D**) (Lee et al., 2013). Expression of *pax1* is observed in somites, however, its prominent expression in the first five of the pharyngeal arches will be the subject of analysis when examining the dorsoventral patterning of the developing pharyngeal region (**Fig. 15F, G & I**) (Sánchez and Sánchez, 2013). All embryos exposed to the vehicle controls showed the expected staining pattern (**Fig. 15B, D, G & I**) (Lee et al., 2013; Sánchez and Sánchez, 2013). Embryos exposed to purmorphamine showed no significant changes in localization of *gcm2* expression when compared to the control embryos (**Fig. 15D, E & K**). Inhibition of Shh signalling resulted in embryos that displayed a significant dorsal shift in the *gcm2* expression domain when compared to control embryos (t (59) = -3.94, p<0.05) (**Fig. 15B, C & K; Supplementary Figure 2**). Thus, the distance between the bottom of the cardiac cavity and the middle of the staining had increased in embryos treated with cyclopamine compared to the control embryos. However, neither purmorphamine or cyclopamine exposure to embryos caused any significant shift in the expression of intermediate marker, *pax1*, along the dorsoventral axis of the developing pharyngeal region compared to controls embryos (**Fig. 15G-J & K**). Interestingly when inhibiting the Shh signalling pathway there was a sharp decrease in the number of embryos that express *pax1* in the 5th pharyngeal arch. This observation will be discussed further in a later section (**Fig. 15G & H**).
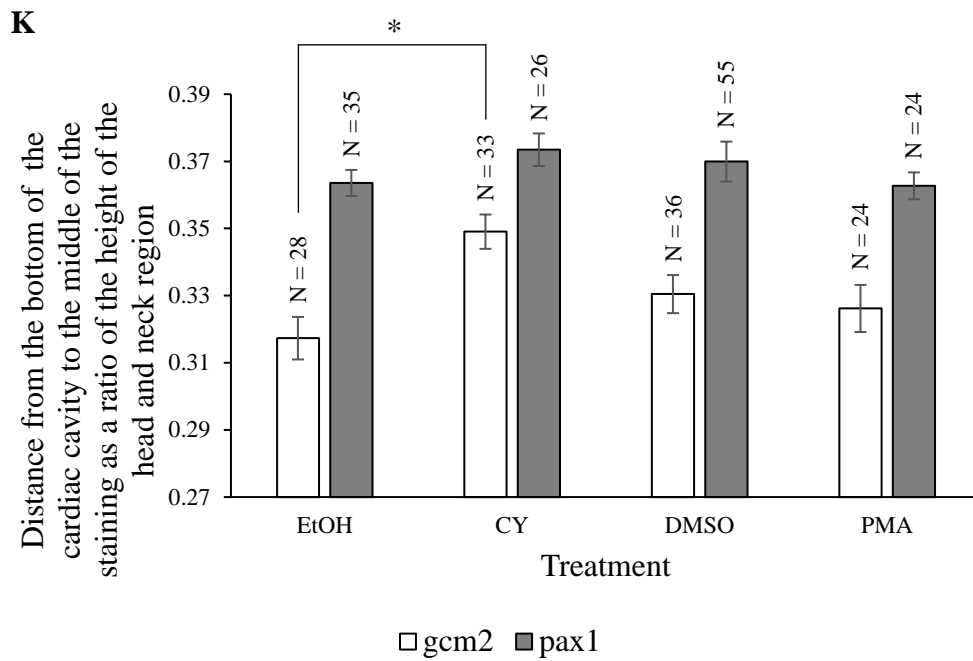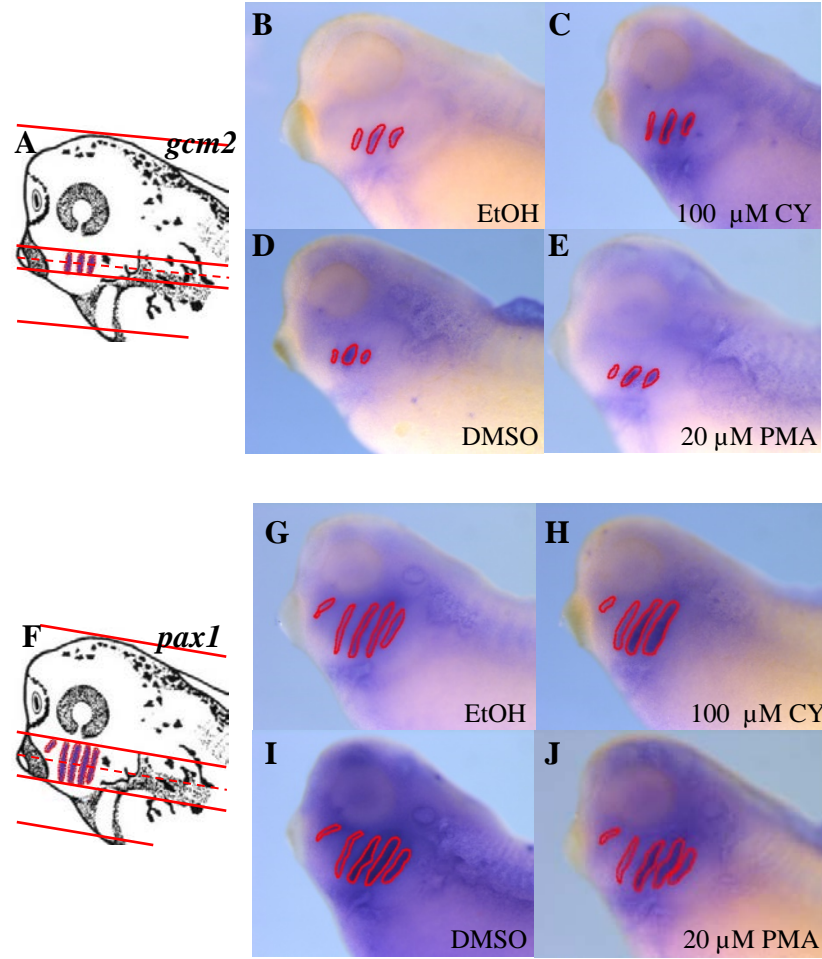
Figure 15. Inhibiting Shh signalling resulted in a dorsal shift in the expression domain of the intermediate marker, *gcm2* but not *pax1*, within the developing pharyngeal region. (A & F) Schematic diagrams depicting the localization of *gcm2* and *pax1* staining with lines demonstrating where markers were placed. The *gcm2* expression domains are restricted to the intermediate region of the 2nd, 3rd, and 4th pharyngeal arches (**B & D**), while, *pax1* expression is observed in the first five of the pharyngeal arches (**G & I**). Exposing embryos to purmorphamine did not result in any significant difference in the localization of *gcm2* (**E**) or *pax1* (**J**) expression compared to control embryos (**D & I**). Exposing embryos to cyclopamine resulted in a significant dorsal shift of the expression domain of *gcm2* (**C**) when compared to the control embryos (**B**) (t (59) = -3.94, p<0.05). Whereas inhibiting Shh signalling resulted in no significant difference in localization of *pax1* (**G**) staining compared to the control embryos (**H**). Significant differences between the control and treated embryos are marked with an asterisk (P < 0.05) according to the two-sample t-test assuming equal variance (**K**). The sharp decrease in the number of embryos that express *pax1* in the 5th pharyngeal arch is exemplified when comparing (**G**) and (**H**). EtOH – ethanol, PMA – purmorphamine, and CY – cyclopamine.

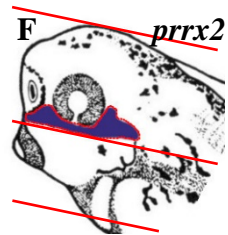Genes that are expressed in the dorsal portion of the developing pharyngeal region include *hoxa3, prrx2,* and *pou3f3* and these were next examined for changes in their expression domain following the manipulation of the Shh signalling pathway. During the development of *X. laevis* embryos, *hoxa3* is expressed in the hindbrain and spinal cord, however, my analysis focuses on the *hoxa3* expression surrounding the 3rd and 4th pharyngeal arches for assessing the dorsoventral patterning of the developing pharyngeal region (**Fig. 16A, B & D**) (McNulty et al., 2005; Square et al., 2015). *Prrx2* expression is observed in the mouth primordium and is expressed in the ventral portion of the developing pharyngeal region (El-Hodiri and Kelly, 2018; Square et al., 2015). However, the focus of my analysis is the expression in the dorsal region of the developing pharyngeal complex (**Fig. 16F, G & I**) (Square et al., 2015). Expression of *pou3f3* is localized to the anterior neural fold, fore- and hindbrain, and the developing kidney (Cosse-Etchepare et al., 2018; Square et al., 2015). My analysis concentrates on the expression in the first, and second pharyngeal arches and was used to assess the dorsoventral patterning of the developing pharyngeal region (**Fig. 16K, L & N**) (Cosse-Etchepare et al., 2018; Square et al., 2015).

All embryos treated with the vehicle controls (3µL of DMSO or 3µl of 95% ethanol) showed the expected staining profiles (**Fig. 16B, D, G, I, L, N & P**) (Cosse-Etchepare et al., 2018; El-Hodiri and Kelly, 2018; Lee et al., 2013; Square et al., 2015). The examination of the expression domains of *hoxa3,* and *prrx2* of embryos following treatment with purmorphamine resulted in no significant change in expression domains when compared to the vehicle controls (**Fig. 16D, E, I, J & P**). In contrast, significant ventral shift in the expression domain of *pou3f3* gene were observed when treated with purmorphamine compared to the expression pattern of control embryos ($t(64) = 2.60$, $p<0.05$) (**Fig. 16N, O & P; Supplementary Figure 5**). Hence, there was a reduced distance between the cardiac cavity and the top of the *pou3f3* staining limit in embryos treated with purmorphamine. There was no significant change in the expression domain of *hoxa3, prrx2* and *pou3f3* in embryos when treated with cyclopamine compared to vehicle controls (**Fig. 16B, C, G, H, L, M & P**). These observations suggest that altering Shh signalling may be one of several signalling pathways regulating the dorsoventral patterning of the dorsal region of the developing pharyngeal complex.

A *hoxa3*

B EtOH

C 100 µM CY

D DMSO

E 20 µM PMA

F *prrx2*

G EtOH

H 100 µM CY

I DMSO

J 20 µM PMA

K *pou3f3*

L EtOH

M 100 µM CY

N DMSO

O 20 µM PMA

P
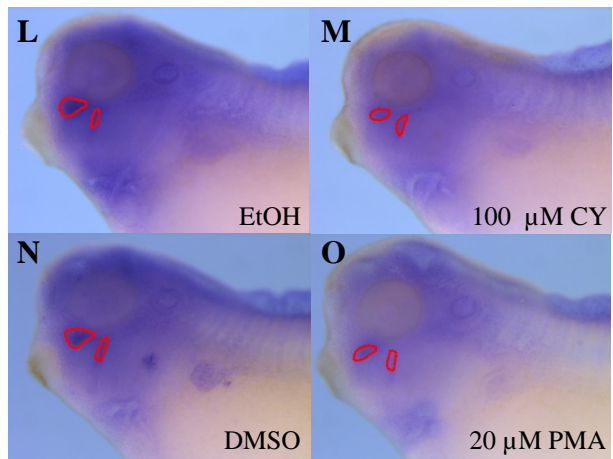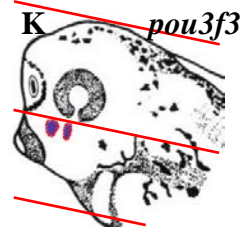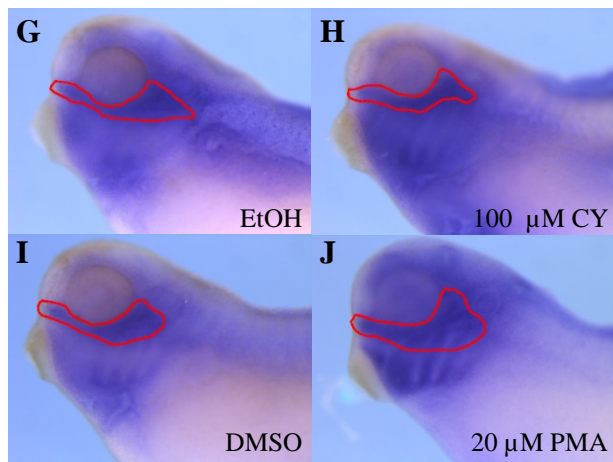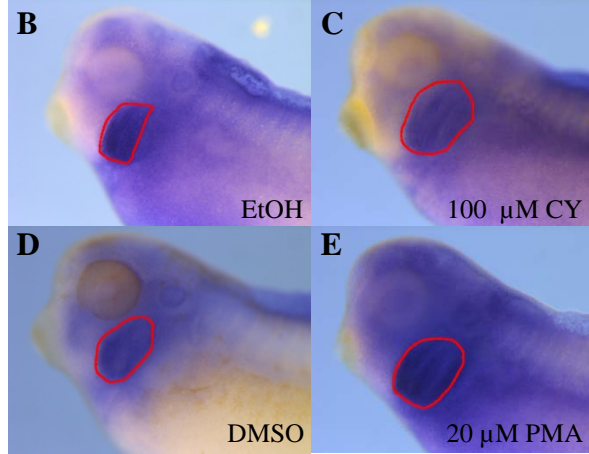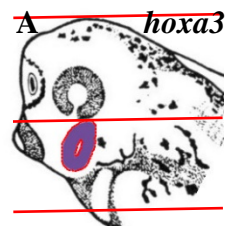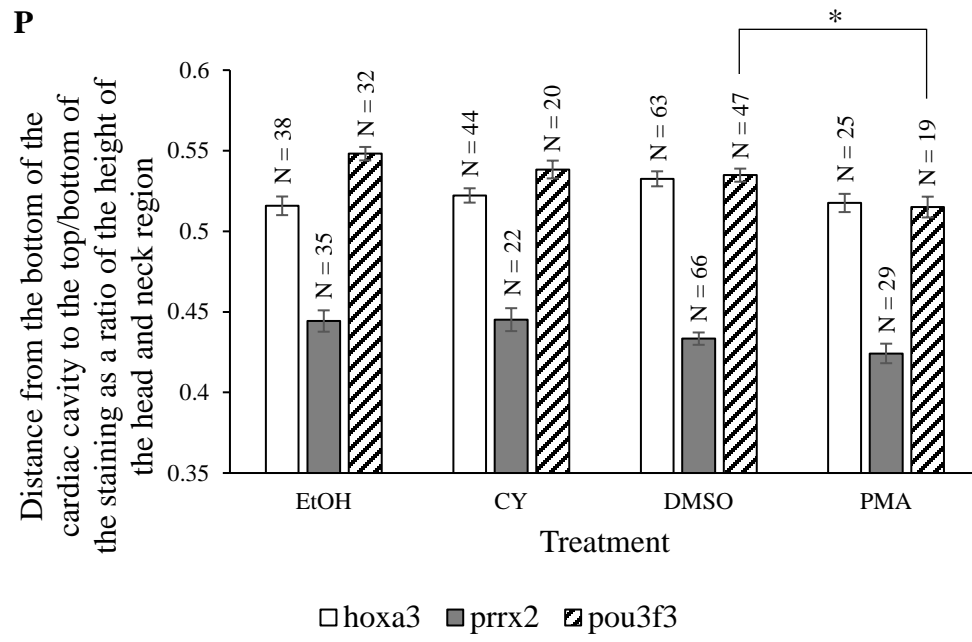
Figure 16. Pharmacological activation of Shh signalling caused a ventral shift in the expression of the dorsal marker, *pou3f3*, in the developing pharyngeal region. **(A, F & K)** Schematic diagrams depicting the localization of *hoxa3*, *prrx2*, and *pou3f3* staining with lines demonstrating where markers were placed. The *hoxa3* expression domain surrounds the 3rd and 4th pharyngeal arches (**B & D**), while, the *prrx2* expression is observed in the ventral portion of the developing pharyngeal region, but the focus of my analysis is the expression in the dorsal region of the developing pharyngeal complex (**G & I**), and *pou3f3* is expressed in first, and second pharyngeal arches (**L & N**). Activating Shh signalling by exposing embryos to purmorphamine resulted in no significant difference in the expression domain of *hoxa3* (**E**) and *prrx2* (**J**) compared to control embryos (**D & I**). Activating the Shh signalling pathway resulted in a significant ventral shift of *pou3f3* (**O**) staining when compared to controls (**N**) ($t(64) = 2.60$, $p<0.05$). Inhibition of Shh signalling, by exposing the embryos to cyclopamine, resulted in no significant change of the *hoxa3* (**C**), *prrx2* (**H**), and *pou3f3* (**M**) expression domains when compared to the control embryos (**B, G & L**). Significant differences between the control and treated embryos are marked with an asterisk ($P < 0.05$) according to the two-sample t-test assuming equal variance (**P**). EtOH – ethanol, PMA – purmorphamine, and CY – cyclopamine.

3.2 Shh signalling regulated the expression of *pax1* in the 5th pharyngeal arch

Further to my observations in **Fig. 15**, I observed that when Shh signalling was inhibited that the staining of *pax1* was lost in the 5th pharyngeal arch. Embryos that had Shh signalling inhibited resulted in only 62.9% (17/27) of the embryos exhibiting staining of *pax1* in the 5th pharyngeal arch (**Fig 17G-I**) compared to the control embryos where all embryos had expression in the 5th arch (24/24) (**Fig 17A-C**). Of those seventeen embryos where *pax1* expression was detected in the 5th pharyngeal arch, 47% (8/17) displayed a reduced *pax1* expression domain (**Fig 17C-F**). Therefore, Shh signalling is necessary for expression of *pax1* in the 5th pharyngeal arch during pharyngeal development in *X. laevis*.
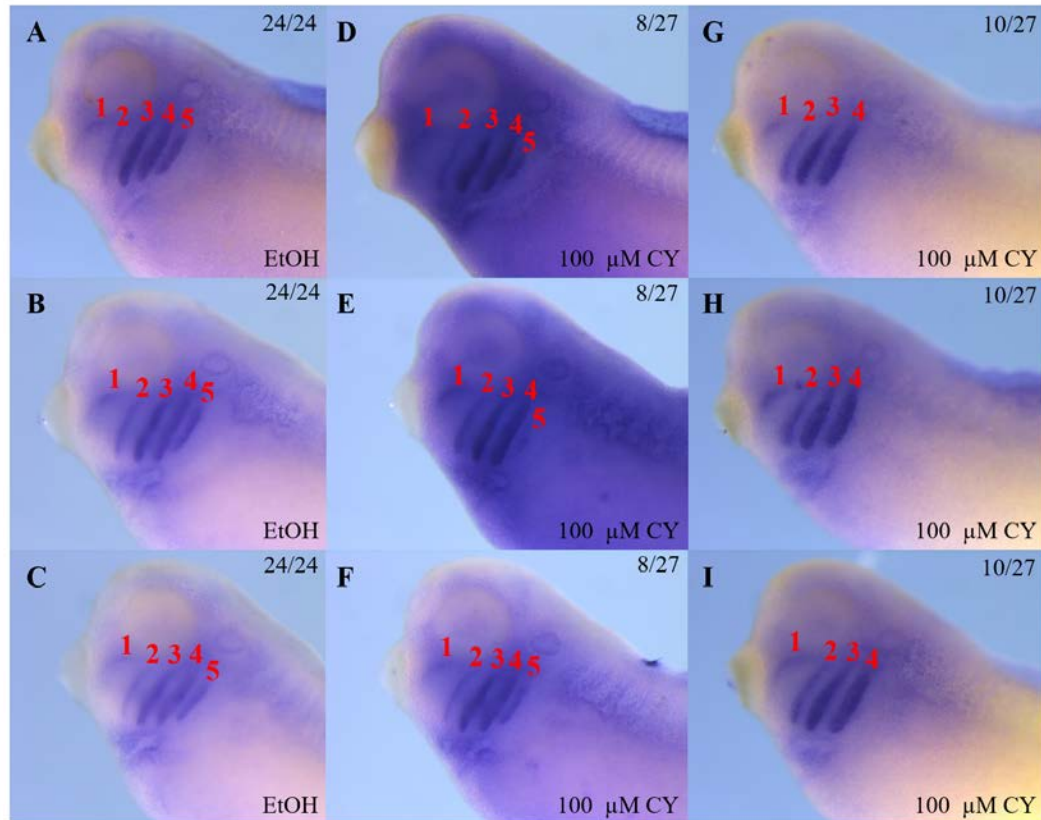
Figure 17. Inhibiting Shh signalling resulted in the loss of expression of *pax1* in the 5th pharyngeal arch. *X. laevis* embryos normally express *pax1* in the 5th pharyngeal arch (24/24) (**A-C**). *X. laevis* embryos in which Shh signalling was inhibited resulted in reduced (8/27) (**D-F**) or complete loss **(G-I)** of *pax1* expression in the 5th pharyngeal arch (10/27).

3.3 Inhibiting Bmp4 signalling resulted in an abnormal dorsoventral patterning of the developing pharyngeal region

In the developing neural tube, Shh is opposed by a gradient of Bmp that is necessary to achieve proper dorsoventral axis patterning (Briscoe et al., 1999; Liem et al., 2000; Liem Jr. et al., 1997; Timmer et al., 2002). To investigate whether the signaling pathway plays a similar role in regulating the dorsoventral patterning of the developing pharyngeal region in *X. laevis,* Bmp4 signalling was inhibited followed by assessment of the same gene expression domains analyzed after altering Shh signalling (Jeong et al., 2008; Square et al., 2015; Talbot et al., 2010).

The ventral region of the developing pharyngeal complex that expresses the *hand1* gene was first examined to investigate whether Bmp4 signalling regulates this pharyngeal region. As noted before the broad staining patterning across the ventral pharyngeal region was of interest (**Fig. 18A & B**). Bmp4 signalling was inhibited by using either dorsomorphin or DHM1 and control embryos were exposed to 3μL of DMSO to control for effects of the DMSO vehicle. Control embryos showed the predicted *hand1* expression pattern (**Fig. 18B**) (Deimling and Drysdale, 2009; Rankin et al., 2012). Embryos treated with dorsomorphin displayed no significant change of the *hand1* expression domain when compared to the control embryos (**Fig. 18A & B**). However, embryos exposed to DMH1 showed a significant ventral shift of the *hand1* expression domain when compared to the control embryos since a smaller distance was observed between the bottom of the cardiac cavity and the top of the staining (F=45.3, P < 0.05) (**Fig. 18A & C; Supplementary Figure 6**).
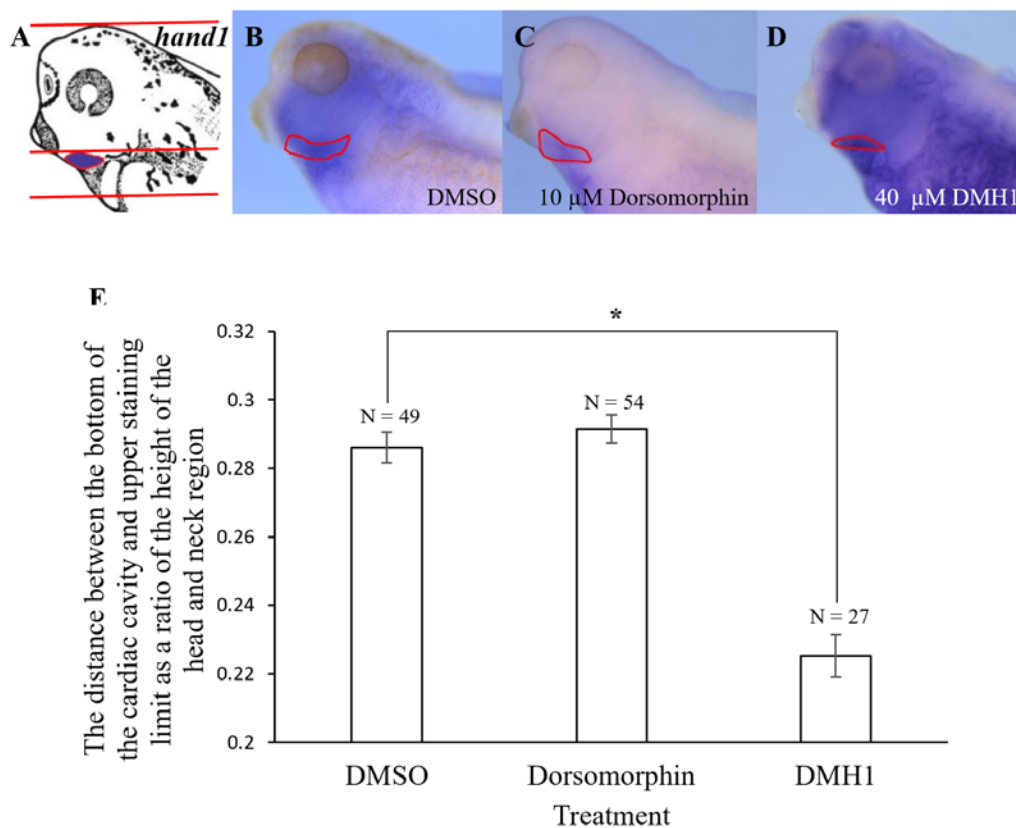
Figure 18. Inhibiting Bmp4 signalling resulted in a ventral shift of the *hand1* expression domain. **(A)** Schematic diagram depicting the expression domain of *hand1* in the developing pharyngeal region with lines demonstrating where the markers were placed. The *hand1* gene is normally expressed in the broad ventral region of the developing pharyngeal complex **(B)**. Inhibiting Bmp4 signalling by exposing the embryos to dorsomorphin **(C)** did not change the positioning of the *hand1* expression domain along the dorsoventral axis, while, DMH1 treatment **(D)** resulted in a significant ventral shift of the *hand1* expression domain when compared to control embryos **(B)** (F=45.3, P < 0.05). Significant differences between the control and treated embryos are marked with an asterisk (P < 0.05) according to Tukey's B test **(E)**.

To test if the effect of inhibiting Bmp4 signalling extended to gene expression patterns that characterize the intermediate region of the developing pharyngeal complex, the *gcm2* and *pax1* expression domains were examined (**Fig. 19A & E**). As with the Shh experiments, *gcm2's* expression in the intermediate region of the 2nd, 3rd, and 4th pharyngeal arches (**Fig. 19A & B**), and *pax1's* expression in the first five of the pharyngeal arches were the focus of analysis (**Fig. 19E & F**). All embryos exposed to the vehicle control (3µL of DMSO) displayed the expected staining profiles (**Fig. 19B & F**) (Lee et al., 2013; Sánchez and Sánchez, 2013). Inhibiting the Bmp4 signalling during embryonic development of the pharyngeal region resulted in a significant ventral shift in the expression domains of *gcm2* when compared to the control embryos (F=10.2, P < 0.05) (**Fig. 19B-D & I; Supplementary Figure 7**). This resulted in a smaller distance between the bottom of the cardiac cavity and the midpoint of the staining when Bmp4 was inhibited. Exposing the embryos to dorsomorphin did not result in a significant change of the *pax1* expression domain but inhibiting Bmp4 signalling through the application of DMH1 produced a significant ventral shift in the expression domain of *pax1* when compared to the control embryos (F=3.2, P < 0.05) (**Fig. 19F-H & I; Supplementary Figure 8**). Consequently, a reduced distance between the bottom of the cardiac cavity and midpoint of the staining could be observed when the embryos were treated with DMH1. Unlike the experiments in which Shh signalling was inhibited, *pax1* expression was present in the 5th pharyngeal arch when Bmp4 signalling was inhibited demonstrating that Bmp4 is not required for *pax1* expression in the 5th pharyngeal (**Fig. 19G & H**).
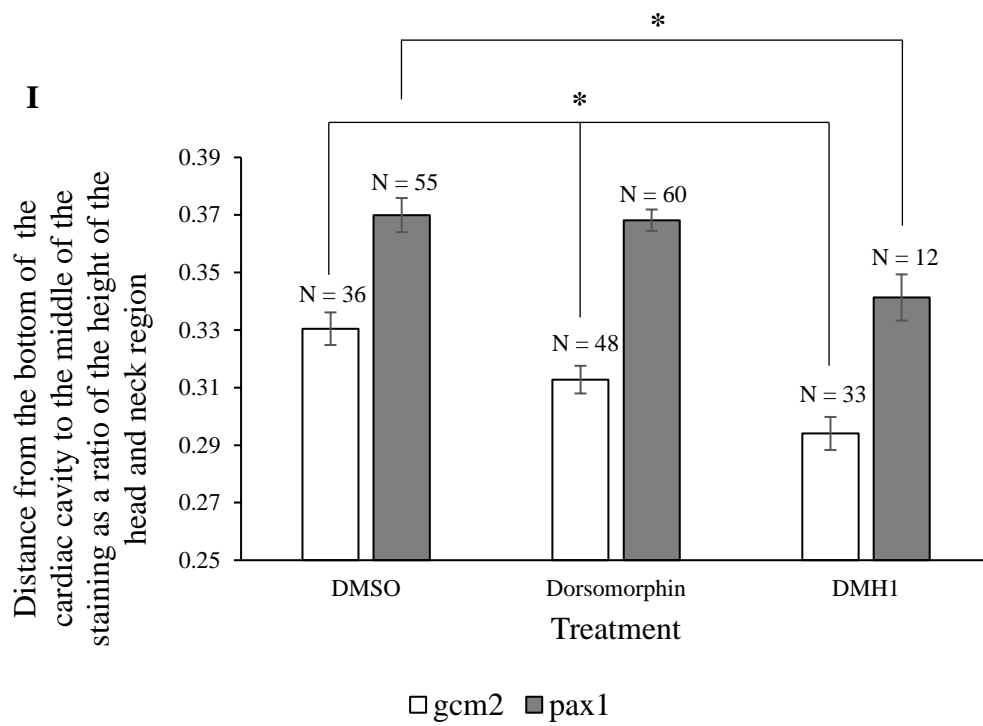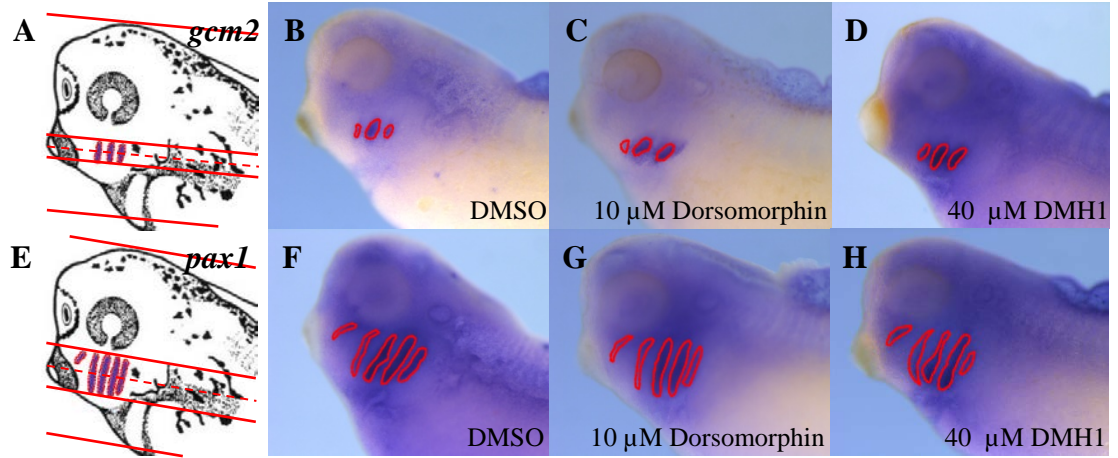
Figure 19. Inhibiting Bmp4 signalling resulted in a ventral shift of the *gcm2* and *pax1* expression domain in the developing pharyngeal region. **(A & E)** Schematic diagrams depict the localization of *gcm2* and *pax1* staining within the developing pharyngeal region with lines demonstrating where markers were placed. Inhibiting Bmp4 signalling by exposing the embryos to dorsomorphin or DMH1 resulted in a significant ventral shift of the *gcm2* **(C & D)** when compared to control embryos (**B**) (F=10.2, $P < 0.05$). Inhibition of Bmp4 signalling by treating the embryos with DMH1 resulted in a significant ventral shift of the *pax1* (**H**) expression domain when compared to controls (**F**), whereas, treatment with dorsomorphin (**G**) did not reproduce those results (F=3.2, $P < 0.05$). Significant differences between the control and treated embryos are marked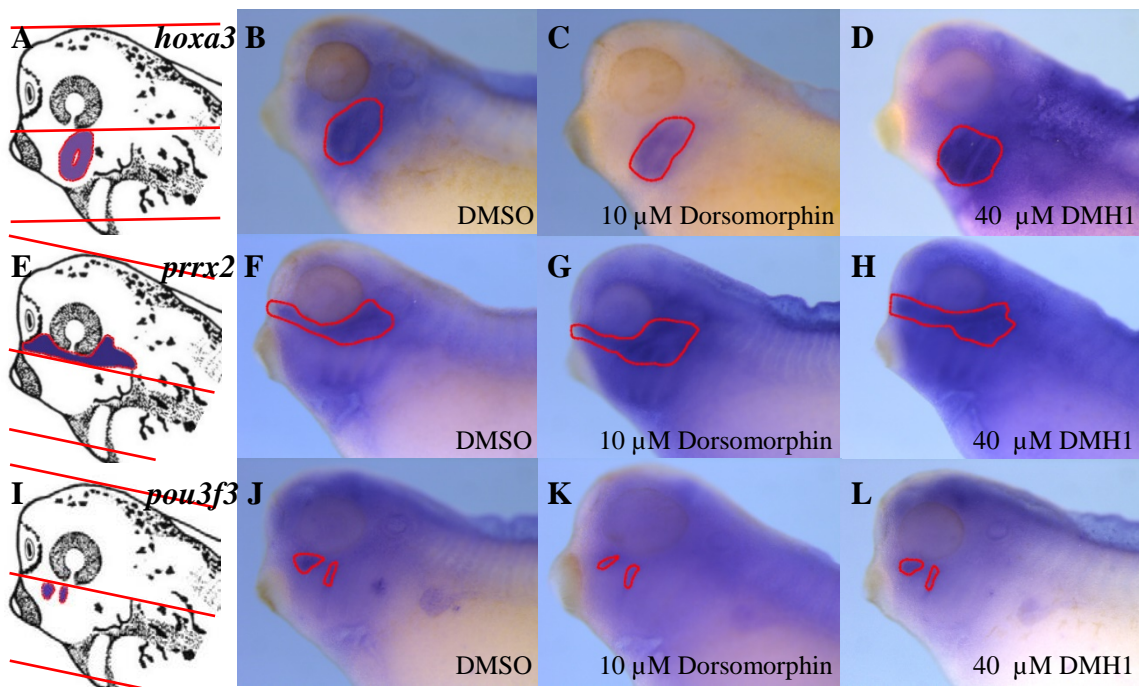 with an asterisk ($P < 0.05$) according to Tukey's B test (**I**). Inhibition of Bmp4 signalling had no effect on *pax1* expression in the 5th pharyngeal arch (**G & H**) in contrast to what was observed when Shh signalling was inhibited.

Finally, I examined the expression domains of *hoxa3*, *prrx2*, and *pou3f3* that are normally expressed in the dorsal region of the developing pharyngeal complex (**Fig. 20A, E & I**). Embryos treated with the vehicle control (3µL of DMSO) displayed the expected expression domains (**Fig. 20B, F & J**) (Cosse-Etchepare et al., 2018; El-Hodiri and Kelly, 2018; Lee et al., 2013; Square et al., 2015). Inhibiting Bmp4 signalling by exposing embryos to DMH1 during embryonic development of the pharyngeal region resulted in a significant ventral shift of the *hoxa3* expression domain when compared to the control embryos (F=13.1, P < 0.05) (**Fig. 20B, D & M; Supplementary Figure 9**). This ventral shift resulted in a smaller distance between the bottom of the cardiac cavity and the top of the staining when the embryos were treated with DMH1. However, treating the embryos with dorsomorphin to inhibit Bmp4 signalling did not reproduce the ventral shift of the *hoxa3* expression domain as observed when the embryos were treated with DMH1 (**Fig. 20B, C & M**). There was no significant change in the expression domain of *prrx2* and *pou3f3* when Bmp4 signalling was inhibited during the development of the pharyngeal region when compared to the controls (**Fig. 20J-L, F-H & M**).
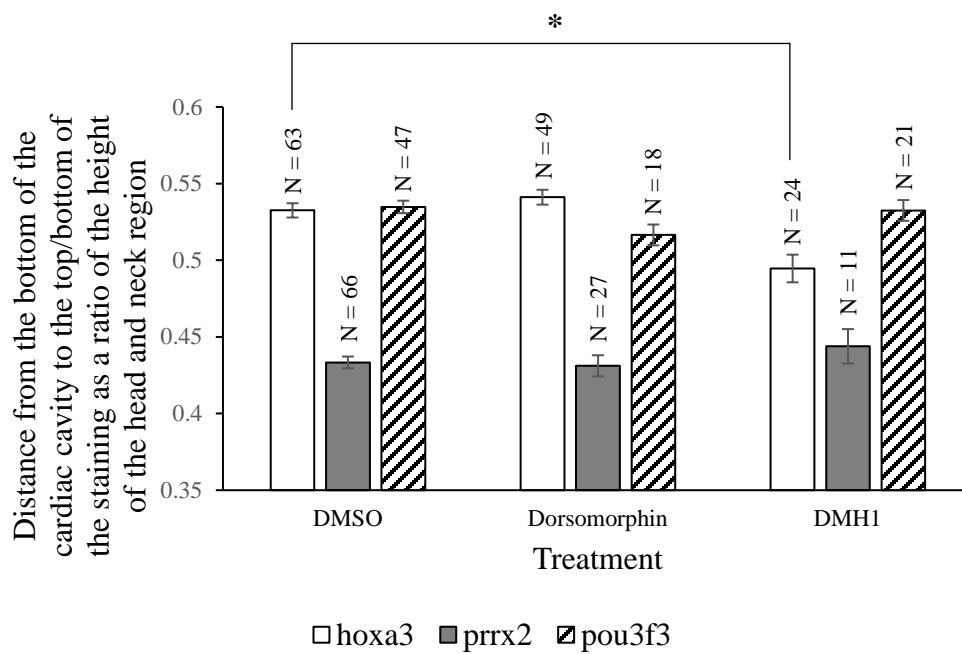
Figure 20. Inhibiting Bmp4 signalling resulted in a ventral shift of the dorsal marker, *hoxa3***. (A, E & I)** Schematic diagrams depicting the localizations of *hoxa3*, *prrx2*, and *pou3f3* expression within the developing pharyngeal region with lines demonstrating where markers were placed. Inhibiting Bmp4 signalling by exposing the embryos to DMH1 resulted in a significant ventral shift of *hoxa3* **(D)** staining when compared to control embryos **(B)** (F=13.1, P < 0.05). However, no significant difference was observed between the *hoxa3* expression domain of control embryos **(B)** and embryos treated with dorsomorphin **(C)** along the dorsoventral axis. Inhibiting Bmp4 signalling had no effect on the *prrx2* and *pou3f3* expression domains **(G & H, K & L)** when compared to control embryos **(F & J)**. Significant differences between the control and treated embryos are marked with an asterisk (P < 0.05) according to Tukey's B test **(M)**.

3.4 hand1 played an active role in dorsoventral patterning of the developing pharyngeal region

In dorsoventral patterning of the neural tube, key transcription factors are expressed at different levels along the dorsal ventral axis in response to the Shh and Bmp gradients and are necessary for defining specific neuronal fates along that axis (Gowan et al., 2001; Persson et al., 2002; Pierani et al., 1999; Timmer et al., 2002). To test if a similar model can be applied to the pharyngeal region, I tested whether *hand1* plays an active role in patterning the developing pharyngeal region or if it is simply expressed in the ventral developing pharyngeal region. The basic helix-loop-helix transcription factor, *hand1*, is a key player in many development processes, including cardiac and respiratory system morphogenesis (Fernandez-Teran et al., 2003; Hoyos et al., 2016; Rankin et al., 2016). In order to test if *hand1* plays an active role, I utilized CRISPR/Cas9 genome editing technology to create mutations in the *hand1* gene. The expression domain of the markers of the pharyngeal pattern were then compared between control and mutant embryos.

To understand the efficiency of *hand1* mutagenesis using the CRISPR/Cas9, the target regions of the genomic DNA extracted from control or CRISPR/Cas9 injected embryos were amplified by PCR and then subjected to a T7 endonuclease assay. As expected, un-injected embryos showed only a single short *hand1* chromosome PCR product (lane #1-5) (**Fig. 21A**) and a single long *hand1* chromosome PCR product (**Fig. 21B**) after the T7 endonuclease assay. Therefore, based on the T7 endonuclease assay, 100% (18/18) of the un-injected embryos tested did not have any sequence variation present in the long or short form of the *hand1* chromosome. CRISPR/Cas9 injected embryos (**Fig. 21A & B**) displayed multiple PCR products demonstrating that a mutation had been introduced at the expected site in *hand1* chromosome in all embryos injected with the appropriate guide RNA and Cas9 protein. Based on the T7 endonuclease assay, at least one copy of the *hand1* gene was mutated in 90% (19/21) of the embryos tested.
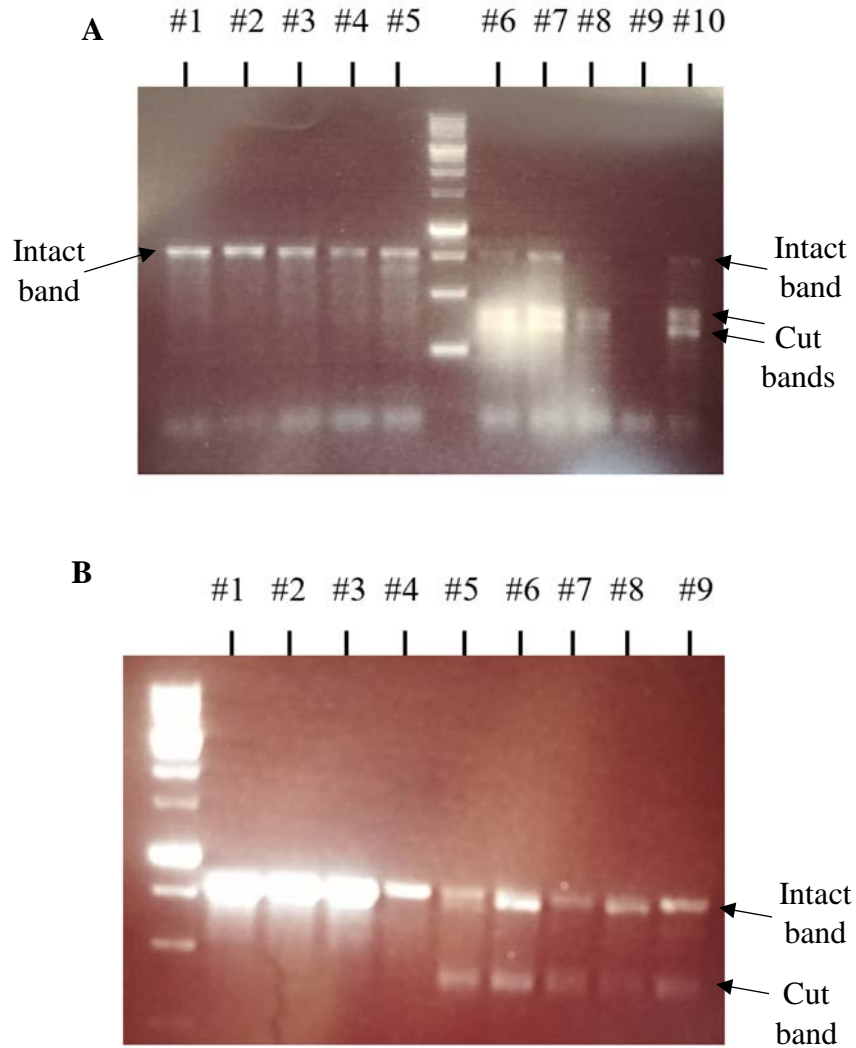
Figure 21. T7E1 assay results demonstrated that CRISPR/Cas9 genome editing was successful at causing mutations in the *hand1* gene. (A) Image of *hand1s* gel with single control embryos (lane #1-5) which display a single (intact) band indicating no sequence variations are present in the *hand1s*. Single injected embryos (lane #6-10) displayed multiple (cut) bands indicating that mutations were present in the hand1s. **(B)** Image of *hand1l* gel with single control embryos (lane #1-4) which display a single (intact) band indicating no mutations were present in the *hand1l*. Single injected embryos (lane #5-9) displayed multiple (cut) bands indicating that mutations have been introduced into the target region of the *hand1l*.

The *hand1* mutants were used to investigate whether *hand1* activity is downstream of Shh and Bmp4 signalling and in turn plays a role in regulating the intermediate portion of the developing pharyngeal complex that expresses *gcm2,* and *pax1* (**Fig. 22A & D**). Control embryos were either not injected or injected with dH$_2$O to control for effects of injection with the Cas9 protein and *hand1* sgRNA. All control embryos displayed the expected staining profiles (**Fig. 22B & E**) (Lee et al., 2013; Sánchez and Sánchez, 2013). CRISPR/Cas9 injected embryos displayed a significant dorsal shift of their *gcm2* expression domain when compared to the control embryos (F=8.3, P < 0.05) (**Fig. 22B, C & G; Supplementary Figure 10**). Therefore, a larger distance between the bottom of the cardiac cavity and midpoint of the staining could be observed when the *hand1* gene was mutated in the embryos. However, there were no changes to the *pax1* expression domain when comparing the CRISPR/Cas9 injected embryos and controls (**Fig. 22E, F & G**).

74
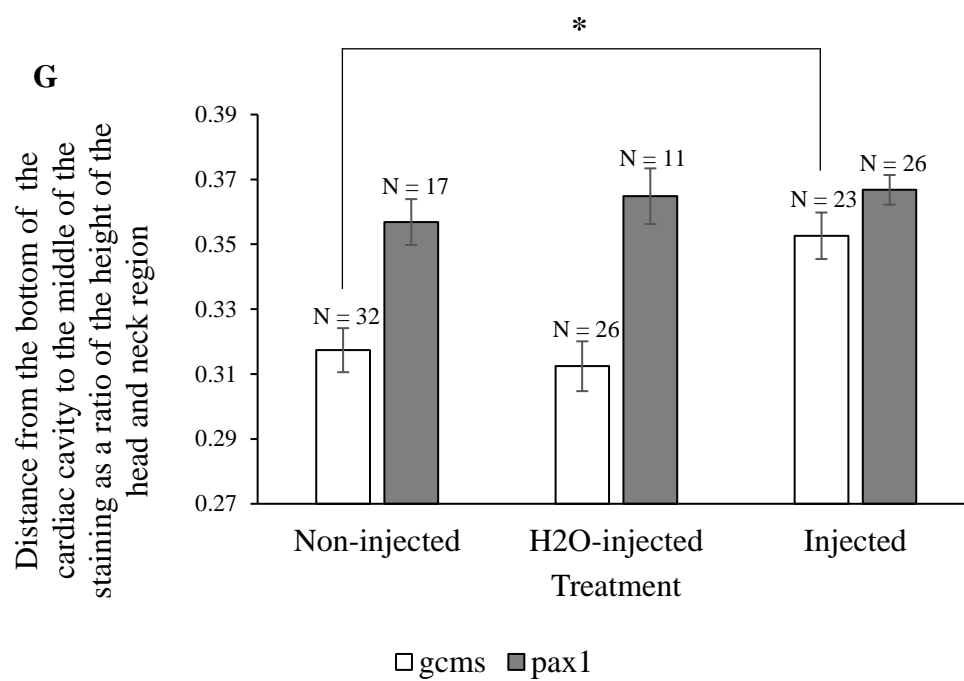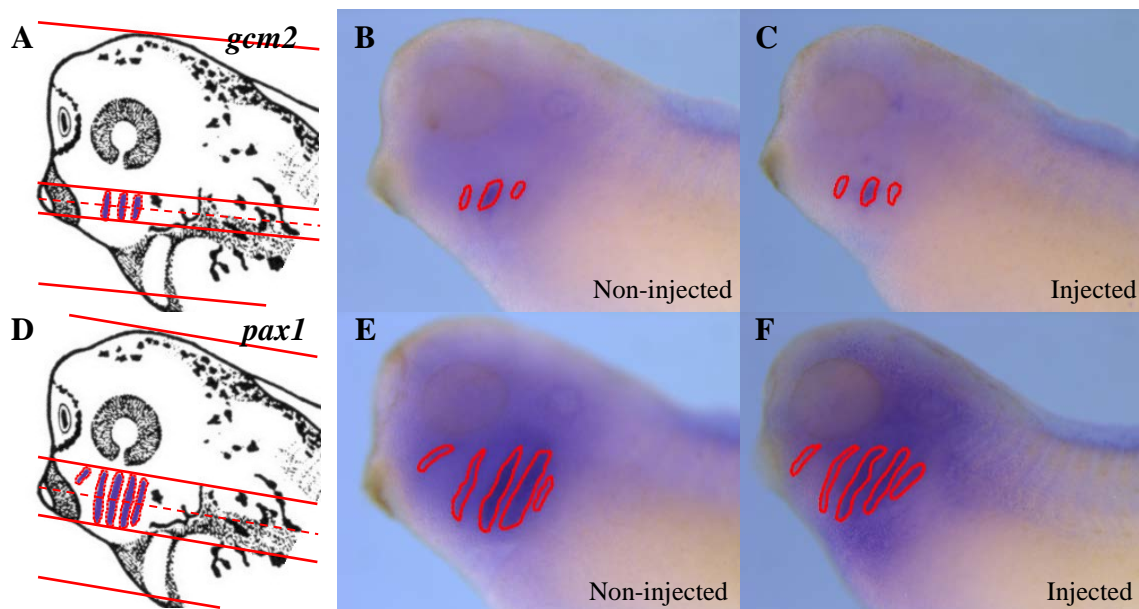
Figure 22. Embryos that had *hand1* mutated using CRISPR/Cas9 showed a dorsal shift in the expression domain of *gcm2* but not *pax1*. (A & D) Schematic diagrams depicting the normal expression domain of *gcm2* and *pax1* in the pharyngeal region with lines demonstrating where markers were placed. Mutating *hand1* using CRISPR/Cas9 technology resulted in a significant dorsal shift of the localization of *gcm2* expression domain **(C)** compared to control embryos **(B)** (F=8.3, $P < 0.05$). Mutating *hand1* using CRISPR/Cas9 technology did not result in any significant difference in expression domain of *pax1* **(F)** when compared to control embryos **(E).** Significant differences between the control and treated embryos are marked with an asterisk ($P < 0.05$) according to Tukey's B test **(G)**.

Finally, the expression domain of the dorsal marker, *prrx2*, of the pharyngeal pattern, was compared between *hand1* mutants and control embryos (**Fig. 23**). The expression of *prrx2* which is restricted to the dorsal region of the developing pharyngeal complex was subject to analysis to determine if *hand1* indeed regulated the dorsoventral patterning of the developing pharyngeal complex downstream of Shh and Bmp4. (**Fig. 23A**). All non-injected, and dH$_2$O-injected embryos showed expected staining profiles (**Fig. 23B**) (Cosse-Etchepare et al., 2018; El-Hodiri and Kelly, 2018; Lee et al., 2013; Square et al., 2015). The embryos which had *hand1* mutated displayed no significant change in the *prrx2* expression domain when compared to the non-injected and dH$_2$O-injected embryos (**Fig. 23B, C & D**).
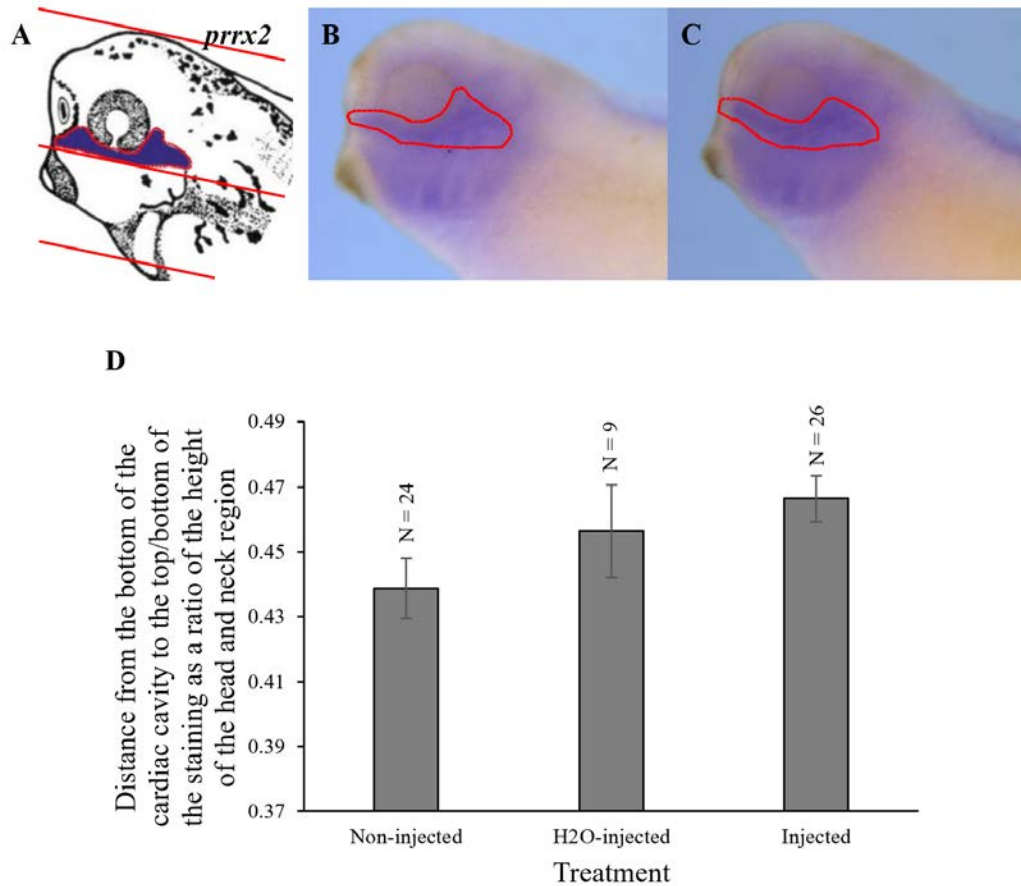
Figure 23. Mutations in *hand1* resulted in no change of the dorsal marker, prrx2, expression domain within the developing pharyngeal region. (**A**) Schematic diagrams depicting the expression domain of *prrx2* with lines demonstrating where markers were placed. Mutating the *hand1* gene resulted in no significant difference in the expression domain of *prrx2* (**C**) compared to non-injected and H_2O-injected embryos (**B**). Significant differences between the control and treated embryos are marked with an asterisk ($P < 0.05$) according to Tukey's B test (**D**).

Chapter 4: Discussion

The purpose of this thesis was to test the hypothesis that the correct dorsoventral gene expression pattern observed in the developing pharyngeal region is regulated by opposing gradients of Shh and Bmp4 signalling in *X. laevis*. I was able to demonstrate gene expression pattern changes in response to altered Shh and Bmp4 signalling that supported the central hypothesis. In addition, I tested whether one of the genes whose expression, changed, *hand1*, played a role in the establishing the pattern as well. During the process of analyzing the changes in *pax1* expression domains, I was also able to demonstrate that Shh is necessary for the expression of *pax1* in the 5th pharyngeal arch. In these following sections, I will discuss how my results support my central hypothesis and the findings that *pax1* expression in the 5th pharyngeal arch requires Shh. I will also discuss future experiments that could further advance our knowledge of how specific signalling pathways regulate craniofacial morphogenesis and patterning.

4.1 Shh signalling regulates the dorsoventral patterning of the developing pharyngeal region

The first evidence that supports the hypothesis that Shh signalling regulates the dorsoventral patterning of the developing pharyngeal region is the shift in the expression domain of genes that are differentially expressed within the developing pharyngeal region when Shh signalling was either activated or repressed. Comparison of the position of the expression domains as related to established morphological landmarks strongly supports the hypothesis that the correct dorsoventral gene expression pattern observed in the developing pharyngeal region is regulated by Shh signalling. Inhibiting Shh signalling resulted in the predicted dorsal shift of the *hand1* expression domain on the ventral side of the embryo, and the *gcm2* expression domain in the intermediate region suggesting that Shh restricts their expression. In the dorsal region activating Shh signalling resulted in a ventral shift of the *pou3f3* expression domain suggesting that Shh supports *pou3f3* expression (**Fig. 14-16**).

The changes observed are consistent with a model of Shh and Bmp4 gradients similar to those observed in the dorsoventral patterning of the neural tube (Ericson et al., 1996; Roelink et al., 1995; Sander et al., 2000). I predict that similarly to the dorsoventral

patterning of the neural tube, Shh signalling molecules are found in a gradient along the developing pharyngeal region, where higher levels are observed near the dorsal pole with decreasing levels towards the ventral-most region (Ericson et al., 1996; Koide et al., 2006; Roelink et al., 1995; Sander et al., 2000). Cells along the dorsoventral axis of the developing pharyngeal region are exposed to varying levels of the Shh ligand that provides positional information that then results in either activation or repression of transcription factors. Increasing or decreasing the signal that the cells receive results in incorrect positional information causing an overall shift of the expression domain of genes along the dorsoventral axis of the developing pharyngeal region.

One set of data that did not match my predicted outcomes was the lack of significant ventral or dorsal shift of the *pax1* expression domain in the intermediate region of the developing pharyngeal complex (**Fig. 15**). One explanation is that its broad expression profile, which spans the entire developing pharyngeal region, requires both manipulation of Shh and Bmp4 signalling pathways for a significant shift of its expression domain. The *pax1* expression spans the complete dorsoventral axis of the developing pharyngeal region, it is less susceptible to the loss of one of the two signalling pathways since cells expressing the *pax1* gene are be exposed to a broad range of Shh or Bmp signal in normal embryos. Therefore, to test this hypothesis embryos should be exposed to an activator of the Shh signalling pathway and an inhibitor of the Bmp4 signalling pathway to determine if manipulation of both signalling pathways is required for a significant shift of the *pax1* expression domain in the ventral direction of the developing pharyngeal region.

Pharmacologically activating Shh signalling resulted in a significant ventral shift of the *pou3f3*'s expression domain, while no changes in the expression domains of *hand1, gcm2 or pax1*, *hoxa3,* or *prrx2* were observed (**Fig. 14-16**). One possible explanation for the lack of an observable ventral shift of the *hand1* gene expression domain in the ventral region and *gcm2* and *pax1* expression domains located in the intermediate region is that the Shh ligand source is dorsal to the developing pharyngeal complex. Increasing the signalling could have an effect at the close proximity in the dorsal region expressing *pou3f3* but fails to change the levels of Shh ligand received by cells in the intermediate region and farther ventral regions resulting in no ventral shift of expression domains along the

dorsoventral axis of the developing pharyngeal region. Removing the Shh signal has much more of a pronounced effect since there is a threshold below which genes start to be regulated differently. The lack of a ventral shift when pharmacologically activating Shh by purmorphamine of the *hand1, gcm2, pax1, hoxa3* and *prrx2* expression domains could also be explained by a threshold with respect to the amount of Shh ligand that cells can receive regarding their positional information. Therefore, cells can be exposed to abnormally high levels of the Shh ligand but this excessive amount of the ligand may not affect how the cells perceive their location along the dorsoventral axis. Experiments could be conducted to determine if spatial separation between the source of the Shh ligand and the Shh sensitive cells is causing no shift in the dorsoventral patterning of the ventral and intermediate regions when activating the Shh signalling.

As well, the lack of significant dorsal shift of the *hoxa3* and *prrx2* expression domains within the developing pharyngeal region can be explained by comparing it to the patterning of the neural tube (**Fig. 16**). The proper dorsoventral patterning of the neural tube requires the three signalling ligands Shh, Wnt, and Bmp (Le Dréau and Martí, 2012). The patterning of the developing pharyngeal region may also require multiple signalling ligands. Solely inhibiting Shh signalling was not sufficient to cause a shift in the expression domains of the *hoxa3* and *prrx2* and to do so may require at least one more signalling pathway to be altered. To confirm this concept, experiments simultaneously altering Shh and other pathways must be conducted to determine if altering multiple signaling pathways is necessary to cause the change in the localization of the *hoxa3* and *prrx2* expression domains. Another experiment that could be conducted would be to isolate tissue from dorsal and ventral regions of the developing pharyngeal complex and to perform RNA sequencing from that tissue. Following the sequencing, any differentially expressed genes that have been previously demonstrated to be involved in patterning could represent potential signalling molecules (eg. wnt) that by altering could determine if they are involved in regulating the patterning of the developing pharyngeal region as well.

Lastly, it may be noted that the ethanol and DMSO controls are not significantly different from one another except for when analyzing the *hoxa3*, and *pou3f3* expression domains. This is consistent with the previous findings that the expression domains are not

always 100% consistent and can vary slightly between embryos and replications of the experiments potentially causing the difference in measurement averages between the two controls.

In summary, my results support the hypothesis that Shh signalling contributes to the correct dorsoventral gene expression pattern observed in the developing pharyngeal region.

4.2 Bmp4 signalling regulates the dorsoventral patterning of the developing pharyngeal region

The ventral shifts observed in the *hand1, gcm2, pax1, and hoxa3* expression domains when Bmp4 was broadly and specifically inhibited supported the hypothesis that the correct dorsoventral gene expression pattern observed in the developing pharyngeal region is regulated by Bmp4 signalling in *X. laevis*. As well, the ventral shift of all these expression domains also supported the prediction that Bmp4 signalling would support ventral expressing regions and suppress dorsal expressing regions. Either broadly or specifically inhibiting Bmp4 signalling resulted in a ventral shift of the *hand1* expression domain, the intermediate region which expresses the *gcm2*, and *pax1* genes, and the dorsal region which expresses the *hoxa3* gene within the developing pharyngeal region (**Fig. 17-19**). Similar to the Shh results these ventral shifts fit with a model of Shh and Bmp4 signalling acting as opposing gradients to pattern the dorsoventral axis as seen in the neural tube (Liem Jr. et al., 1995, 1997; Nguyen et al., 2000; Rankin et al., 2012; Timmer et al., 2002).

Within the developing pharyngeal region there is a high concentration of the Bmp4 ligand near the ventral pole (Rankin et al., 2012). Moving away from the ventral pole, cells are exposed to lower concentrations of the Bmp4 ligand. This gradient provides cells with positional information along the dorsoventral axis resulting in expression or repression of key developmental genes (Liem Jr. et al., 1995, 1997; Nguyen et al., 2000; Rankin et al., 2012; Timmer et al., 2002). Inhibiting Bmp4 signalling results in cells perceiving that they are in a more ventral position compared to their normal position along the dorsoventral axis resulting in a ventral shift of the expression domains of the genes of interest (**Fig. 17-19**).

The expression domains of *prrx2* and *pou3f3* did not display a ventral shift when Bmp4 signalling was inhibited (**Fig. 19**). One explanation for this result is that the expression domain of *prrx2* and *pou3f3* genes are located in the most dorsal region. Inhibiting Bmp4 signalling may have little to no effect on the most dorsal region of the developing pharyngeal complex since limited levels of Bmp4 may reach the dorsal area. Shh signalling may play a stronger role in the dorsoventral patterning of the dorsal region because the cells are closer to the Shh ligand source. The high levels of Bmp4 signalling on the ventral side explains why the most dramatic ventral shift was observed in the expression of *hand1* (**Fig. 18**).

Finally, I would like to address the ventral shift of the *hand1, pax1* and *hoxa3* expression domains when treated with DMH1 but not when treated with dorsomorphin (**Fig. 18-20**). This difference between the treatment groups can be attributed to the fact that DMH1 is a much more selective and effective inhibitor of Bmp4 signalling. Differences in results between dorsomorphin and DMH1 have previously been observed (Ao et al., 2012). Cells treated with dorsomorphin also had delayed expression profiles when compared to cells treated with DMH1 (Ao et al., 2012).

In conclusion, these results support the hypothesis that the correct dorsoventral gene expression pattern observed in the developing pharyngeal region is regulated by Bmp4 signalling.

4.3 Shh signalling is required for *pax1* expression in the 5th pharyngeal arch

During assessment of the intermediate region of the developing pharyngeal complex which expresses *pax1* it became apparent that inhibiting Shh signalling resulted in the disappearance of *pax1* expression in the 5th pharyngeal arch or alternatively, the loss of the 5th pharyngeal arch that expresses *pax1* (**Fig. 17**). This result is not surprising given that Shh has been demonstrated to mediate as a dual functioning signalling pathway in developing structures such as the eye, and limb (Macdonald et al., 1995; Rodrigues et al., 2017). During embryonic development, Shh signalling regulates the patterning of the eye, and the expression of *pax2,* and *pax6*, while also patterning the limb, and controlling the expressing of *hoxd13* (Macdonald et al., 1995; Rodrigues et al., 2017). Interestingly Shh has been demonstrated to be crucial for proper development of the 1st pharyngeal

arch in mice, however, no observable changes occurred to the 1st pharyngeal arch in my experiments (Yamagishi et al., 2006). The difference between results could possibly be attributed to using different model organisms or the different time points at which the pharyngeal arches were examined. As well, when Shh signalling was disrupted in mice, similar reduced gene expression in the pharyngeal arches was observed where multiple transcription targets were downregulated such as *Barx1, goosecoid,* and *dlx2,* as well as, downregulated *fgf8* signalling (Yamagishi et al., 2006). In addition to patterning the dorsal ventral axis of the developing pharyngeal region, the results suggest Shh signalling participates in anteroposterior patterning of the developing pharyngeal region. More specifically Shh signaling is required for specification of the 5th pharyngeal arch or simply be necessary for expression of *pax1* in that arch. Further experiments will be required to determine if Shh signalling is required for *pax1* expression in the 5th pharyngeal arch or is required for the proper development of the 5th pharyngeal arch. One set of experiments that could be conducted would be to examine whether expression domains of genes such as *emx2, nkx3.2b* or *nkx3.3* that are located in the 5th pharyngeal arch are present following inhibition of Shh signalling. If the expression of these genes is observed in the 5th pharyngeal arch, this would suggest that Shh signalling solely regulates *pax1* expression in the 5th pharyngeal arch. If these genes are also not expressed following Shh inhibition, further experiments will be needed to confirm that Shh signaling is then regulating the development of the 5th pharyngeal arch. Another series of experiments that could be conducted would be to allow the embryos to develop to later stages to determine which pharyngeal derives are missing or malformed due to loss of *pax1* expression in the 5th pharyngeal arch. I suspect that derivatives of the 5th pharyngeal arch such as laryngeal cartilage, and intrinsic muscles would either fail to develop or abnormal morphology would be observed leading to impaired functions of the larynx.

4.4 *hand1* gene regulates the dorsoventral patterning of the developing pharyngeal region downstream of Shh and Bmp4 signalling

The hypothesis that the correct dorsoventral gene expression pattern observed in the developing pharyngeal region is regulated by the *hand1* gene downstream of the Shh and

Bmp4 signalling pathways is supported by the shift of the *gcm2* expression domain following mutation of *hand1 gene* using CRISPR/Cas9. As well, the dorsal shift of the *gcm2* expression domain supports the prediction that mutating the *hand1 gene* will result in a dorsal shift of the expression domain because cells aligned along the dorsoventral axis of the developing pharyngeal region may be receiving the incorrect positional information causing the misexpression of the *gcm2* gene (**Fig. 23**).

Hand1 was selected as a potential regulator of the dorsoventral patterning of the developing pharyngeal region because the *hand1* expression profile had the most significant ventral and dorsal shift in expression localization when Bmp4 and Shh signalling were inhibited, respectively. As well, the expression domain of the *hand1* gene has been demonstrated to be under the regulation of Shh signaling (Fernandez-Teran et al., 2003; McFadden et al., 2002). Therefore, based on the results from the Shh signaling series of experiments and work conducted by Fernandez-Teran and colleagues and McFadden and colleagues if *hand1* is mutated and functions downstream of the Shh signalling pathway a dorsal shift of *gcm2, pax1, hoxa3, prrx2*, and *pou3f3* expression domains should be observed similarly to the dorsal shifts of the expression domains when Shh signalling was inhibited (Fernandez-Teran et al., 2003; McFadden et al., 2002). Indeed, a dorsal shift in the expression of *gcm2* was observed. As mentioned in the two previous sections the dorsal shift of the *gcm2* expression domain is due to the incorrect positional information that cells are receiving. Therefore, cells which are dorsal to the normal *gcm2* expression localization now express *gcm2,* while cells which normally express *gcm2,* in the ventral region of the *gcm2* expression domain now repress *gcm2* genes.

However, no significant dorsal shift was observed in the expression domain of *pax1* or *prrx2*. Similar to the pharmacological interventions, due to the fact that *pax1* broad expression domains spans the entire dorsoventral axis of the developing pharyngeal region manipulating both the Shh and Bmp4 signals may be required to cause a shift of the *pax1* expression domain. Manipulating either the Shh or Bmp4 signalling pathway failed to result in a shift of the *pax1* expression domain since its expression is throughout the developing pharyngeal region. Thereby, allowing the unmanipulated signalling pathway to maintain proper dorsoventral patterning when the other signalling system is either

pharmacologically activated or inhibited. Additionally, the *hoxa3,* and *pou3f3* staining localization were trending in the dorsal shift direction similarly to when the *hand1* gene was mutated and embryos were stained for *gcm2*, however, more replicates of the experiments need to be conducted to statistically confirm that potential dorsal shift (**Supplementary Figure 9**).

No significant change in the localization along the dorsoventral axis of the developing pharyngeal region of the *pax1* and *prrx2* expression domains results are explained by my previous experiments investigating whether Shh regulates the patterning of the regions expressing *pax1* and *prrx2*. Those experiments demonstrated that the regions expressing *pax1* and *prrx2* are regulated independently from Shh and Bmp4, therefore, it is not surprising that mutating the *hand1* gene had no effect. During the development of the neural tube Shh, Bmp4, and Wnt signalling are required for the proper dorsoventral patterning (Le Dréau and Martí, 2012). Therefore, Wnt or other signalling molecules could be regulating the dorsoventral patterning of the developing pharyngeal region as well. Manipulating just one of the signalling pathways or one of the transcription factors functioning downstream of these signalling pathways may not have a significant effect on the localization of *pax1* and *prrx2* expression domains (Le Dréau and Martí, 2012; Megason and McMahon, 2002). To test this hypothesis, multiple signalling pathways and transcription factors should be manipulated to observe if any significant changes to *pax1* and *prrx2* domains occurs along the dorsoventral axis.

Overall, the dorsal shift in *gcm2* expression domain resulting from mutating the *hand1* gene supports the hypothesis that the correct dorsoventral gene expression pattern observed in the developing pharyngeal region is regulated by the *hand1* gene downstream of Shh and Bmp4 signalling in *X. laevis*.

4.5 Future investigations of signalling pathways which regulate craniofacial morphogenesis and patterning

In this thesis, I have shown that Shh and Bmp4 play a role in the normal dorsoventral patterning of the developing pharyngeal region. These signalling pathways were either pharmacologically activated or inhibited, prior to the onset of pharyngeal development (stage 13) until stage 35 when the embryos were fixed, and pharyngeal gene expressions

were examined. Hence, this thesis determined the broad window of development where appropriate expression levels of the signalling ligands are needed for proper dorsoventral patterning. Using similar methods, it was established that Shh is required for the specification of the mouth size and that Shh is mandatory at later tadpole stages for perforation of the mouth (Tabler et al., 2014). Jacqueline Tabler and associates likewise first determined a broad window in which Shh signalling was required for proper mouth formation and then further refined the exact developmental timeframe when Shh signalling was required. Therefore, future studies could better define a specific developmental window where Shh and Bmp4 signalling are required for the dorsoventral patterning of the developing pharyngeal region.

If my central hypothesis is correct, a clear prediction would be that there should be a more substantial shift in the pharyngeal pattern if the Shh signalling pathway is activated while the Bmp4 signalling pathway is inhibited during the development and patterning of the pharyngeal region. Activation of Shh and inhibition of Bmp4 concurrently may yield a more substantial shift of genes along the dorsoventral axis since both signalling pathways are being manipulated. I would predict that following treatment there would be a more substantial ventral shift of the *hand1, gcm2, pax1, hoxa3, prrx2* and *pou3f3* expression domains along the dorsoventral axis since both signalling gradients are being disrupted compared to the one signalling gradient that is being disrupted in the present experiments.

The third set of experiments that could continue the work of this thesis would be to investigate the later morphological consequences of disrupting the normal expression of *hand1, gcm2, pax1, hoxa3, prrx2,* and *pou3f3* along the dorsoventral axis of the developing pharyngeal region. The main reason why the genes analyzed in this thesis were chosen was that their expression is restricted to specific areas of the developing pharyngeal region that allowed me to simplify the analysis of the dorsoventral patterning into three broad regions. A second reason why these genes were selected was that they are crucial in the later stages of craniofacial development (Berge et al., 1998; Firulli et al., 2014; Günther et al., 2000; Jeong et al., 2008; Liu et al., 2007; Manley and Capecchi, 1998; Su et al., 2001). With regard to the ventral region of the developing pharyngeal complex, proper expression and phosphoregulation of *hand1* are crucial for craniofacial morphogenesis, and when *hand1* is mutated prominent mid-facial clefts are observed as well as an increase in cell

death within the pharyngeal arches (Firulli et al., 2014). Previous studies have also demonstrated that the proper expression of *gcm2*, and *pax1* are crucial for the proper formation of the thymus and parathyroid (Günther et al., 2000; Liu et al., 2007; Su et al., 2001). Embryos in which the *gcm2* gene was mutated resulted in the parathyroid glands failing to form, and when the *pax1* gene was misexpressed embryos displayed defects in the morphology of both organs, incomplete separation of the organs from the pharyngeal pouch, and increased cell death during the earlier stages of organogenesis (Günther et al., 2000; Liu et al., 2007; Su et al., 2001). Finally, with respect to the *hoxa3, prrx2* and *pou3f3* genes chosen as markers for the dorsal region of the developing pharyngeal complex, they have been shown to be crucial for the proper development of the thymus, thyroid, parathyroid, and bones of the facial region (Berge et al., 1998; Jeong et al., 2008; Manley and Capecchi, 1998). When the *hoxa3* gene is silenced embryos display phenotypic defects in the thyroid and the parathyroid such as decreased number of C cells in the thyroid lobes (Manley and Capecchi, 1998). Whereas knocking out the expression of both the *prrx1* and *prrx2* genes resulted in multiple phenotypic defects in the craniofacial region. These include shortened dentaries, cleft mandible, and defects around the nasal cavity such as cleft palate later causing respiratory issues in the mice (Berge et al., 1998). When *pou3f3* was knocked out in mice embryos, a significant reduction in the size of the squamosal bone, jugal bone, as well as the failure of the stapes to detach from the styloid process were all observed (Jeong et al., 2008). Consequently, disrupting the dorsoventral patterning of these genes in the developing pharyngeal region would expect to cause these phenotypic defects since all of the aforementioned abnormally developed elements originate from the pharyngeal region during embryonic development. Therefore, bright-field microscopy and Alizarin red staining could be used to examine bone and cartilage *of X. laevis* embryos allowed to develop to later tadpole stages. Specific markers for structures such as the thyroid and parathyroid could be utilized to determine if disrupting the expression domains of these genes along the dorsoventral axis of the developing pharyngeal region will result in abnormal phenotypes previously documented.

4.6 Conclusions

Understanding the signalling pathways and transcription factors which regulate the developing pharyngeal region along the dorsoventral axis is necessary to understand

craniofacial development especially the more developmentally complex structures such as the pharynx. This thesis has uncovered evidence that the Shh and Bmp4 patterning system similar to the well-established patterning in the neural tube is used to also regulate the dorsoventral axis of the developing pharyngeal region. Additionally, this thesis implies a mechanism that links the pathways and known results of craniofacial development. The first major product of this thesis is the demonstration that Shh and Bmp4 signalling regulate the dorsoventral patterning of the developing pharyngeal region in *X. laevis* during stages 13 to 35, and secondly that *hand1* is a regulator of the patterning downstream of the signalling ligands. Finally, this research has also identified Shh signalling as a regulator of *pax1* expression in the 5th pharyngeal arch. Further investigation will be needed to determine the exact windows at which Shh, and Bmp4 signalling, and the *hand1* gene are required for proper dorsoventral patterning of the developing pharyngeal region to advance our knowledge of craniofacial development in *X. laevis*.

Appendix: Early *X. laevis* Embryogenesis
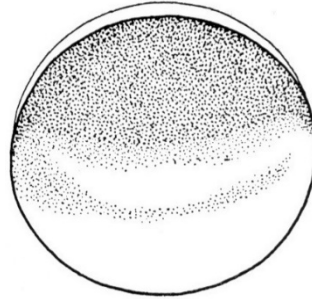
Stage 1 (egg), ventral view

0 mn pf @ 23°C
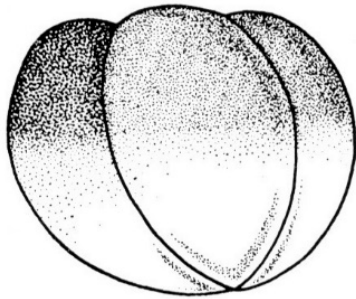
Stage 3 (4-cell), dorsal-lateral view

2 hr pf @ 23°C
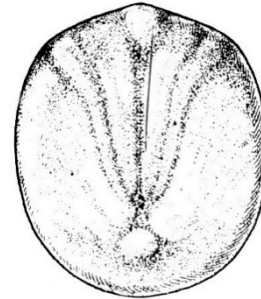
Stage 13, posterior-dorsal view

14 hr 45 min pf @ 23°C
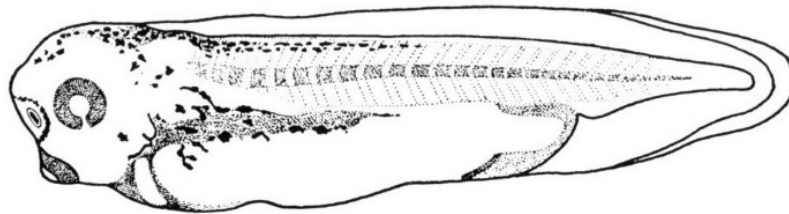
Stage 35-36, lateral view

2 days, 2 hr pf @ 23°C

*All images were obtained from www.xenbase.org, according to Nieuwkoop and Faber's Normal Table of *Xenopus laevis* (Daudin, 1994); Images are morphological representations and not drawn to scale
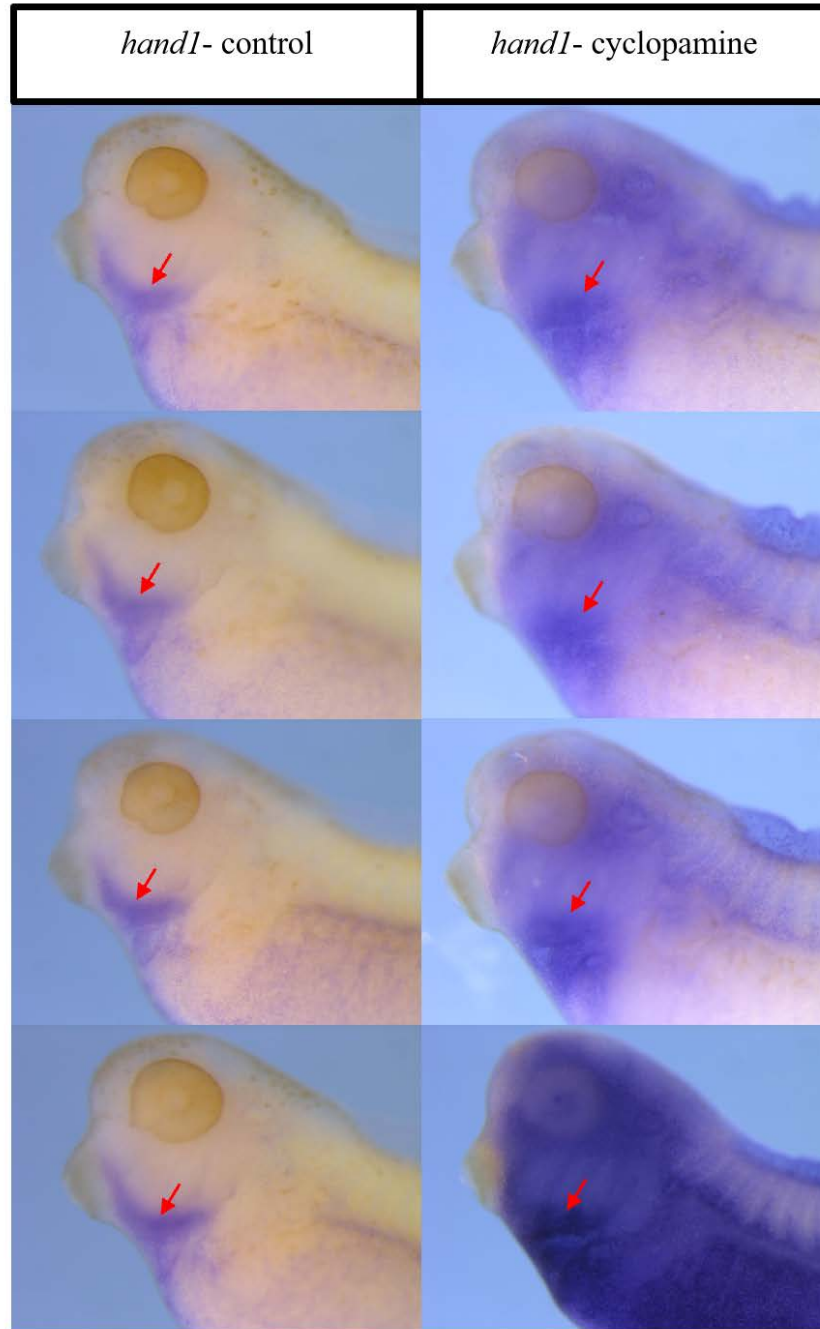
Supplementary Figure 1. Images demonstrating that inhibiting Shh signalling resulted in a dorsal shift of *hand1* expression within the pharyngeal region. Inhibition of Shh signalling by exposing embryos to cyclopamine resulted in a significant dorsal shift of the *hand1* expression domain when compared to control embryos. Arrows indicate *hand1* expression of interest within the pharyngeal region.

gcm2 - control	*gcm2* - cyclopamine
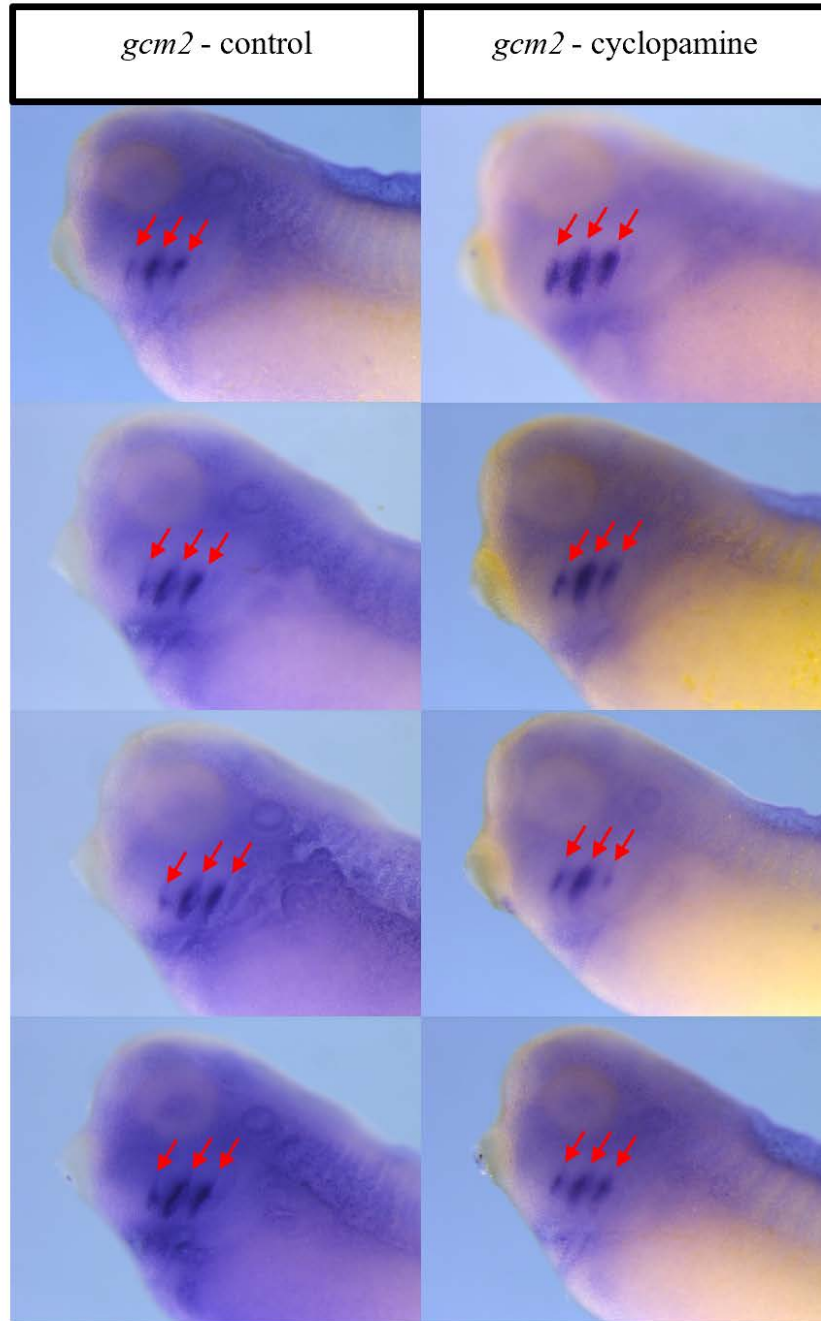
Supplementary Figure 2. Images showing inhibition of Shh signalling resulted in a dorsal shift in the expression domain of the intermediate marker *gcm2* within the developing pharyngeal region. Exposing embryos to cyclopamine resulted in a significant dorsal shift of the expression domain of *gcm2* when compared to the control embryos. Arrows indicate *gcm2* expression of interest within the pharyngeal region.

Supplementary Figure 3. Images demonstrating that altering the Shh signalling pathway caused a shift of *pou3f3* expression along the dorsoventral axis of the developing pharyngeal region. Exposing the embryos with purmorphamine results in a significant ventral shift of the expression domain of *pou3f3* when compared to the control embryos. Arrows indicate *pou3f3* expression of interest within the pharyngeal region.

| *hand1*- control | *hand1*- DMH1 |
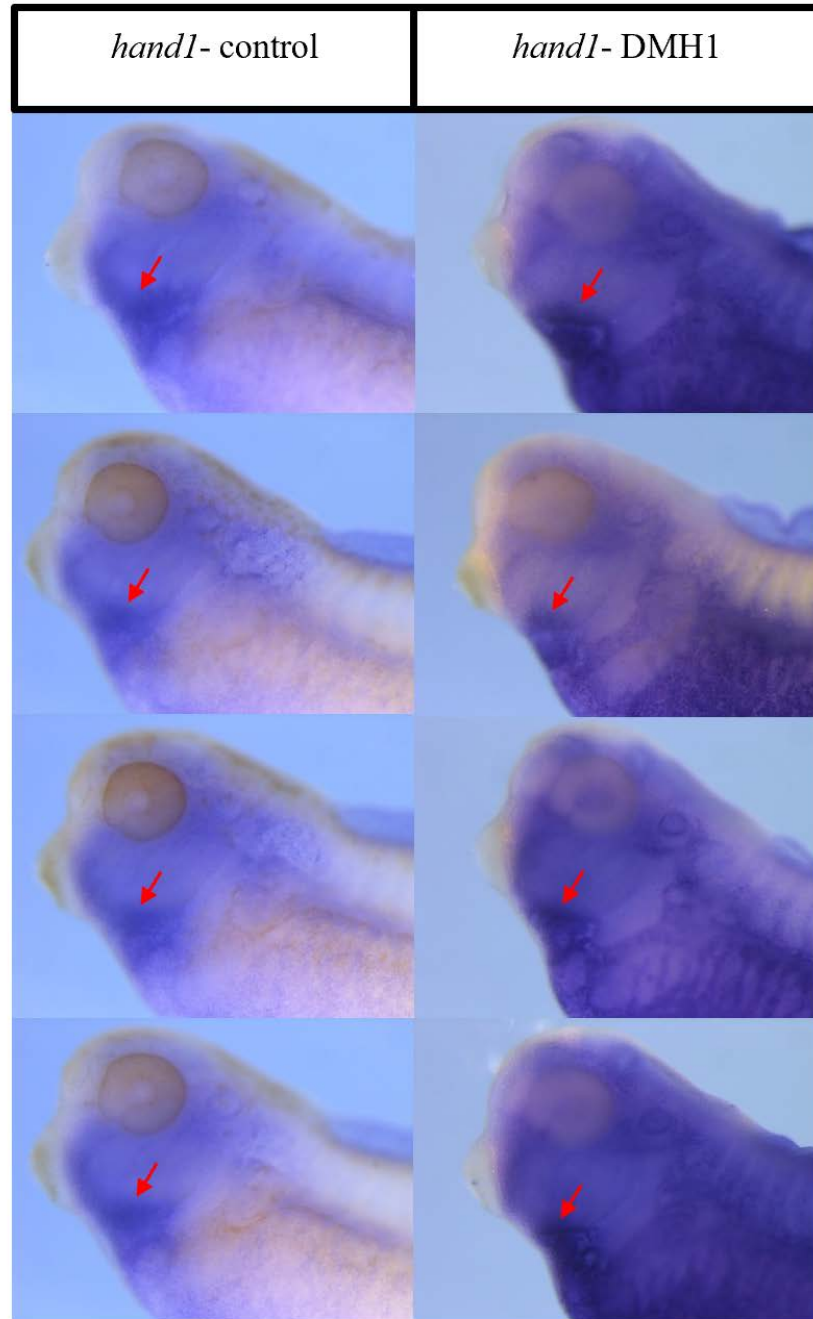
Supplementary Figure 4. Images demonstrating that inhibiting Bmp4 signalling resulted in a ventral shift of *hand1* expression within the pharyngeal region. Inhibition of Bmp4 signalling by exposing embryos to DMH1 resulted in a significant ventral shift of the *hand1* expression domain when compared to control embryos. Arrows indicate *hand1* expression of interest within the pharyngeal region.
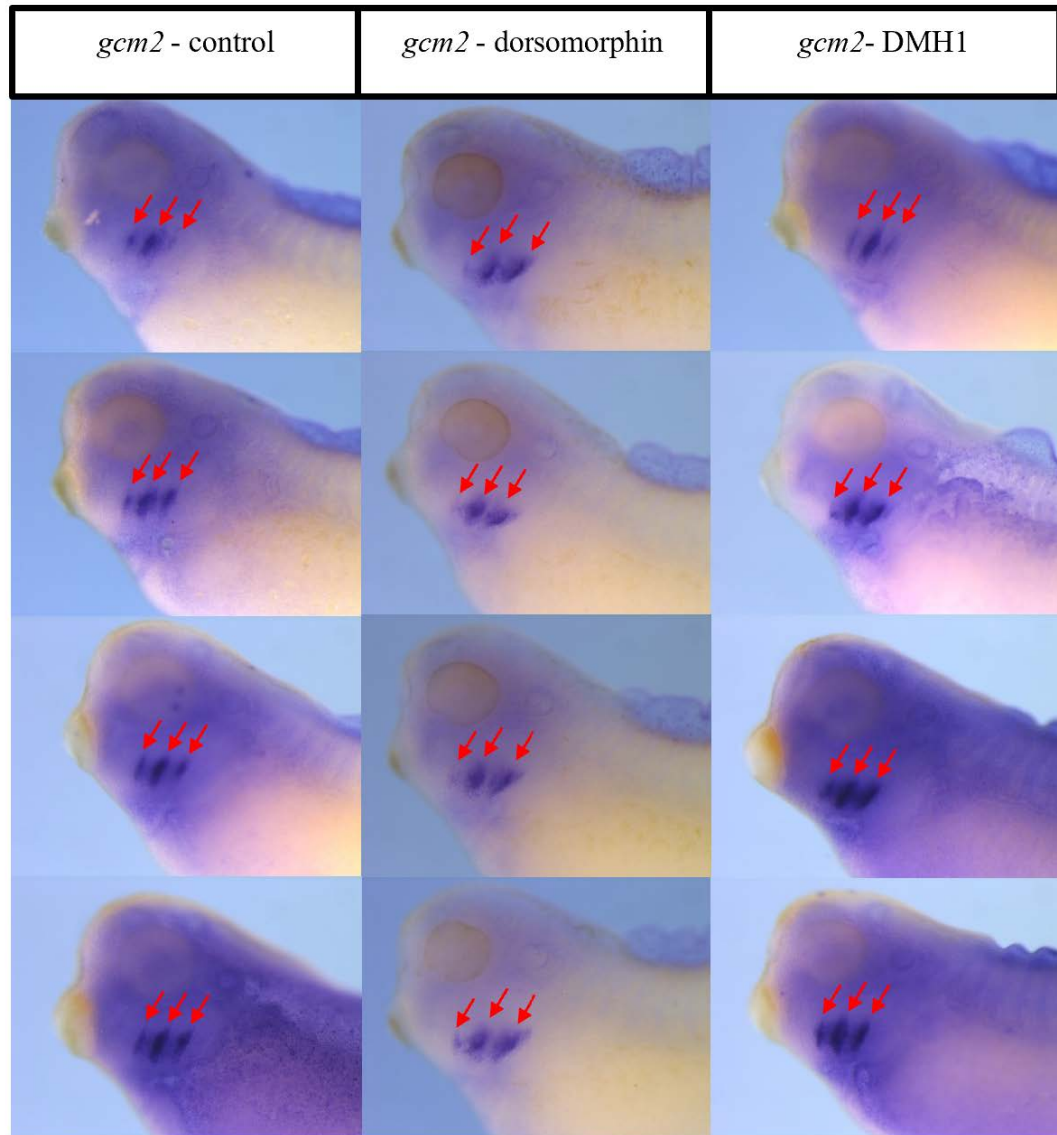
Supplementary Figure 5. Images showing that inhibiting Bmp4 signalling resulted in a ventral shift of *gcm2* expression within the pharyngeal region. Inhibition of Bmp4 signalling by exposing embryos to Dorsomorphin and DMH1 resulted in a significant ventral shift of the *gcm2* expression domain when compared to control embryos. Arrows indicate *gcm2* expression of interest within the pharyngeal region.

pax1 - control	*pax1* - DMH1
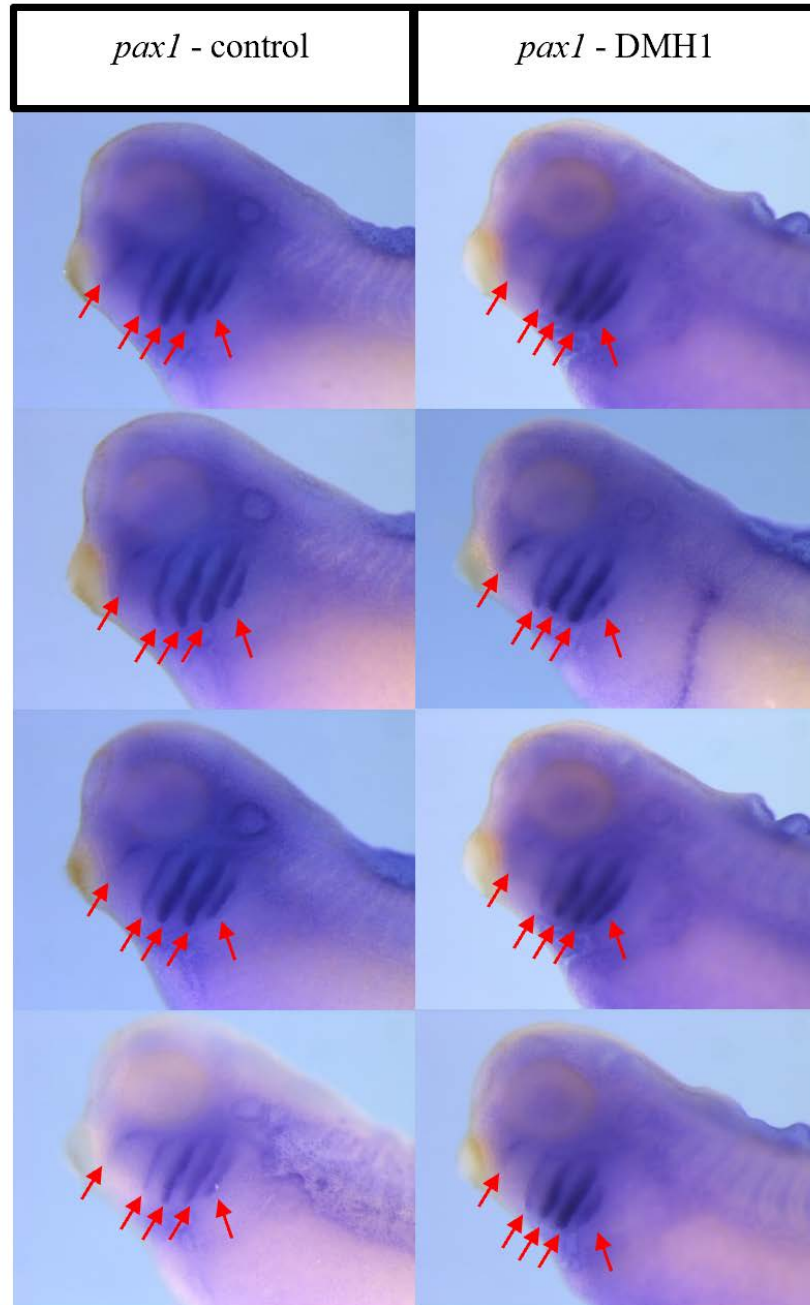
Supplementary Figure 6. Images demonstrating that inhibiting Bmp4 signalling resulted in a ventral shift of *pax1* expression within the pharyngeal region. Inhibition of Bmp4 signalling by exposing embryos to DMH1 resulted in a significant ventral shift of the *pax1* expression domain when compared to control embryos. Arrows indicate *pax1* expression of interest within the pharyngeal region.

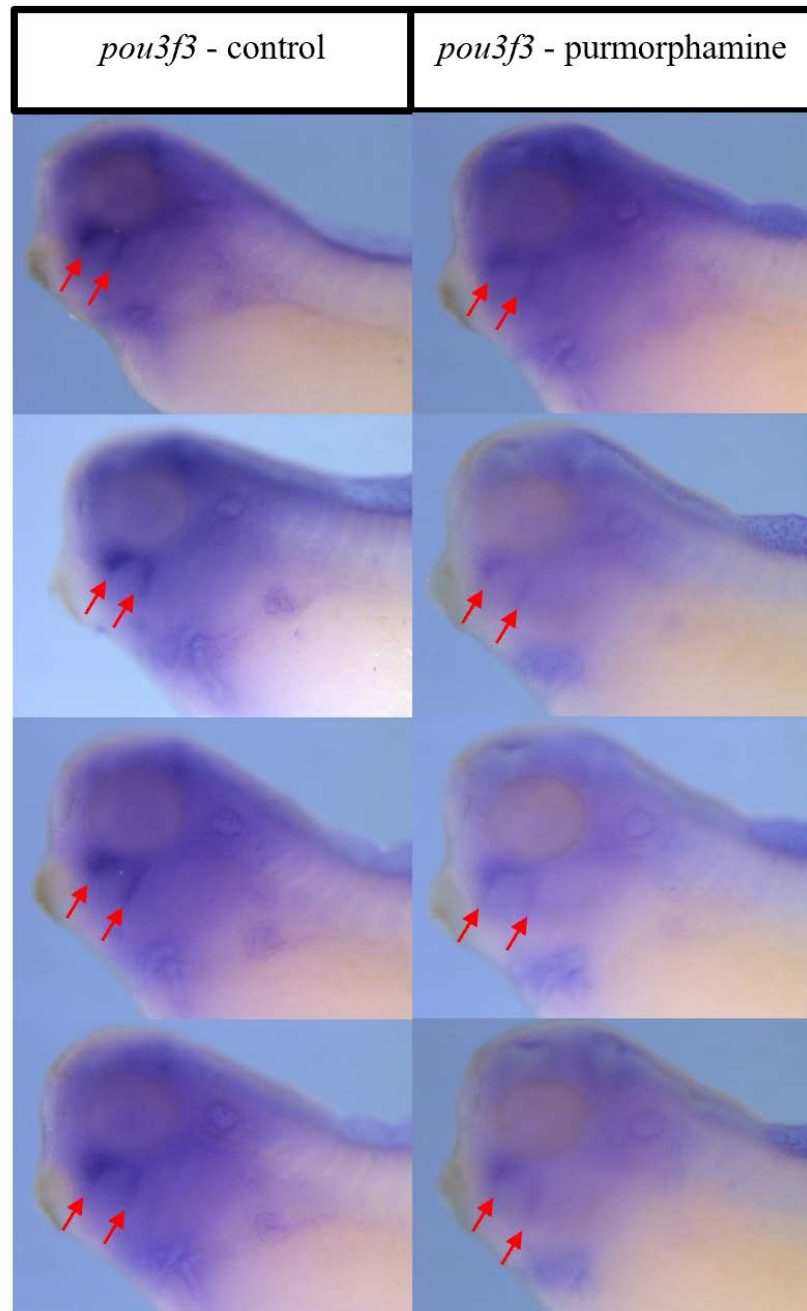| *hoxa3* - control	*hoxa3* - DMH1
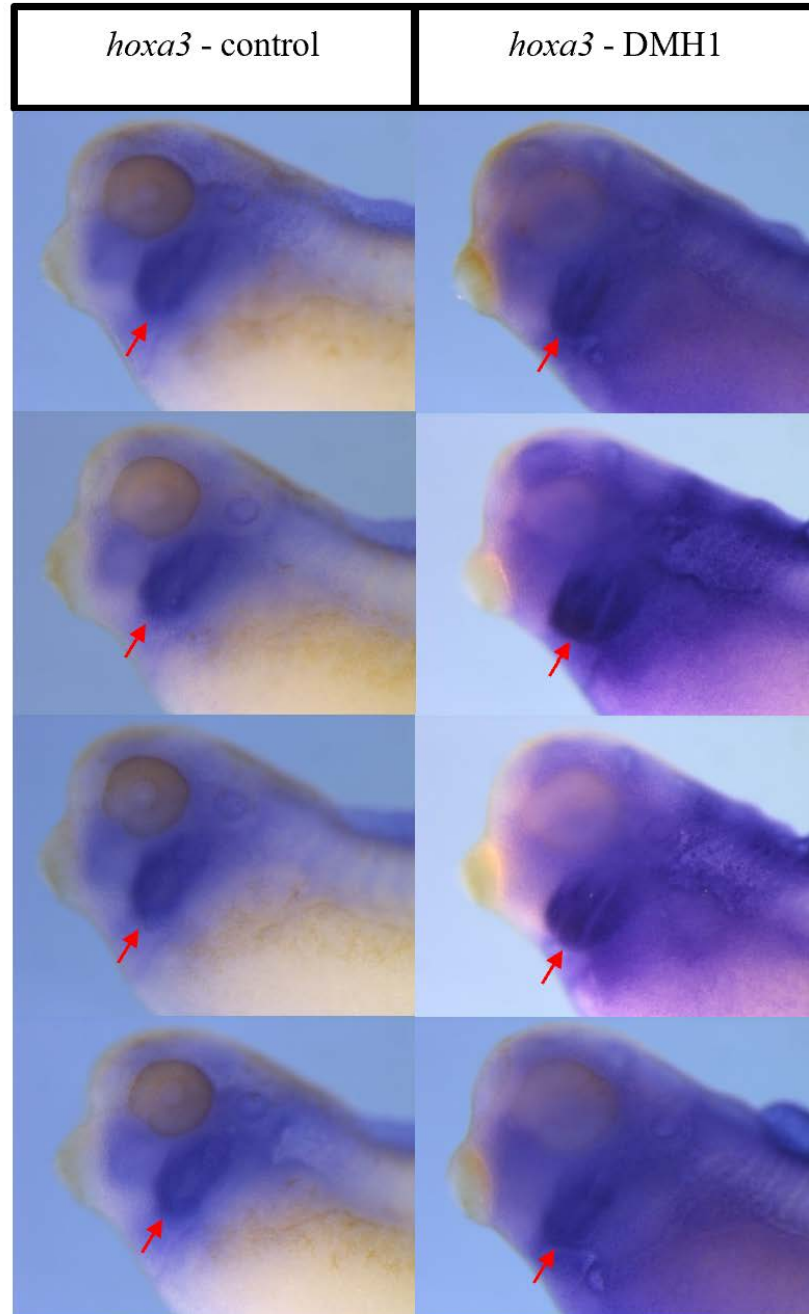
Supplementary Figure 7. Images demonstrating that inhibiting Bmp4 signalling resulted in a ventral shift of *hoxa3* expression within the pharyngeal region. Inhibition of Bmp4 signalling by exposing embryos to DMH1 resulted in a significant ventral shift of the *hoxa3* expression domain when compared to control embryos. Arrows indicate *hoxa3* expression of interest within the pharyngeal region.

gcm2 - control	*gcm2* - injected
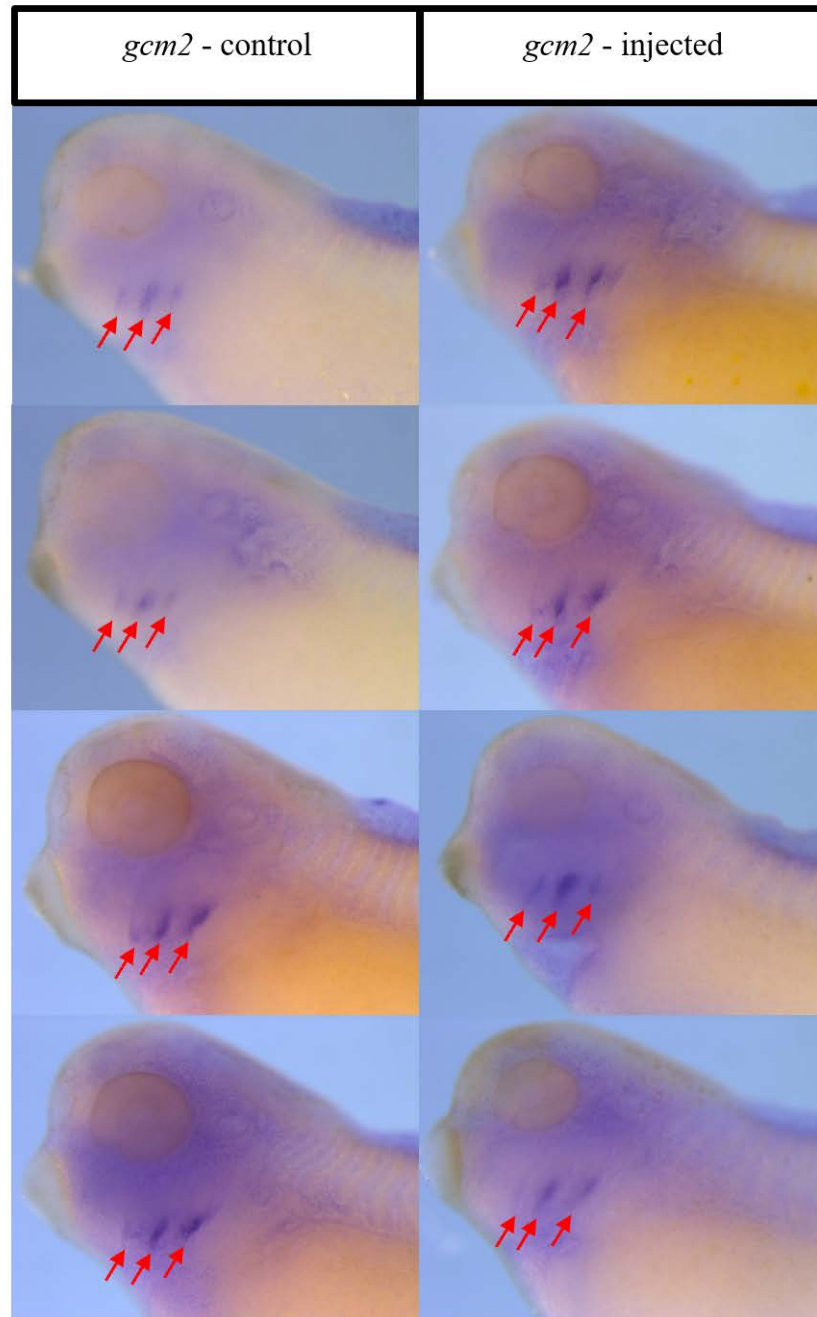
Supplementary Figure 8. **Images of embryos that had *hand1* mutated using CRISPR/Cas9 showed a dorsal shift in the expression domain of *gcm2*.** Mutating *hand1* using CRISPR/Cas9 technology resulted in a significant dorsal shift of the localization of *gcm2* expression domain compared to control embryos. Arrows indicate *gcm2* expression of interest within the pharyngeal region.
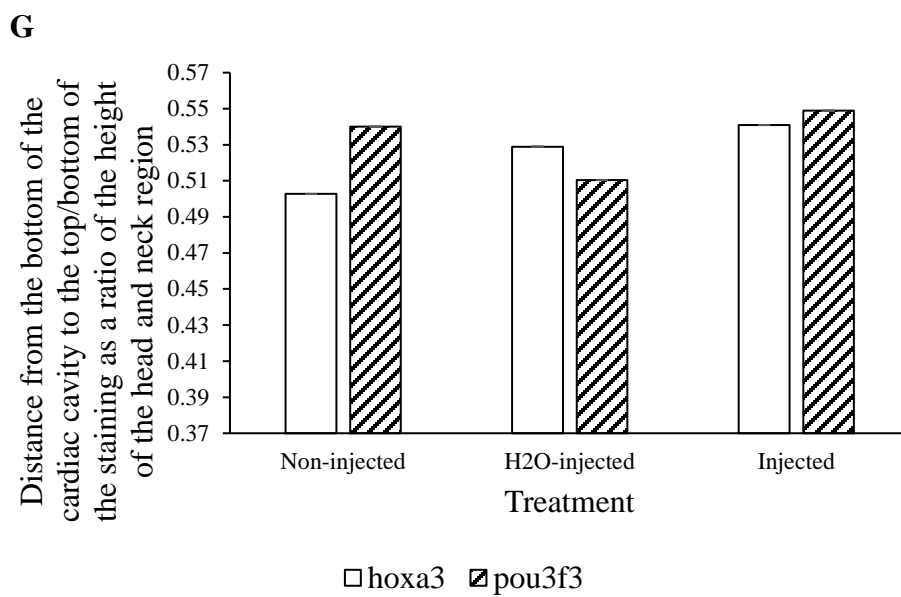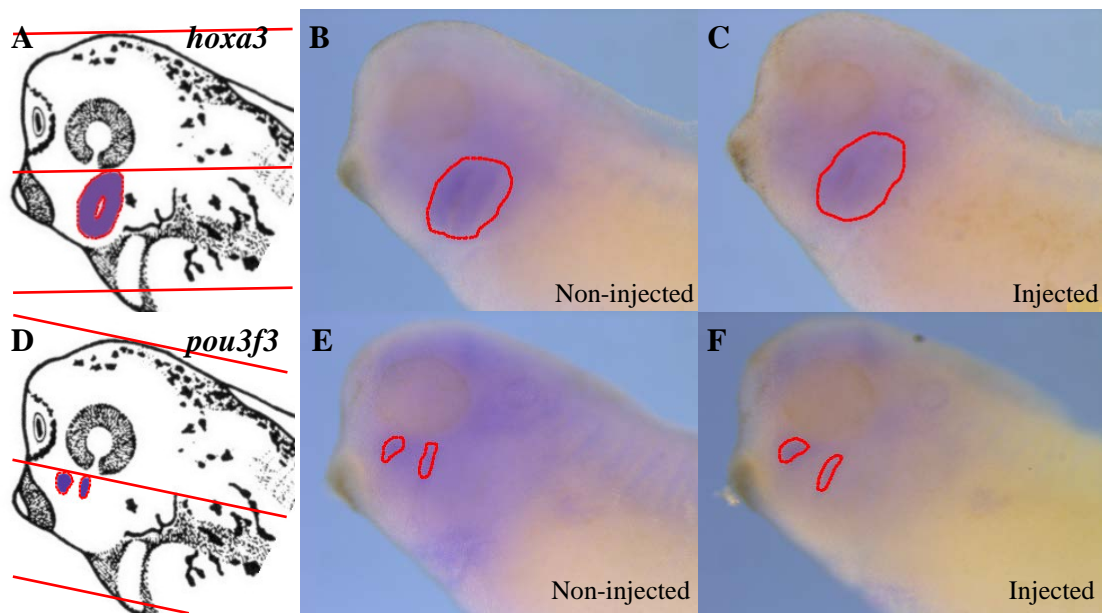
**Supplementary Figure 9. Mutations in the *hand1* gene resulted in a trending dorsal shift of the *hoxa3* expression domain. (A & D)** Schematic diagrams depicting the expression domains of *hoxa3* and *pou3f3* with lines demonstrating where markers were placed. Following mutation of the *hand1* gene a trending dorsal shift of the *hoxa3* expression domain (**C**) was observed in comparison to the control embryos (**B & G**). No observable change of the *pou3f3* expression domain (**E**) was observed in the embryos in which the *hand1* gene was mutated when compared to the control embryos (**F & G**).

References

Altaba, A.R. i, and Melton, D.A. (1989). Involvement of the Xenopus homeobox gene Xhox3 in pattern formation along the anterior-posterior axis. Cell *57*, 317–326.

Angelo, S., Lohr, J., Lee, K.H., Ticho, B.S., Breitbart, R.E., Hill, S., Yost, H.J., and Srivastava, D. (2000). Conservation of sequence and expression of Xenopus and zebrafish dHAND during cardiac, branchial arch and lateral mesoderm development. Mech. Dev. *95*, 231–237.

Ao, A., Hao, J., Hopkins, C.R., and Hong, C.C. (2012). DMH1, a Novel BMP Small Molecule Inhibitor, Increases Cardiomyocyte Progenitors and Promotes Cardiac Differentiation in Mouse Embryonic Stem Cells. PLoS ONE *7*.

Ataliotis, P., Ivins, S., Mohun, T.J., and Scambler, P.J. (2005). XTbx1 is a transcriptional activator involved in head and pharyngeal arch development in Xenopus laevis. Dev. Dyn. *232*, 979–991.

Bailey, J.M., Swanson, B.J., Hamada, T., Eggers, J.P., Singh, P.K., Caffery, T., Ouellette, M.M., and Hollingsworth, M.A. (2008). Sonic Hedgehog Promotes Desmoplasia in Pancreatic Cancer. Clin. Cancer Res. *14*, 5995–6004.

Balic, A., Adams, D., and Mina, M. (2009). Prx1 and Prx2 cooperatively regulate the morphogenesis of the medial region of the mandibular process. Dev. Dyn. Off. Publ. Am. Assoc. Anat. *238*, 2599–2613.

Barnett, C., Yazgan, O., Kuo, H.-C., Malakar, S., Thomas, T., Fitzgerald, A., Harbour, W., Henry, J.J., and Krebs, J.E. (2012). Williams Syndrome Transcription Factor is critical for neural crest cell function in Xenopus laevis. Mech. Dev. *129*, 324–338.

Barth, K.A., Kishimoto, Y., Rohr, K.B., Seydler, C., Schulte-Merker, S., and Wilson, S.W. (1999). Bmp activity establishes a gradient of positional information throughout the entire neural plate. Development *126*, 4977–4987.

Basler, K., Edlund, T., Jessell, T.M., and Yamada, T. (1993). Control of cell pattern in the neural tube: Regulation of cell differentiation by dorsalin-1, a novel TGFβ family member. Cell *73*, 687–702.

Beck, C.W., Whitman, M., and Slack, J.M.W. (2001). The Role of BMP Signaling in Outgrowth and Patterning of the Xenopus Tail Bud. Dev. Biol. *238*, 303–314.

Bei, M., and Maas, R. (1998). FGFs and BMP4 induce both Msx1-independent and Msx1-dependent signaling pathways in early tooth development. Development *125*, 4325–4333.

Berge, D. ten, Brouwer, A., Korving, J., Martin, J.F., and Meijlink, F. (1998). Prx1 and Prx2 in skeletogenesis: roles in the craniofacial region, inner ear and limbs. Development *125*, 3831–3842.

Bhattacharya, D., Marfo, C.A., Li, D., Lane, M., and Khokha, M.K. (2015). CRISPR/Cas9: An inexpensive, efficient loss of function tool to screen human disease genes in Xenopus. Dev. Biol. *408*, 196–204.

Blitz, I.L., Biesinger, J., Xie, X., and Cho, K.W.Y. (2013). Biallelic genome modification in F0 Xenopus tropicalis embryos using the CRISPR/Cas system. Genesis *51*, 827–834.

Blum, M., and Ott, T. (2018). Xenopus: An Undervalued Model Organism to Study and Model Human Genetic Disease. Cells Tissues Organs 1–11.

Briscoe, J., Sussel, L., Serup, P., Hartigan-O'Connor, D., Jessell, T.M., Rubenstein, J.L.R., and Ericson, J. (1999). Homeobox gene Nkx2.2 and specification of neuronal identity by graded Sonic hedgehog signalling. Nature *398*, 622–627.

Campione, M., Steinbeisser, H., Schweickert, A., Deissler, K., Bebber, F. van, Lowe, L.A., Nowotschin, S., Viebahn, C., Haffter, P., Kuehn, M.R., et al. (1999). The homeobox gene Pitx2: mediator of asymmetric left-right signaling in vertebrate heart and gut looping. Development *126*, 1225–1234.

Chamoun, Z., Mann, R.K., Nellen, D., Kessler, D.P. von, Bellotto, M., Beachy, P.A., and Basler, K. (2001). Skinny Hedgehog, an Acyltransferase Required for Palmitoylation and Activity of the Hedgehog Signal. Science *293*, 2080–2084.

Chen, J.K., Taipale, J., Cooper, M.K., and Beachy, P.A. (2002). Inhibition of Hedgehog signaling by direct binding of cyclopamine to Smoothened. Genes Dev. *16*, 2743–2748.

Chojnowski, J.L., Trau, H.A., Masuda, K., and Manley, N.R. (2016). Temporal and spatial requirements for Hoxa3 in mouse embryonic development. Dev. Biol. *415*, 33–45.

Choudhry, Z., Rikani, A.A., Choudhry, A.M., Tariq, S., Zakaria, F., Asghar, M.W., Sarfraz, M.K., Haider, K., Shafiq, A.A., and Mobassarah, N.J. (2014). Sonic hedgehog signalling pathway: a complex network. Ann. Neurosci. *21*, 28–31.

Christen, B., and Slack, J.M.W. (1997). FGF-8Is Associated with Anteroposterior Patterning and Limb Regeneration inXenopus. Dev. Biol. *192*, 455–466.

Collop, A.H., Broomfield, J.A.S., Chandraratna, R.A.S., Yong, Z., Deimling, S.J., Kolker, S.J., Weeks, D.L., and Drysdale, T.A. (2006). Retinoic acid signaling is essential for formation of the heart tube in Xenopus. Dev. Biol. *291*, 96–109.

Correa, P., Akerström, G., and Westin, G. (2002). Underexpression of Gcm2, a master regulatory gene of parathyroid gland development, in adenomas of primary hyperparathyroidism. Clin. Endocrinol. (Oxf.) *57*, 501–505.

Cosse-Etchepare, C., Gervi, I., Buisson, I., Formery, L., Schubert, M., Riou, J.-F., Umbhauer, M., and Le Bouffant, R. (2018). Pou3f transcription factor expression during embryonic development highlights distinct pou3f3 and pou3f4 localization in the Xenopus laevis kidney. Int. J. Dev. Biol. *62*, 325–333.

Dale, L., and Slack, J.M.W. (1987). Fate map for the 32-cell stage of Xenopus laevis. 26.

Deimling, S.J., and Drysdale, T.A. (2009). Retinoic acid regulates anterior–posterior patterning within the lateral plate mesoderm of Xenopus. Mech. Dev. *126*, 913–923.

Deimling, S.J., and Drysdale, T.A. (2011). Fgf is required to regulate anterior–posterior patterning in the Xenopus lateral plate mesoderm. Mech. Dev. *128*, 327–341.

DeLay, B.D., Corkins, M.E., Hanania, H.L., Salanga, M., Deng, J.M., Sudou, N., Taira, M., Horb, M.E., and Miller, R.K. (2018). Tissue-Specific Gene Inactivation in Xenopus laevis: Knockout of lhx1 in the Kidney with CRISPR/Cas9. Genetics *208*, 673–686.

Dickinson, A.J.G. (2016). Using frogs faces to dissect the mechanisms underlying human orofacial defects. Semin. Cell Dev. Biol. *51*, 54–63.

Dickinson, A.J.G., and Sive, H. (2006). Development of the primary mouth in Xenopus laevis. Dev. Biol. *295*, 700–713.

Drossopoulou, G., Lewis, K.E., Sanz-Ezquerro, J.J., Nikbakht, N., McMahon, A.P., Hofmann, C., and Tickle, C. (2000). A model for anteroposterior patterning of the vertebrate limb based on sequential long- and short-range Shh signalling and Bmp signalling. Development *127*, 1337–1348.

El-Hodiri, H.M., and Kelly, L.E. (2018). Visualization of Gene Expression Patterns by In Situ Hybridization on Early Stages of Development of Xenopus laevis. Methods Mol. Biol. Clifton NJ *1797*, 325–335.

Ericson, J., Muhr, J., Placzek, M., Lints, T., Jessel, T.M., and Edlund, T. (1995). Sonic hedgehog induces the differentiation of ventral forebrain neurons: A common signal for ventral patterning within the neural tube. Cell *81*, 747–756.

Ericson, J., Morton, S., Kawakami, A., Roelink, H., and Jessell, T.M. (1996). Two Critical Periods of Sonic Hedgehog Signaling Required for the Specification of Motor Neuron Identity. Cell *87*, 661–673.

Escriva, H., Holland, N.D., Gronemeyer, H., Laudet, V., and Holland, L.Z. (2002). The retinoic acid signaling pathway regulates anterior/posterior patterning in the nerve cord and pharynx of amphioxus, a chordate lacking neural crest. Development *129*, 2905–2916.

Ferguson, C.A., and Graham, A. (2004). Redefining the head–trunk interface for the neural crest. Dev. Biol. *269*, 70–80.

Fernandez-Teran, M., Piedra, M.E., Rodriguez-Rey, J.C., Talamillo, A., and Ros, M.A. (2003). Expression and regulation of eHAND during limb development. Dev. Dyn. *226*, 690–701.

Firulli, B.A., Fuchs, R.K., Vincentz, J.W., Clouthier, D.E., and Firulli, A.B. (2014). Hand1 phosphoregulation within the distal arch neural crest is essential for craniofacial morphogenesis. Development *141*, 3050–3061.

Firulli, B.A., Milliar, H., Toolan, K.P., Harkin, J., Fuchs, R.K., Robling, A.G., and Firulli, A.B. (2017). Defective Hand1 phosphoregulation uncovers essential roles for Hand1 in limb morphogenesis. Development *144*, 2480–2489.

Frisdal, A., and Trainor, P.A. (2014). Development and evolution of the pharyngeal apparatus. Wiley Interdiscip. Rev. Dev. Biol. *3*, 403–418.

Gao, Y., Zhou, Y., Xu, A., and Wu, D. (2008). Effects of an AMP-activated protein kinase inhibitor, compound C, on adipogenic differentiation of 3T3-L1 cells. Biol. Pharm. Bull. *31*, 1716–1722.

Gendron-Maguire, M., Mallo, M., Zhang, M., and Gridley, T. (1993). Hoxa-2 mutant mice exhibit homeotic transformation of skeletal elements derived from cranial neural crest. Cell *75*, 1317–1331.

Gordon, L., Mansh, M., Kinsman, H., and Morris, A.R. (2010). Xenopus sonic hedgehog guides retinal axons along the optic tract. Dev. Dyn. *239*, 2921–2932.

Gowan, K., Helms, A.W., Hunsaker, T.L., Collisson, T., Ebert, P.J., Odom, R., and Johnson, J.E. (2001). Crossinhibitory Activities of Ngn1 and Math1 Allow Specification of Distinct Dorsal Interneurons. Neuron *31*, 219–232.

Graham, A., and Smith, A. (2001). Patterning the pharyngeal arches. BioEssays *23*, 54–61.

Gray, R.S., Bayly, R.D., Green, S.A., Agarwala, S., Lowe, C.J., and Wallingford, J.B. (2009). Diversification of the expression patterns and developmental functions of the Dishevelled gene family during chordate evolution. Dev. Dyn. Off. Publ. Am. Assoc. Anat. *238*, 2044–2057.

Günther, T., Chen, Z.-F., Kim, J., Priemel, M., Rueger, J.M., Amling, M., Moseley, J.M., Martin, T.J., Anderson, D.J., and Karsenty, G. (2000). Genetic ablation of parathyroid glands reveals another source of parathyroid hormone. Nature *406*, 199–203.

Hao, J., Ho, J.N., Lewis, J.A., Karim, K.A., Daniels, R.N., Gentry, P.R., Hopkins, C.R., Lindsley, C.W., and Hong, C.C. (2010). In Vivo Structure−Activity Relationship Study of Dorsomorphin Analogues Identifies Selective VEGF and BMP Inhibitors. ACS Chem. Biol. *5*, 245–253.

Hao, J., Lee, R., Chang, A., Fan, J., Labib, C., Parsa, C., Orlando, R., Andresen, B., and Huang, Y. (2014). DMH1, a Small Molecule Inhibitor of BMP Type I Receptors, Suppresses Growth and Invasion of Lung Cancer. PLOS ONE *9*, e90748.

Haremaki, T., Deglincerti, A., and Brivanlou, A.H. (2015). Huntingtin is required for ciliogenesis and neurogenesis during early Xenopus development. Dev. Biol. *408*, 305–315.

Ho, L., Symes, K., Yordán, C., Gudas, L.J., and Mercola, M. (1994). Localization of PDGF A and PDGFRα mRNA in Xenopus embryos suggests signalling from neural ectoderm and pharyngeal endoderm to neural crest cells. Mech. Dev. *48*, 165–174.

Hoyos, J.M., Ferraro, A., Sacchetti, S., Keller, S., De Martino, I., Borbone, E., Pallante, P., Fedele, M., Montanaro, D., Esposito, F., et al. (2016). HAND1 gene expression is negatively regulated by the High Mobility Group A1 proteins and is drastically reduced in human thyroid carcinomas. Oncogene *35*, 5930.

Hunt, P., Gulisano, M., Cook, M., Sham, M.-H., Faiella, A., Wilkinson, D., Boncinelli, E., and Krumlauf, R. (1991a). A distinct Hox code for the branchial region of the vertebrate head. Nature *353*, 861–864.

Hunt, P., Whiting, J., Nonchev, S., Sham, M.H., Marshall, H., Graham, A., Cook, M., Allemann, R., Rigby, P.W., and Gulisano, M. (1991b). The branchial Hox code and its implications for gene regulation, patterning of the nervous system and head evolution. Dev. Camb. Engl. Suppl. *Suppl 2*, 63–77.

Jeong, J., Li, X., McEvilly, R.J., Rosenfeld, M.G., Lufkin, T., and Rubenstein, J.L.R. (2008). Dlx genes pattern mammalian jaw primordium by regulating both lower jaw-specific and upper jaw-specific genetic programs. Development *135*, 2905–2916.

Jones, N.C., and Trainor, P.A. (2004). The therapeutic potential of stem cells in the treatment of craniofacial abnormalities. Expert Opin. Biol. Ther. *4*, 645–657.

Kebebew, E., Peng, M., Wong, M.G., Ginzinger, D., Duh, Q.-Y., and Clark, O.H. (2004). GCMB gene, a master regulator of parathyroid gland development, expression, and regulation in hyperparathyroidism. Surgery *136*, 1261–1266.

Koide, T., Hayata, T., and Cho, K.W.Y. (2006). Negative regulation of Hedgehog signaling by the cholesterogenic enzyme 7-dehydrocholesterol reductase. Development *133*, 2395–2405.

Kontges, G., and Lumsden, A. (1996). Rhombencephalic neural crest segmentation is preserved throughout craniofacial ontogeny. Development *122*, 3229–3242.

Laufer, E., Nelson, C.E., Johnson, R.L., Morgan, B.A., and Tabin, C. (1994). Sonic hedgehog and Fgf-4 act through a signaling cascade and feedback loop to integrate growth and patterning of the developing limb bud. Cell *79*, 993–1003.

Le Dréau, G., and Martí, E. (2012). Dorsal-ventral patterning of the neural tube: a tale of three signals. Dev. Neurobiol. *72*, 1471–1481.

Lee, Y.-H., Williams, A., Hong, C.-S., You, Y., Senoo, M., and Saint-Jeannet, J.-P. (2013). Early development of the thymus in Xenopus laevis. Dev. Dyn. Off. Publ. Am. Assoc. Anat. *242*, 164–178.

Lewis, P.M., Dunn, M.P., McMahon, J.A., Logan, M., Martin, J.F., St-Jacques, B., and McMahon, A.P. (2001). Cholesterol Modification of Sonic Hedgehog Is Required for Long-Range Signaling Activity and Effective Modulation of Signaling by Ptc1. Cell *105*, 599–612.

Liem, K.F., Jessell, T.M., and Briscoe, J. (2000). Regulation of the neural patterning activity of sonic hedgehog by secreted BMP inhibitors expressed by notochord and somites. Development *127*, 4855–4866.

Liem Jr., K.F., Tremml, G., Roelink, H., and Jessell, T.M. (1995). Dorsal differentiation of neural plate cells induced by BMP-mediated signals from epidermal ectoderm. Cell *82*, 969–979.

Liem Jr., K.F., Tremml, G., and Jessell, T.M. (1997). A Role for the Roof Plate and Its Resident TGFβ-Related Proteins in Neuronal Patterning in the Dorsal Spinal Cord. Cell *91*, 127–138.

Liu, C., Lou, C.-H., Shah, V., Ritter, R., Talley, J., Soibam, B., Benham, A., Zhu, H., Perez, E., Shieh, Y.-E., et al. (2016). Identification of microRNAs and microRNA targets in Xenopus gastrulae: The role of miR-26 in the regulation of Smad1. Dev. Biol. *409*, 26–38.

Liu, Z., Yu, S., and Manley, N.R. (2007). Gcm2 is required for the differentiation and survival of parathyroid precursor cells in the parathyroid/thymus primordia. Dev. Biol. *305*, 333–346.

Macdonald, R., Barth, K.A., Xu, Q., Holder, N., Mikkola, I., and Wilson, S.W. (1995). Midline signalling is required for Pax gene regulation and patterning of the eyes. Development *121*, 3267–3278.

Machold, R., Hayashi, S., Rutlin, M., Muzumdar, M.D., Nery, S., Corbin, J.G., Gritli-Linde, A., Dellovade, T., Porter, J.A., Rubin, L.L., et al. (2003). Sonic Hedgehog Is Required for Progenitor Cell Maintenance in Telencephalic Stem Cell Niches. Neuron *39*, 937–950.

Maconochie, M., Krishnamurthy, R., Nonchev, S., Meier, P., Manzanares, M., Mitchell, P.J., and Krumlauf, R. (1999). Regulation of Hoxa2 in cranial neural crest cells involves members of the AP-2 family. Development *126*, 1483–1494.

Manley, N.R., and Capecchi, M.R. (1998). HoxGroup 3 Paralogs Regulate the Development and Migration of the Thymus, Thyroid, and Parathyroid Glands. Dev. Biol. *195*, 1–15.

Matsuda, Y., Uno, Y., Kondo, M., Gilchrist, M.J., Zorn, A.M., Rokhsar, D.S., Schmid, M., and Taira, M. (2015). A New Nomenclature of Xenopus laevis Chromosomes Based on the Phylogenetic Relationship to Silurana/Xenopus tropicalis. Cytogenet. Genome Res. *145*, 187–191.

McFadden, D.G., McAnally, J., Richardson, J.A., Charité, J., and Olson, E.N. (2002). Misexpression of dHAND induces ectopic digits in the developing limb bud in the absence of direct DNA binding. Development *129*, 3077–3088.

McMahon, J.A., Takada, S., Zimmerman, L.B., Fan, C.-M., Harland, R.M., and McMahon, A.P. (1998). Noggin-mediated antagonism of BMP signaling is required for growth and patterning of the neural tube and somite. Genes Dev. *12*, 1438–1452.

McNulty, C.L., Peres, J.N., Bardine, N., van den Akker, W.M.R., and Durston, A.J. (2005). Knockdown of the complete Hox paralogous group 1 leads to dramatic hindbrain and neural crest defects. Dev. Camb. Engl. *132*, 2861–2871.

Megason, S.G., and McMahon, A.P. (2002). A mitogen gradient of dorsal midline Wnts organizes growth in the CNS. Development *129*, 2087–2098.

Minoux, M., and Rijli, F.M. (2010). Molecular mechanisms of cranial neural crest cell migration and patterning in craniofacial development. Development *137*, 2605–2621.

Nguyen, V.H., Trout, J., Connors, S.A., Andermann, P., Weinberg, E., and Mullins, M.C. (2000). Dorsal and intermediate neuronal cell types of the spinal cord are established by a BMP signaling pathway. Development *127*, 1209–1220.

Nie, S., and Bronner, M.E. (2015). Dual developmental role of transcriptional regulator Ets1 in Xenopus cardiac neural crest vs. heart mesoderm. Cardiovasc. Res. *106*, 67–75.

Nishinakamura, R., and Sakaguchi, M. (2014). BMP signaling and its modifiers in kidney development. Pediatr. Nephrol. *29*, 681–686.

Noden, D.M., and Trainor, P.A. (2005). Relations and interactions between cranial mesoderm and neural crest populations. J. Anat. *207*, 575–601.

P.D. Nieuwkoop, and J. Faber (1994). Normal table of Xenopus laevis (Daudin). A symmetrical and chronological survey of the development from the fertilized egg till the end of metamorphosis (New York: Garland Publishing).

Persson, M., Stamataki, D., Welscher, P. te, Andersson, E., Böse, J., Rüther, U., Ericson, J., and Briscoe, J. (2002). Dorsal-ventral patterning of the spinal cord requires Gli3 transcriptional repressor activity. Genes Dev. *16*, 2865–2878.

Pickar-Oliver, A., and Gersbach, C.A. (2019). The next generation of CRISPR–Cas technologies and applications. Nat. Rev. Mol. Cell Biol. *20*, 490–507.

Pieper, M., Ahrens, K., Rink, E., Peter, A., and Schlosser, G. (2012). Differential distribution of competence for panplacodal and neural crest induction to non-neural and neural ectoderm. Development *139*, 1175–1187.

Pierani, A., Brenner-Morton, S., Chiang, C., and Jessell, T.M. (1999). A Sonic Hedgehog–Independent, Retinoid-Activated Pathway of Neurogenesis in the Ventral Spinal Cord. Cell *97*, 903–915.

Qian, S.-W., Tang, Y., Li, X., Liu, Y., Zhang, Y.-Y., Huang, H.-Y., Xue, R.-D., Yu, H.-Y., Guo, L., Gao, H.-D., et al. (2013). BMP4-mediated brown fat-like changes in white adipose tissue alter glucose and energy homeostasis. Proc. Natl. Acad. Sci. *110*, E798–E807.

Rankin, S.A., Gallas, A.L., Neto, A., Gómez-Skarmeta, J.L., and Zorn, A.M. (2012). Suppression of Bmp4 signaling by the zinc-finger repressors Osr1 and Osr2 is required for Wnt/β-catenin-mediated lung specification in Xenopus. Dev. Camb. Engl. *139*, 3010–3020.

Rankin, S.A., Thi Tran, H., Wlizla, M., Mancini, P., Shifley, E.T., Bloor, S.D., Han, L., Vleminckx, K., Wert, S.E., and Zorn, A.M. (2015). A Molecular atlas of Xenopus respiratory system development. Dev. Dyn. *244*, 69–85.

Rankin, S.A., Han, L., McCracken, K.W., Kenny, A.P., Anglin, C.T., Grigg, E.A., Crawford, C.M., Wells, J.M., Shannon, J.M., and Zorn, A.M. (2016). A Retinoic Acid-Hedgehog Cascade Coordinates Mesoderm-Inducing Signals and Endoderm Competence during Lung Specification. Cell Rep. *16*, 66–78.

Rijli, F.M., Mark, M., Lakkaraju, S., Dierich, A., Dollé, P., and Chambon, P. (1993). A homeotic transformation is generated in the rostral branchial region of the head by disruption of Hoxa-2, which acts as a selector gene. Cell *75*, 1333–1349.

Riley, P., Anaon-Cartwight, L., and Cross, J.C. (1998). The Hand1 bHLH transcription factor is essential for placentation and cardiac morphogenesis. Nat. Genet. *18*, 271–275.

Rinon, A., Lazar, S., Marshall, H., Büchmann-Møller, S., Neufeld, A., Elhanany-Tamir, H., Taketo, M.M., Sommer, L., Krumlauf, R., and Tzahor, E. (2007). Cranial neural crest cells regulate head muscle patterning and differentiation during vertebrate embryogenesis. Development *134*, 3065–3075.

Rodrigues, A.R., Yakushiji-Kaminatsui, N., Atsuta, Y., Andrey, G., Schorderet, P., Duboule, D., and Tabin, C.J. (2017). Integration of Shh and Fgf signaling in controlling Hox gene expression in cultured limb cells. Proc. Natl. Acad. Sci. *114*, 3139–3144.

Roelink, H., Porter, J.A., Chiang, C., Tanabe, Y., Chang, D.T., Beachy, P.A., and Jessell, T.M. (1995). Floor plate and motor neuron induction by different concentrations of the amino-terminal cleavage product of sonic hedgehog autoproteolysis. Cell *81*, 445–455.

Ryan, A.K., and Rosenfeld, M.G. (1997). POU domain family values: flexibility, partnerships, and developmental codes. Genes Dev. *11*, 1207–1225.

Sánchez, R.S., and Sánchez, S.S. (2013). Characterization of pax1, pax9, and uncx sclerotomal genes during Xenopus laevis embryogenesis. Dev. Dyn. *242*, 572–579.

Sánchez, R.S., and Sánchez, S.S. (2015). Paraxis is required for somite morphogenesis and differentiation in Xenopus laevis. Dev. Dyn. *244*, 973–987.

Sander, M., Paydar, S., Ericson, J., Briscoe, J., Berber, E., German, M., Jessell, T.M., and Rubenstein, J.L. (2000). Ventral neural patterning by Nkx homeobox genes: Nkx6.1 controls somatic motor neuron and ventral interneuron fates. Genes Dev. *14*, 2134–2139.

Scambler, P.J. (2000). The 22q11 deletion syndromes. Hum. Mol. Genet. *9*, 2421–2426.

Schmidt, J.E., Suzuki, A., Ueno, N., and Kimelman, D. (1995). Localized BMP-4 Mediates Dorsal/Ventral Patterning in the Early Xenopus Embryo. Dev. Biol. *169*, 37–50.

Session, A.M., Uno, Y., Kwon, T., Chapman, J.A., Toyoda, A., Takahashi, S., Fukui, A., Hikosaka, A., Suzuki, A., Kondo, M., et al. (2016). Genome evolution in the allotetraploid frog Xenopus laevis. Nature *538*, 336–343.

Sinha, S., and Chen, J.K. (2006). Purmorphamine activates the Hedgehog pathway by targeting Smoothened. Nat. Chem. Biol. *2*, 29–30.

Smart, N., Hill, A.A., Cross, J.C., and Riley, P.R. (2002). A differential screen for putative targets of the bHLH transcription factor Hand1 in cardiac morphogenesis. Mech. Dev. *119*, S65–S71.

Sparrow, D.B., Kotecha, S., Towers, N., and Mohun, T.J. (1998). Xenopus eHAND: a marker for the developing cardiovascular system of the embryo that is regulated by bone morphogenetic proteins. Mech. Dev. *71*, 151–163.

Square, T., Jandzik, D., Cattell, M., Coe, A., Doherty, J., and Medeiros, D.M. (2015). A gene expression map of the larval Xenopus laevis head reveals developmental changes underlying the evolution of new skeletal elements. Dev. Biol. *397*, 293–304.

Stewart, K., Uetani, N., Hendriks, W., Tremblay, M.L., and Bouchard, M. (2013). Inactivation of LAR family phosphatase genes Ptprs and Ptprf causes craniofacial malformations resembling Pierre-Robin sequence. Development *140*, 3413–3422.

Su, D., Ellis, S., Napier, A., Lee, K., and Manley, N.R. (2001). Hoxa3 and Pax1 Regulate Epithelial Cell Death and Proliferation during Thymus and Parathyroid Organogenesis. Dev. Biol. *236*, 316–329.

Suzuki, A., Thies, R.S., Yamaji, N., Song, J.J., Wozney, J.M., Murakami, K., and Ueno, N. (1994). A truncated bone morphogenetic protein receptor affects dorsal-ventral patterning in the early Xenopus embryo. Proc. Natl. Acad. Sci. *91*, 10255–10259.

Tabler, J.M., Bolger, T.G., Wallingford, J., and Liu, K.J. (2014). Hedgehog activity controls opening of the primary mouth. Dev. Biol. *396*, 1–7.

Talbot, J.C., Johnson, S.L., and Kimmel, C.B. (2010). hand2 and Dlx genes specify dorsal, intermediate and ventral domains within zebrafish pharyngeal arches. Development *137*, 2507–2517.

Tandon, P., Conlon, F., Furlow, J.D., and Horb, M.E. (2017). Expanding the genetic toolkit in Xenopus: Approaches and opportunities for human disease modeling. Dev. Biol. *426*, 325–335.

Tickle, C., and Towers, M. (2017). Sonic Hedgehog Signaling in Limb Development. Front. Cell Dev. Biol. *5*.

Timmer, J.R., Wang, C., and Niswander, L. (2002). BMP signaling patterns the dorsal and intermediate neural tube via regulation of homeobox and helix-loop-helix transcription factors. Development *129*, 2459–2472.

Trainor, P.A., and Krumlauf, R. (2000). Patterning the cranial neural crest: Hinbrain segmentation and *hox* gene plasticity. Nat. Rev. Neurosci. *1*, 116–124.

Tümpel, S., Maconochie, M., Wiedemann, L.M., and Krumlauf, R. (2002). Conservation and Diversity in the cis-Regulatory Networks That Integrate Information Controlling Expression of Hoxa2 in Hindbrain and Cranial Neural Crest Cells in Vertebrates. Dev. Biol. *246*, 45–56.

Tümpel, S., Cambronero, F., Sims, C., Krumlauf, R., and Wiedemann, L.M. (2008). A regulatory module embedded in the coding region of Hoxa2 controls expression in rhombomere 2. Proc. Natl. Acad. Sci. *105*, 20077–20082.

Vallstedt, A., Muhr, J., Pattyn, A., Pierani, A., Mendelsohn, M., Sander, M., Jessell, T.M., and Ericson, J. (2001). Different Levels of Repressor Activity Assign Redundant and Specific Roles to Nkx6 Genes in Motor Neuron and Interneuron Specification. Neuron *31*, 743–755.

Weaver, C., and Kimelman, D. (2004). Move it or lose it: axis specification in Xenopus. Development *131*, 3491–3499.

Wheeler, G.N., and Brändli, A.W. (2009). Simple vertebrate models for chemical genetics and drug discovery screens: lessons from zebrafish and Xenopus. Dev. Dyn. Off. Publ. Am. Assoc. Anat. *238*, 1287–1308.

Yamada, T., Pfaff, S.L., Edlund, T., and Jessell, T.M. (1993). Control of cell pattern in the neural tube: Motor neuron induction by diffusible factors from notochord and floor plate. Cell *73*, 673–686.

Yamagishi, C., Yamagishi, H., Maeda, J., Tsuchihashi, T., Ivey, K., Hu, T., and Srivastava, D. (2006). Sonic hedgehog is essential for first pharyngeal arch development. Pediatr. Res. *59*, 349–354.

Yang, H., Wang, H., Shivalila, C.S., Cheng, A.W., Shi, L., and Jaenisch, R. (2013). One-Step Generation of Mice Carrying Reporter and Conditional Alleles by CRISPR/Cas-Mediated Genome Engineering. Cell *154*, 1370–1379.

Yost, H.J. (1990). Inhibition of proteoglycan synthesis eliminates left-right asymmetry in Xenopus laevis cardiac looping. Dev. Camb. Engl. *110*, 865–874.

Yu, J., Carroll, T.J., and McMahon, A.P. (2002). Sonic hedgehog regulates proliferation and differentiation of mesenchymal cells in the mouse metanephric kidney. Development *129*, 5301–5312.

Yu, P.B., Hong, C.C., Sachidanandan, C., Babitt, J.L., Deng, D.Y., Hoyng, S.A., Lin, H.Y., Bloch, K.D., and Peterson, R.T. (2008). Dorsomorphin inhibits BMP signals required for embryogenesis and iron metabolism. Nat. Chem. Biol. *4*, 33–41.

Zeng, X., Goetz, J.A., Suber, L.M., Scott Jr, W.J., Schreiner, C.M., and Robbins, D.J. (2001). A freely diffusible form of Sonic hedgehog mediates long-range signalling. Nature *411*, 716–720.

Curriculum Vitae

Name: Alexander Cameron Szpak

Place of Birth: Calgary, Alberta

Date of Birth: May 19, 1994

Post-secondary   Honours Specialization in Biology
education and   Western University
degrees: 2012-2016

                                    M.Sc. in Biology (Collaborative Program in
                                    Developmental Biology
                                    Western University
                                    2016-2019

Contributions to   17th Annual International *Xenopus* Conference,
research and   Poster Presentation "Mechanisms that regulate
development: dorsoventral patterning of the pharynx in Xenopus
                                    laevis"
                                    Seattle, Washington
                                    August 12-16, 2018

                                    Western's Annual Developmental Biology Day
                                    Poster Presentation "Mechanisms that regulate
                                    dorsoventral patterning of the pharynx in Xenopus
                                    laevis"
                                    London, Ontario
                                    May 2018

Western's Annual Pediatrics Research Day

Poster Presentation "Mechanisms that regulate dorsoventral patterning of the pharynx in Xenopus laevis"

London, Ontario

May 2018

London Health Research Day

Poster Presentation "Mechanisms that regulate dorsoventral patterning of the pharynx in Xenopus laevis"

London, Ontario

May 2018

9th Canadian Developmental Biology Conference

Poster Presentation "Mechanisms that regulate dorsoventral patterning of the pharynx in Xenopus laevis"

Mont-Tremblant, Quebec

March 19-22, 2018

Western's Biology Graduate Research Forum

Poster Presentation "Mechanisms that regulate dorsoventral patterning of the pharynx in Xenopus laevis"

London, Ontario

October 2017

Western's Annual Developmental Biology Day
Poster Presentation "Mechanisms that regulate
dorsoventral patterning of the pharynx in Xenopus
laevis"
London, Ontario
May 2017

Western's Annual Pediatrics Research Day
Poster Presentation "Mechanisms that regulate
dorsoventral patterning of the pharynx in Xenopus
laevis"
London, Ontario
May 2017

Western's Annual Developmental Biology Day
Poster Presentation "Mechanisms that regulate
dorsoventral patterning of the pharynx in Xenopus
laevis"
London, Ontario
May 2016